125

STOCHASTIC STRUCTURAL ANALYSIS OF ENGINEERING COMPONENTS USING THE FINITE ELEMENT METHOD

by

Marc Anton Weber
B.Sc. (Eng)(Mech) (UCT)
M.Sc. (Eng) (UCT)

A thesis presented for the Degree of
Doctor of Philosophy

Department of Mechanical Engineering
University of Cape Town

August 1993

Declaration

This is to certify that the results, calculations and any other work presented in this thesis are essentially my own work, and that no part of it has been submitted for a degree at any other university.

Signed by candidate

M A Weber

August 1993

Abstract

This thesis investigates probabilistic and stochastic methods for structural analysis which can be integrated into existing, commercially available finite element programs. It develops general probabilistic finite element routines which can be implemented within deterministic finite element programs without requiring major code development. These routines are implemented in the general purpose finite element program ABAQUS through its user element subroutine facility and two probabilistic finite elements are developed: a three-dimensional beam element limited to linear material behaviour and a two-dimensional plane element involving elastic-plastic material behaviour. The plane element incorporates plane strain, plane stress and axisymmetric formulations. The numerical accuracy and robustness of the routines are verified and application of the probabilistic finite element method is illustrated in two case studies, one involving a four-story, two-bay frame structure, the other a reactor pressure vessel nozzle.

The probabilistic finite element routines developed in this thesis integrate point estimate methods and mean value first order methods within the same program. Both methods require a systematic sequence involving the perturbation of the random parameters to be evaluated, although the perturbation sequence of the methods differ. It is shown that computer-time saving techniques such as Taylor series and iterative perturbation schemes, developed for mean value based methods, can also be used to solve point estimate method problems. These efficient techniques are limited to linear problems; nonlinear problems must use full perturbation schemes. Finally, it is shown that all these probabilistic methods and perturbation schemes can be integrated within one program and can follow many of the existing deterministic program structures and subroutines. An overall strategy for converting deterministic finite element programs to probabilistic finite element programs is outlined.

The point estimate method is capable of estimating the mean and standard deviation of component response directly within the probabilistic finite element analysis, from which the cumulative distribution of the response and the probability of failure of the component can be estimated. Some post-processing is required in the case of the mean value first order method, and a post-processing program based on fast probability integration is developed. The mean value-fast probability integration programs are capable of making good initial estimates of the mean and standard deviation of component response, the cumulative distribution of the response, the probability of failure of the component and the most probable points at failure. These initial estimates can be improved by repeating the procedure at the most probable points. A simple analysis procedure is developed for solving problems involving random parameters which are statistically independent for different parts of the model.

A crucial feature in the integration of probabilistic routines into ABAQUS or other deterministic finite element programs is the addition of a perturbation control module which controls the perturbation sequence and solution algorithms of the different perturbation schemes and writes results to a database file. Since the overall program structure of the deterministic finite element can be maintained, the additional code required to convert a deterministic element to a probabilistic element is limited and can be easily integrated within existing program structures. Existing program sub-units can be used for both the deterministic and probabilistic routines and, except for some input/output routines, the additional code required affects existing programs only at the element level.

Acknowledgement

I acknowledge, and sincerely appreciate, the help of the following people and organisations:

- Professor R K Penny, under whose supervision this thesis was conducted, for his continuing interest and support,
- colleagues of the Centre for Research into Computational and Applied Mechanics and the Department of Mechanical Engineering at the University of Cape Town, for their willing assistance,
- the Division of Materials Science of Technology of the Council for Scientific and Industrial Research and the Foundation for Research and Development, for their financial assistance, and,
- my parents, Ton and Anneke Weber, for their interest and support, and Elizabeth Dreyer for her understanding and patience during the preparation of this manuscript.

Table of Contents

List of Terms

Convention

Standard terminology as found in the literature has been used in this thesis as far as possible. Where different workers have used different terminology, the most consistent combination of terminology has been adopted in an effort to achieve a clear and concise text. Where the use of standard terminology would have led to confusion in the text, minor terminology changes have been effected. Nevertheless, the wide scope of topics considered in this thesis has led to some terms having multiple definitions. This should not lead to confusion in the text as these terms are not used in combination and terms are defined in the text when they are used. A consistent typographical format has been used in the definition of finite element terms, which has been followed as far as possible in other sections of the thesis, and which is defined below:

Bold typeface, upper case	Matrix
Bold typeface, lower case	Vector
Normal typeface	Single parameter Function Matrix/vector component

List of Terms

$\mathbf{B}$	Strain-displacement matrix
$\mathbf{D}$	Constitutive matrix
$\mathbf{J}$	Jacobian matrix
$\mathbf{K}$	Stiffness matrix
$\mathbf{R}$	Rotation matrix
$\mathbf{u}$	Displacement vector
$\mathbf{f}$, $\mathbf{r}$	Load vector, reaction vector
$\mathbf{f}^{INT}$, $\mathbf{f}^{RES}$	Internal force vector, residual vector
$\boldsymbol{\varepsilon}$, $\mathbf{e}$	Strain vector, deviatoric strain vector
$\boldsymbol{\sigma}$, $\mathbf{s}$	Stress vector, deviatoric stress vector
A, I, J	Cross-sectional area, moment of area, polar moment of area
E, G, K, H	Elastic, shear, bulk, hardening modulus
F, S, M, T	Force, shear force, bending moment, torque
P	Point load (units: force)
$Z(\mathbf{x})$, $Z_1(\mathbf{x})$	Response function, linearised response function
$H(\mathbf{x})$	Higher order terms in response function

Z_f	Limit state, failure criterion
Φ	Standard normal cumulative distribution function
a	Response function coefficients
$b_{\pm}$, ρ	Point estimate weighting factor, correlation coefficient
$\tilde{e}^{pl}$	Equivalent plastic strain
$f_{\mathbf{x}}$	Probability distribution function
$g(\mathbf{x})$	Limit state function
p, w	Pressure (units: force/area), distributed load (units: force/length)
p_f	Probability of failure
β	Reliability index, safety index
δ, θ	Deflection, rotation
ν	Poisson's ratio
μ, σ_Z, σ_{Z_f}	Mean, standard deviation of response, failure criterion
σ^*	Mises equivalent stress
σ_y, σ_y^o	Yield stress, initial yield stress
Mean, STD, COV	Mean, standard deviation, coefficent of variance (used in tables)

Operators

$\mathrm{E}[\cdot]$	Expectation
$\sigma[\cdot]$, $\sigma^2[\cdot]$	Standard deviation, variance/covariance
$\delta[r_j]$	Perturbation amount of random parameter r_j

Subscripts

len, *vol*	Element length, volume
0	Deterministic part
r, 1, 2	Random parts
$\pm$	Point estimate method perturbation

Superscripts

G, L	Global, local coordinates
el, *pl*	Elastic, plastic
o, $n-1$, n	Initial, previous, current value
$*$	Most probable point

Accents

$\hat{}$	Elastic predictor value
$\breve{}$	Perturbed parameter
$\bar{}$	Mean value

1 Introduction

Engineers derive mathematical models to represent the physical behaviour of structures and components in numerical form. The aim of these models is to be able to predict the behaviour of a structure or component by "solving" a numerical representation of a design problem. Sometimes these models are based on the physical characteristics of the problem, sometimes they are empirical, usually they are a combination. Yet they all have in common that some *model parameters* are required in order to obtain results. Typical model parameters are material properties, geometry, environmental factors and the loads acting on a structure. Uncertainty or randomness in model parameters has been a problem facing engineers ever since the first design calculations were performed.

To solve the problem requires that specific values be assigned to the model parameters. Yet the engineer knows that, in many problems, it is impossible to assign specific, constant values to these parameters. For example, although an engineer can measure material properties by performing tests, there is always some variation in material composition, scatter in the results and some inaccuracies in the measurement technique. Similarly, operational conditions vary with time, and even if historical records are available, there is always the probability that more extreme conditions will occur in the future.

Engineers, safety-conscious as they are, have designed structures and components which possess an inherent conservatism through the use of safety or overload factors. In many problems these safety factors are specified by Codes of Practice and Standards and represent the knowledge and experience of many engineers over a long period of time. Yet failures do occur, sometimes catastrophic. At the same time structures exist which are overly conservative. In any case, the use of extra material can in itself cause premature failure – as in problems involving thermal transients.

With the current emphasis on efficient and economic designs, which aim to maximise performance and minimise cost and material, the use of overly conservative safety factors is no longer justified. At the same time the occurrence of failures needs to be minimised and reliable operation needs to be ensured during the design stage from commissioning through to retirement of plant.

The driving forces towards reliable operation are threefold, namely concerns for safety, cost and the environment. The safety aspect is the most important of these as the loss of life in the event of catastrophic failure cannot be recompensed. Cost is important since unreliable operation can cause maintenance expenses which are of the order of, or larger than, the original cost of the component. Structural failures often result in the destruction of other plant and property, leading to enormous downtime, replacement, insurance and litigation costs. Catastrophic failures of nuclear and chemical plant and

off-shore structures can result in environmental disasters which affect the health of current and future generations.

As a consequence the uncertainty and/or randomness of inputs and parameters needs to be included in the design procedure: it is required to establish at the design stage which are the most sensitive parameters in the model (and whether they are likely to vary much), and it is required to establish how reliable a design is. Of equal practical importance is the life assessment and/or uprating of aged plant: material parameters have degraded and current values are not known accurately, flaws of unknown size are present, operation history is often not known precisely, future operation may suffer from unpredicted load and temperature excursions, and it is required to know whether operation of the plant can be safely continued, and for how long.

One of the main tools available to engineers to model and analyse complex structures and components is the finite element method. This had its origins in the aircraft industry in the 1950's. When used with care, commercially available finite element programs are capable of solving a wide variety of problems and offer users a choice of element formulations, mesh generation techniques, material models, solution schemes and other model options. Through the rapid development of desktop computer hardware at affordable prices in the 1980's, these programs have become increasingly accessible to engineers who include the finite element method in a range of standard tools in the design process.

Commercially available finite element programs are deterministic: material parameters, environmental conditions, loading and geometry are assumed to be constant parameters of the finite element model. Lately, some of the finite element programs have incorporated optimisation procedures which can assess the sensitivity of the model to some of its parameters. However, these programs do not formally include uncertainty or randomness in their procedures and estimates of reliability cannot be made directly from the finite element analyses.

Advanced probabilistic methods for structural analysis have been derived which include the randomness of parameters in the design procedure. These are based on either classical probability theory or Bayesian probability theory. Traditional methods, such as Monte Carlo simulation techniques and Weibull analyses, are able to determine accurately the reliability of individual components and structures. However, due to the large number of evaluations required, these may not be effective methods if the problem under consideration is highly complex and finite element programs are required to analyse the structure, and in such cases the required computing time (and cost) may be prohibitive.

Point estimate methods are able to reduce the computational requirements for probabilistic structural analysis considerably, but their use within finite element programs has

been limited. Mean value based methods have been derived recently for use within finite element programs, but have been implemented only in specific purpose programs not commercially available to engineers.

There is a need therefore to adapt existing finite element programs to include probabilistic or stochastic procedures. As a contribution towards this aim, the objectives of this thesis are:

- To investigate probabilistic methods for structural analysis which can be integrated into finite element programs. These probabilistic methods must:
  - improve on the computational requirements of traditional probabilistic methods for structural analysis,
  - be able to estimate the mean and standard deviation of component response,
  - be able to estimate the probability distribution of component response,
  - be able to estimate the probability of failure of a component,
  - be able to deal with linear and non-linear problems, and
  - be able to deal with correlation between random parameters.
- To develop general probabilistic finite element routines which can be implemented within deterministic finite element programs. The constraints on these probabilistic finite element routines are:
  - they must maintain existing program structures as far as possible,
  - they must involve limited additional code development,
  - they must take into account the hardware and software limitations of commercially available finite element programs, and
  - their operation by the user must be similar to that of deterministic finite element programs.

Chapter 2 critically reviews the literature on probabilistic and stochastic methods for structural analysis and on finite element methods. The objective of this review is to investigate which probabilistic structural analysis methods lend themselves to integration into existing finite element programs and how to achieve this within the constraints and objectives set above.

It is shown that two probabilistic methods, namely point estimate methods and mean value first order methods, can be integrated within the same finite element program. Both methods require a systematic sequence involving the perturbation of the random

parameters to be evaluated, although the perturbation sequence of the methods differ. It is shown that computer-time saving techniques such as Taylor series and iterative perturbation schemes, developed for mean value based methods, can also be used to solve point estimate method problems. These efficient techniques are limited to linear problems; nonlinear problems must use full perturbation schemes. Finally, it is shown that all these probabilistic methods and perturbation schemes can be integrated within one program and can follow many of the existing deterministic program structures and subroutines. An overall strategy for converting deterministic finite element programs to probabilistic finite element programs is derived.

Chapters 3, 4 and 5 describe how this strategy can be implemented in a general purpose finite element program through the user element subroutine facility available in ABAQUS. Chapter 3 describes the development of two standard deterministic finite element routines, one a linear three-dimensional beam element, the other an elastic-plastic two-dimensional plane element. The conversion of these deterministic routines to probabilistic routines is described in Chapter 4. Chapter 5 describes the post-processing routines which are required. Chapters 4 and 5 also discuss the implementation of these routines in existing deterministic finite element programs.

Chapter 6 presents the results of a number of verification problems which were analysed. The results are compared with at least one other method. Chapter 7 presents two case studies in which the procedures developed in this thesis are used in the analysis of a four-story, two-bay frame structure and a reactor pressure vessel nozzle.

Chapter 8 summarises the findings of the thesis and presents some conclusions.

2 Review of the Literature

2.1 The Finite Element Method – History and Developments

The Finite Element Method (FEM) has its roots in the aircraft industry: the development of fast, turbo-jet powered aircraft led to a relentless drive for minimum weight coupled to maximum safety (Martin and Carey, 1973). Traditional structural analysis methods – mostly beam theory methods and/or redundant force methods based on equilibrium conditions and Castigliano's theorem, both of which aim to assess stresses and deflections in the components as a whole – were insufficient in dealing with geometrically complex components such as swept wings and other components involving discontinuities. Hrennikoff (1941) and Levy (1947) were among the first to publish a method which idealised a swept wing into a framework of simple structural units, namely shear planes, spars and ribs, to which the force method could then be applied. This method was then generalised and matrix methods, based on the force method, were developed.

Matrix methods required the derivation of the flexibility matrix for the structural unit under consideration. An alternative approach based on the stiffness matrix (i.e. the inverse of the flexibility matrix) was first proposed by Levy (1953) but he was not able to derive stiffness matrices for all the structural units required to model aircraft components: although the bending capacities of spars and ribs could be modelled satisfactorily, the bending capacity of plates was still lumped with the spar and rib elements. The finite element method in its present form was originated through the derivation of the stiffness matrix for a triangular plate element (Turner et al., 1956). The term "finite element" was proposed by Clough (1960).

Initially, the matrices derived using the matrix methods were solved by hand using Gauss-reduction techniques and simple calculators. This limited the size of the models and the complexity and number of elements that could be used. Since the finite element matrices could be derived in a standardised manner, these matrices could be solved systematically using the digital electronic computers that were being developed at that time. The new techniques reduced the time spent on analysis, allowed more complex structures to be modelled and limited the need for expensive physical testing (Turner et al., 1956).

During the sixties the wider applications of FEM were being recognised by structural engineering disciplines outside the aircraft industry, notably by engineers involved in the design and analysis of off-shore structures, power generation, chemical and petro-chemical plant, and automotive and defence hardware. A number of conferences on FEM helped to achieve this; for example the First Conference on Matrix Methods in Structural Mechanics held in October 1965 by the US Air Force Institute of Technology (Przemieniecki, 1966).

A number of standard texts on FEM and matrix methods were published at this time, which transferred the finite element method to a wider audience. Foremost among these were the books by Zienkiewicz and Cheung (1967) and Przemieniecki (1968).

Although the initial use of FEM involved the analysis of linear elastic structures subject to static loading, it was recognised that the method could also be used for the analysis of, among others, heat transfer problems, fluid flow problems, structural dynamics problems, electromagnetism, soil and rock mechanics problems and eigenvalue problems. The method was also extended to the solution of nonlinear structural problems (Oden, 1972), in particular problems involving metal plasticity (Martin, 1975) and high temperature metal creep (Penny and Marriott, 1971).

The advances in FEM during the sixties and early seventies, and the increasing availability of powerful computers led to the development of the first commercially available and general purpose finite element programs (e.g. ABAQUS, MSC/NASTRAN, MARC, ANSYS). These programs were written in the FORTRAN programming language, and were installed on large mainframe computers. Use was limited to the larger companies and research and development organisations due to the high cost of the programs and the required hardware. Operation of the programs was limited to small groups of specialists (Paulsen, 1986).

During the seventies advances in FEM proliferated, with the development of new element formulations (especially iso-parametric elements), increased element libraries to deal with a wider range of applications, new integration techniques and solution procedures to deal with highly complex nonlinear behaviour and to improve efficiency, and so on. Installation was still limited to large mainframe computers.

The eighties saw the rapid development in desktop computer hardware, with powerful workstations and personal computers being introduced to the market at prices affordable by all engineers. As a consequence a number of finite element programs were brought on the market which could be installed on a variety of machines, ranging from mainframes to personal computers. Typical of these programs are ANSYS, ALGOR and LUSAS. Irons and Ahmad (1980) encapsulated their vision for the development of the finite element method in the following paragraph:

> "The new market for finite elements will be dominated by the ordinary designer. Every small design team will have a local un-costed computer, effectively a modernistic sliderule. The designer will submit his ten-element jobs, almost daily, without even consulting his section leader. The total number of such jobs will be astronomical, and there will be no good engineering reason to restrict them. Rather, what stifles the creative designer is the present em-

> phasis on large jobs, 'check-stressing' a big, complicated scheme too late for radical design changes. It is timid, unimaginative engineering to anticipate a law case in everything one does. In the long run it cannot be competitive."

The situation today reveals that their vision of FEM has largely been achieved: commercially available finite element programs can solve a wide variety of problems and have powerful pre-processors which can assist with meshing problems and can interface with many Computer Aided Drawing programs. They have advanced post-processors which can present results in graphical format. Material models can be linear and nonlinear. An increasing number of engineers have gained exposure to FEM and consider FEM as one of a range of standard tools available to analyse structures and components.

Finite element models are used in many design and life assessment problems. However, these models can only predict behaviour according to the information supplied. In many problems this information, which includes material, environmental and loading parameters and the geometry of the model, is ill-defined either through uncertainty in its values (i.e. the model parameters have not been measured or specified accurately: e.g. the material has not yet been chosen in the design and an optimisation with respect to material properties is required; the material has degraded with time and the current values are uncertain), or through randomness in its values (i.e. the model parameters are known to vary randomly: e.g. wind loads; batch-to-batch variations in material properties; variations with temperature). This is nothing new and, in the past, uncertainty and/or randomness were counteracted by safety factors, often through design code specifications.

With the current emphasis on efficient and economic designs, for which performance must be maximised and cost and material must be minimised, the use of overly conservative safety factors is no longer justified. The uncertainty or randomness needs to be included in the design procedure: the design process should establish which are the most sensitive parameters in the model (and whether they are likely to vary much), and how reliable a design is. Of equal importance is the life assessment and/or uprating of aged plant: material parameters have degraded and current values are not known accurately, flaws of unknown size are present, operation history is often not known precisely, future operation may suffer from unpredicted loading and temperature excursions, and it is required to know whether operation of the plant can be safely continued, and for how long.

The analysis of static structural problems using commercially available finite element programs is deterministic. This means that material parameters, loading, environmental conditions and geometry are assumed to be constant parameters of the model. No allowance is made for variance in these model parameters. ANSYS Version 4.2 incorporates a linear design sensitivity analysis (or optimisation) option which has been adapted to make estimates of reliability (Gopalakrishna and Donaldson, 1991), but the program is

not specifically geared to do so. A similar linear design sensitivity analysis option exists in MSC/NASTRAN, from which estimates of reliability have been (Riha et al., 1992). ABAQUS Version 5.2 incorporates a linear perturbation option where the loading can be perturbed linearly (ABAQUS User's Manual, 1992). The main purpose of this option appears to be to enable inclusion of structural dynamic analysis at various stages of a path dependent nonlinear analysis without disturbing the time stepping of the solution procedure. It is not geared to obtaining estimates of reliability.

No account can be made of material and/or load variation in commercially available finite element programs for the systematic and direct calculation of the reliability of a component. A number of specific purpose programs have been developed to calculate reliability directly using finite element methods, the most prominent of which is NESSUS (Cruse et al., 1989; Millwater et al., 1992). However, these programs are not generally available to engineers. Most of the published work on probabilistic finite element methods has been on well-defined linear problems. Recently some work has been published involving nonlinear problems but often these cover specific cases with limiting assumptions.

2.2 The Need for Reliability Assessment

Systematic reliability assessments were first performed by the aircraft industry after World War I: as commercial air traffic proliferated, the safety of air travel needed to be improved and reliable operation needed to be ensured. Since then reliability assessment and reliability management has pervaded all sectors of engineering.

Three main factors, namely concerns for safety, cost and the environment, have led to a drive for reliable operation. Of these, the safety aspect is the most important, as the loss of life due to catastrophic failure cannot be recompensed. The cost aspect enters at two levels: unreliable operation can cause maintenance expenses which are of the order of, or larger than, the original cost of the component and structural failures often result in the destruction of other plant and property, leading to enormous downtime, replacement, insurance and litigation costs. Recently environmental concerns have placed more stringent requirements for reliability on nuclear and chemical plant and off-shore structures as catastrophic failure of these can result in environmental disasters which affect the health of current and future generations.

The assessment of reliability is therefore an important facet in the design and analysis of components or structures, especially if these are highly stressed, perform critical functions or are being used beyond their original design lifetime. With this in mind reliability can be defined as follows:

> The reliability of a system or component is the probability that, when operating under stated environmental conditions, the system or component will perform its intended function adequately for a specified interval of time (Kapur and Lamberson, 1977).

When used in the reliability assessment of a component, three aspects of this definition need to be determined: firstly, what are the stated environmental conditions, how can they be quantified and are they deterministic or probabilistic. Secondly, what is "adequate performance", and how can failure to perform adequately be characterised and quantified, and thirdly, how can the interval of reliable operation be determined?

This thesis is concerned with the numerical analysis of engineering problems involving randomness or uncertainty in the model parameters. In this type of problems, where the probabilistic response and/or reliability of a component or structure needs to be estimated, a probabilistic method is used which formally accounts for uncertainty in data, knowledge or model parameters. The earlier definition of reliability can then be adapted in terms of numerical probabilistic structural analysis as follows:

> Reliability is the probability that a specified limit state or failure criterion will not be exceeded.

In traditional engineering terms, reliability is the probability that the working stresses due to the applied loading, denoted S, will not exceed the strength or "resistance" of the component, denoted R (Carter, 1972). If the working stress and component strength are deterministic the safety margin can be defined as $(R - S)$. If stress and strength are not deterministic and have inherent randomness or uncertainty, the safety margin is reduced. This is illustrated in Figure 2.1 where the mean design working stress $\bar{S}$ may be increased due to, for instance, stress raisers (A), unknown loads and environmental conditions (B), unknown internal or residual stresses (C), unknown material parameters (D), and other factors. The mean strength $\bar{R}$ may be similarly reduced by material degradation with time due to creep, fatigue, corrosion and wear (E), unknown initial strength (F), undetected defects (G), production variations (H) and so on.

Failure occurs when the increased working stress exceeds the reduced strength. If the working stress and component strength are represented by probabilistic density functions, the probability of failure corresponds to the region of overlap of the stress and strength curves illustrated schematically in Figure 2.2. The figure illustrates why in a large sample of components some may fail prematurely, even if (seemingly) conservative safety factors are used. For the purpose of a reliability analysis, and realising that the range of component strength is rarely infinite but is usually bounded in the extreme, it

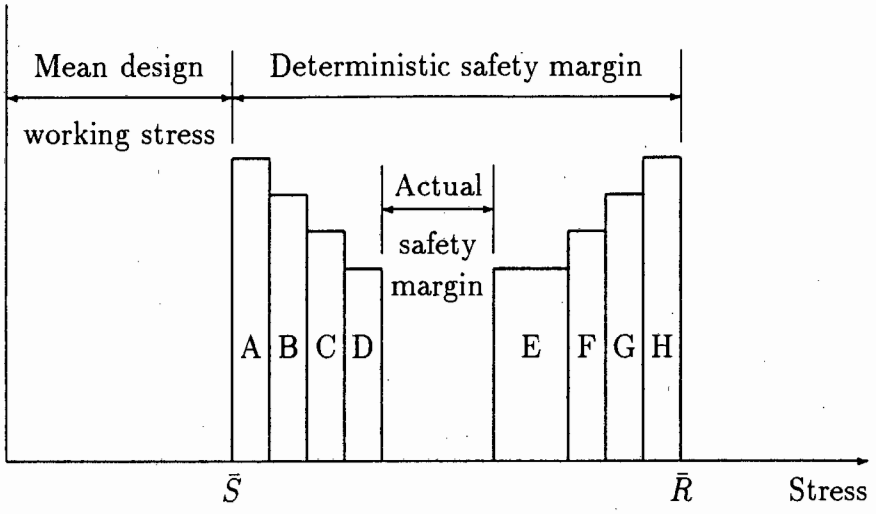

Figure 2.1: Schematic representation of working stress and component strength variation

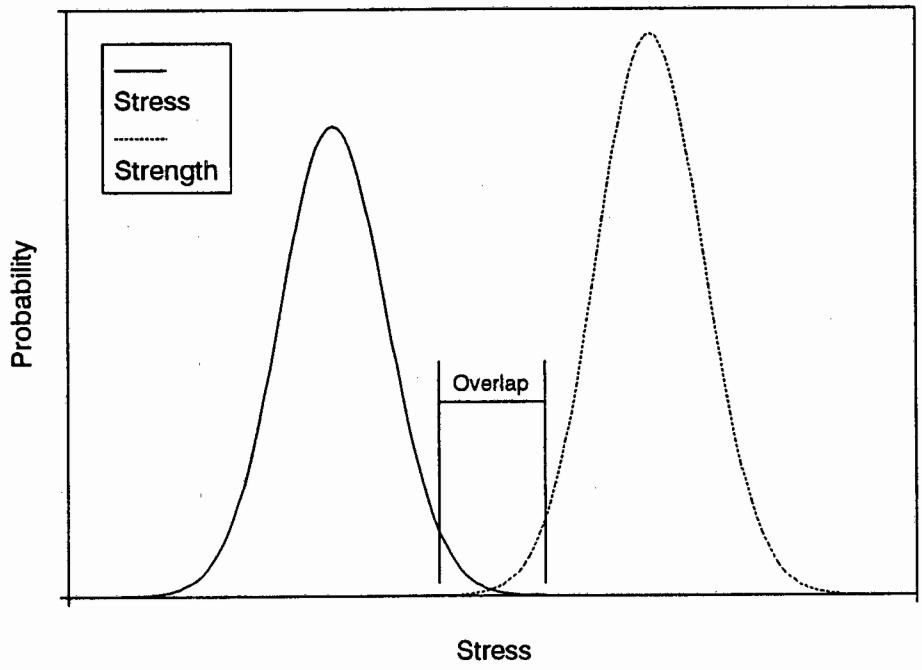

Figure 2.2: Probabilistic representation of working stress and component strength

is possible to make a lower bound estimate of the reliability of the component by calculating the probability that the working stress will lie to the left of the region of overlap in Figure 2.2. More advanced analyses take the randomness of the strength into account.

The first objective of the numerical reliability analysis is to find the probability distribution of a characteristic model response parameter, and to compare this with an appropriate lower bound failure criterion. As a minimum the mean and standard deviation of the response parameter should be known, although knowledge of the complete probability

distribution should be aimed for. A further objective is to include the randomness of the strength of the component in the analysis

The failure criteria chosen in probabilistic structural problems to characterise the limit state may or may not be completely consistent with the mechanical behaviour of the structure or component: in the case of framed structures one option is to define the limit state by the combined effects of axial forces and bending moments (SABS-0162, 1984; Arnbjerg-Nielsen and Bjerager, 1988). Another option is to define an excessive deflection (Der Kiureghian and Ke, 1985). For pressure containing structures, failure could be defined as the violation of the yield condition at a point (Klingmüller, 1982), as a limiting post-yield stress level (Millwater et al., 1991), as an excessive plastic strain at a point (Faravelli, 1989), as an excessive tensile stress which causes fracture, or as a crack length of a critical size or growing at a critical rate (Tsai and Wu, 1993).

Ideally, reliability assessment of a component or structure should form part of the design process, since reliability is an inherent attribute of a component or system, in the same way that capacity or power rating is an attribute. Subsequent testing and production will not raise the reliability without a basic design change. In many problems however, components or structures were designed according to Codes of Practice or similar design procedures, and reliability was built into the design through safety or overload factors. Reliability assessments now become necessary when used plant is uprated to operate beyond the intended loading or environmental conditions, when it is necessary to extend the lifetime of aged plant beyond the original design lifetime, when the original design models omitted to take all possible failure modes into account, or when the structure survived extreme environmental conditions or has known damage and safety of further operation needs to be assessed.

In many industrial situations, engineering plant can be described as a system involving many components. The components themselves can be systems of smaller sub-components (Carter, 1972). The reliability of a system will always involve the reliability of the individual components making up that system. Therefore it is necessary to be able to assess the reliability both of single components and of systems made from these parts.

The reliability of systems assembled using a number of smaller components can be calculated routinely if the reliability of all components making up the system is known and if their relationship with respect to failure can be determined (Ang and Tang, 1984). A variety of techniques is available, some of which have been implemented in computer programs (e.g. Mechanical Reliability Program, Powertronic Systems). These techniques are used mostly in the reliability analysis of high volume electronic and mechanical components, as reliability data for individual components is either listed in reliability databanks or can be calculated or estimated from existing failure data. Applications in the mechanical

engineering field are usually in high production items such as automotive and aeronautical components for which the acquisition of reliability data is economically feasible through the availability of extensive performance data.

Limited construction components such as nuclear pressure vessels, defence and astronautical components, on- and off-shore structures and other specialised designs, for which previous performance data is usually limited, and for which physical reliability testing is not economically viable, require reliability estimates to be made from a combination of sound engineering judgement and advanced modelling techniques such as *probabilistic structural mechanics* (Balkey et al., 1986). These techniques usually combine traditional structural analysis methods with second moment probabilistic methods and require knowledge of the first and second moments of the random or uncertain variables (i.e. the mean and covariance). Accurate knowledge of the distribution of random variables is not essential, and these distributions become no more than conceptual vehicles for transforming information based on engineering judgement into the probabilistic model (Ditlevsen, 1982).

Precise information about random variables is rarely known and through probabilistic structural mechanics appropriate and sound engineering experience can complement the observed, but limited, data: usually only information regarding mean and standard deviation can be obtained and even the extent of variance of material parameters, environmental conditions, loading and geometry is often not known precisely (Schütz, 1993). Values for covariance, spatial correlation and probability distribution are often assigned using engineering judgement, since measured data is either difficult or impossible to obtain (Shinozuka, 1987; Deodatis, 1990; Millwater et al., 1991). Vanmarcke (1982) indicated that a complex random field model, which includes interdependence and spatial correlation between the random variables on a microscopic level in the probabilistic model, may be unwarranted by the macroscopic structural behaviour. Simpler probabilistic methods, which consider only the mean and standard deviation of the random parameters, will give useful answers to designers without the complexities of the more detailed methods.

The majority of probabilistic analysis methods found in the literature involve elastic structures. However structural failures are normally associated with extreme values of the component parameters or with accidental occurrences under which it is unthinkable that the structure can remain elastic. At the same time design codes often aim to specify designs in which excursions into the plastic zone are avoided even under the most adverse conditions (SABS-219, 1978). Both elastic and inelastic behaviour must therefore be incorporated in the probabilistic analysis procedures. Inelastic material parameters such as initial yield stress and hardening properties have an inherent randomness and uncertainty that is usually higher than in elastic parameters (Casciati, 1982), and those uncertainties should not be neglected in probabilistic structural analysis methods.

2.3 Probabilistic Methods for Structural Analysis

Codes of Practice and Standards have helped to ensure safe and reliable components by specifying safety or overload factors which were required to be built into the design. In an increasing number of situations this approach is no longer sufficient: in assessments of the integrity or residual life of plant, for example, it is often difficult to assign singular, deterministic values to unknowns and uncertainties (Balkey et al., 1986).

Led by the developments for probability-based load criteria for the design of buildings and structures (NBS Special Publication 577, 1980), Code forming bodies have started to include probabilistic and reliability analysis methods in the Codes and Standards in order to refine and rationalise Code margins, allowables, inspection requirements and evaluation procedures (SABS-0160, 1989; ASME Ad Hoc Task Group on Reliability, 1990; Mahadevan and Haldar, 1991). However, it appears that the Codes will not prescribe reliability analyses to be part of the design requirements. They will use reliability analyses in the specification of (essentially deterministic) guidelines and will justify safety or overload factors through probabilistic analyses. The need for the reliability assessment of new and aged components and structures remains, and robust techniques for such assessment methods need to be developed and refined.

A probabilistic problem in the engineering sense can be posed in general terms as follows: given a function of random variables, $Z = Z(\mathbf{x})$ where $\mathbf{x} = (x_1, x_2, \ldots, x_n)$, and the joint probability function $f_{\mathbf{x}}$ of $\mathbf{x}$, what is the probability distribution of Z? When Z is a simple function, the probability moments of Z result from direct integration (Ang and Tang, 1975):

$$\bar{Z} = \mathrm{E}[Z] = \int_{-\infty}^{\infty} Z\, f_Z(Z)\, \mathrm{d}Z = \int_{-\infty}^{\infty} Z(\mathbf{x})\, f_{\mathbf{x}}(\mathbf{x})\, \mathrm{d}\mathbf{x} \tag{2.1}$$

and

$$\begin{aligned} \sigma_Z &= \mathrm{E}[(Z - \bar{Z})^2] = \int_{-\infty}^{\infty} (Z - \bar{Z})^2\, f_Z(Z)\, \mathrm{d}Z \\ &= \int_{-\infty}^{\infty} (Z(\mathbf{x}) - \bar{Z})^2\, f_{\mathbf{x}}(\mathbf{x})\, \mathrm{d}\mathbf{x} \end{aligned} \tag{2.2}$$

and so on for further probability moments of Z. The probability distribution of Z can then be estimated from the probability moments. A practical example of this approach is in a study by Arbabi et al. (1991) of railway tracks with randomly varying axle loads: the tracks are modelled as an infinite beam on an elastic foundation with a random concentrated load acting at the centre of the beam. The method is extended to include multiple random variables, resulting in a significant increase in complexity for a simple model. The

method is specific to the problem under consideration, and a solution procedure needs to be developed for each different problem. The advantage of the method is that parametric studies are simple and efficient once a solution procedure has been developed. In most engineering problems however, the joint density function $f_{\mathbf{x}}$ is not known explicitly and the function Z is complex, and direct integration methods are not feasible.

One method readily available to deal with inherently complex problems is the *Monte Carlo simulation* technique (Haugen, 1968; Ang and Tang, 1984). This technique involves the repeated deterministic analysis of a problem whereby for each analysis the uncertain parameters are allowed to vary randomly within a specified probability function. A specified response function is evaluated for each simulation and compared with specified failure criteria (which may be random). Whenever the response exceeds the failure criteria, an occurrence of failure is recorded. The probability of failure is then estimated as the recorded number of failures divided by the total number of simulations. At the same time the probability distribution of the response can be approximated using histogram techniques (i.e. counting the number of occurrences within a set of small intervals).

The technique is numerically accurate but requires a large number of repeated calculations, usually of the order of 10,000 (and as many as 1,000,000 in some instances), especially if small probabilities of failure must be calculated or if the number of random parameters is large (Lawrence, 1989). The number of simulations can be reduced if only a portion of the response probability function is of interest; for example the tails of the response probability distribution function. Variance reduction, importance sampling and/or stratified sampling techniques are then required (Schuëller and Stix, 1987; Bjerager, 1989; Decker, 1991). However, in problems where the response function is implicit (as in finite element analyses) these selective sampling techniques may not be easy to implement (Wu et al., 1987).

Monte Carlo simulation techniques are extremely powerful if the component response can be modelled as a simple explicit formulation and if the probability distributions of the uncertain or random parameters are well known. Good examples are in crack-propagation problems which can be represented by relatively straightforward fracture mechanics formulations (Sih, 1973). These simple formulations can then be implemented in Monte Carlo simulation programs (Sire et al., 1992; Tsai and Wu, 1993). Other examples are in the probabilistic simulation of deterministic, Code-prescribed calculations for components such as pressure vessels (Weber and Penny, 1991). Repeated solutions are then economically feasible and Monte Carlo simulation of such components can give valuable answers to engineers designing components that involve uncertainty in material behaviour, loading or environmental conditions and/or geometry.

The overall accuracy of the Monte Carlo method in predicting reliability depends on the accuracy with which the random parameters and failure criteria can be characterised. In

the initial design stages, it may be impossible to describe the random parameters and the failure criteria except by gross assumptions. It would then be inefficient to run a large number of Monte Carlo simulations in an attempt to estimate reliability. However if a simple model can be formed at this stage to represent the problem as an approximate function of the (expected) random parameters, it is possible (and economically feasible) to use the Monte Carlo simulation approach to perform parametric sensitivity studies by exercising a random simulation a limited number of times. This approach will indicate the important parameters efficiently and could form the basis of further, more detailed, reliability studies. An example of this approach is found in a study of the effect of spatial variations in yield strength and elastic and plastic hardening moduli on the size of the plastic zone at a nozzle/pressure vessel weld using a finite element analysis exercised a limited number of times (Penny, 1989).

When a component cannot be reduced to a simple model, finite element modelling is usually the only viable solution procedure. However, even with the recent advances in finite element methods and computer hardware, the speed of analysis is not yet such that engineers using standard equipment (workstations or personal computers) can afford to perform the thousands of production runs necessary for accurate Monte Carlo simulation procedures and for these types of problems less expensive methods for probability and reliability analysis need to be developed.

An alternative method for estimating the random response of a complex structure is the *point estimate method* (PEM) (Rosenblueth, 1975; Wong, 1985; Harr, 1987). The response function, which can be explicit or implicit (as, for instance, in a finite element analysis), is evaluated at a limited number of points. The points are obtained by perturbing the mean parameters by adding or subtracting one standard deviation. The probability moments of the response are estimated systematically from the point estimates.

The method can include the effects of correlation between the random parameters, although the procedures become complex (albeit systematic) if the number of random parameters is large, and it is simple to include correlation if the procedure is computerised. 2^n point estimates are required, corresponding to the possible permutations of positive and negative perturbations of n random parameters. If a finite element model is used, involving a large number of random variables and/or elements, the method can become excessively expensive in computer time. The method has been used by Harr (1987) in the analysis of beams with random yield strength, section modulus and applied moment. The method is discussed in more detail in Section 2.5.

A similar method is the *response surface method* (Wong, 1985; Faravelli, 1989). In this method, the unknown response function is approximated by a suitable explicit function, known as the response surface. When used together with a numerical model in the form

of a computer code, for instance a finite element program, the code is exercised a limited number of times to find a set of point estimates near the deterministic solution. The point estimates are used to fit an approximating function (not necessarily a linear function) to replace the unknown (implicit) response function. This approximating function or response surface is then used to estimate the probability moments, usually by implementing it in a Monte Carlo simulation program (Garribba, 1982).

The specific points can be the same as for the point estimate method (i.e. positive and negative perturbations of the mean by one standard deviation), in which case the two methods are identical, but other choices of estimation points can be used. If a nonlinear response surface is assumed, the estimation points have to be chosen carefully and this makes the method difficult to implement as a systematic procedure in a computer program. Nevertheless the method is very versatile and therefore very powerful. The method has been used by Faravelli (1989) in the reliability analysis of a pressure vessel with random yield strength and elastic and plastic hardening moduli, involving spatial as well as parameter correlation.

If numerical modelling is required through, for instance, a finite element analysis, the point estimate and response surface methods reduce the computational requirements compared with Monte Carlo methods, but a considerable number of (essentially deterministic) computer runs is still required to find the point estimates required.

Recently, a method known as the *stochastic* or *probabilistic finite element method* (SFEM or PFEM) has been described in the literature (Benaroya and Rehak, 1988). This method has had considerable success in assessing the reliability of complex structures and components within acceptable computing time limits when compared to, for example, Monte Carlo techniques (Lawrence, 1986). The objective of the method is to compute the response gradients with respect to the random variables. The probability moments of the response can be calculated from the response gradients. It is also possible to estimate the reliability of a component from the response gradients using fast probability integration methods, discussed in Section 2.7.

A number of different formulations has been proposed. In the most common of these the random load and stiffness matrices are expanded into a Taylor series, usually truncated at the second-order terms (Nakagiri et al., 1989). Standard finite element techniques are then used to calculate first- or second-order approximations for the random response and the expanded terms are implemented such that only the deterministic stiffness matrix needs to be inverted. Although the method was initially developed to solve random dynamic problems, the method has been successfully applied to static problems involving random or uncertain parameters. Alternative methods include iterative perturbation schemes (Dias et al., 1989). These methods are discussed in more detail in Section 2.6.

A more extensive account of the methods can be found in a review by Liu and Belytschko (1989). Stochastic finite element techniques or derivatives thereof have been used by various authors to solve a wide variety of problems: Liu et al. have considered elastic-plastic cantilever beams (1986, 1987), truss systems (1986) as well as plane strain problems (1988) under uncertain loads and stiffness. Besterfield et al. (1990, 1991) have considered cracked plate problems with uncertain material properties, crack geometry and loading. Lawrence (1986, 1987) has considered beam elements, plane stress elements and plate bending elements. Der Khiureghian and Ke (1985) and Der Khiureghian and De Stefano (1991) have considered the reliability of frame structures with random material parameters, geometry, under uncertain loads and with uncertain failure criteria. Handa and Andersson (1981) have considered frame structures with random loads, material parameters and geometry. Nakagiri et al. (1989) and Hisada and Nakagiri (1981, 1985) have considered frame structures with uncertain material and section properties and uncertain failure conditions as well as a fracture mechanics problem. Arnbjerg-Nielsen and Bjerager (1988) have considered space frame structures with uncertain material properties, loading and cross-sectional parameters. Arbabi et al. (1991) and Arbabi and Loh (1991) have considered railway tracks with uncertain loading and material parameters. Bulleit and Yates (1991) have analysed wood truss systems with random material parameters and loadings. Liaw and Yang (1989) have considered beams and columns with random material parameters and loading. Teigen et al. (1991b) have considered concrete structures with random loads and nonlinear material properties. Dias et al. (1989) apply an iterative perturbation scheme to a rotating cantilever beam with varying material properties, cross-sectional parameters and rotational speed. Hien and Kleiber (1989, 1990, 1991a, 1991b) have adapted the stochastic finite element technique to the design sensitivity analysis of beams and cylinders in static and dynamic problems with material parameters, section parameters and loads as design variables. The NESSUS software system was developed to assist in the structural analysis of components used in space propulsion systems where material properties, environmental conditions and geometrical parameters are random (Millwater et al., 1989). The program has been used in the analysis of beam vibration and shell buckling problems (Cruse et al., 1988a), in the linear static and vibration analysis of turbine blades (Cruse et al., 1988b; Rajagopal et al., 1989; Thacker et al., 1990), in the analysis of problems involving random stress-strain curves (Millwater et al., 1991) and the analysis of fracture mechanics problems (Thacker et al., 1991; Millwater et al., 1992). Recently other probabilistic methods, including conventional Monte Carlo simulation, Latin Hypercube sampling methods and system reliability assessment methods have been added to the NESSUS system (Millwater et al., 1992).

Although this is not a complete summary of all the available methods for probabilistic structural analysis of statically loaded components, the best-known methods and workers

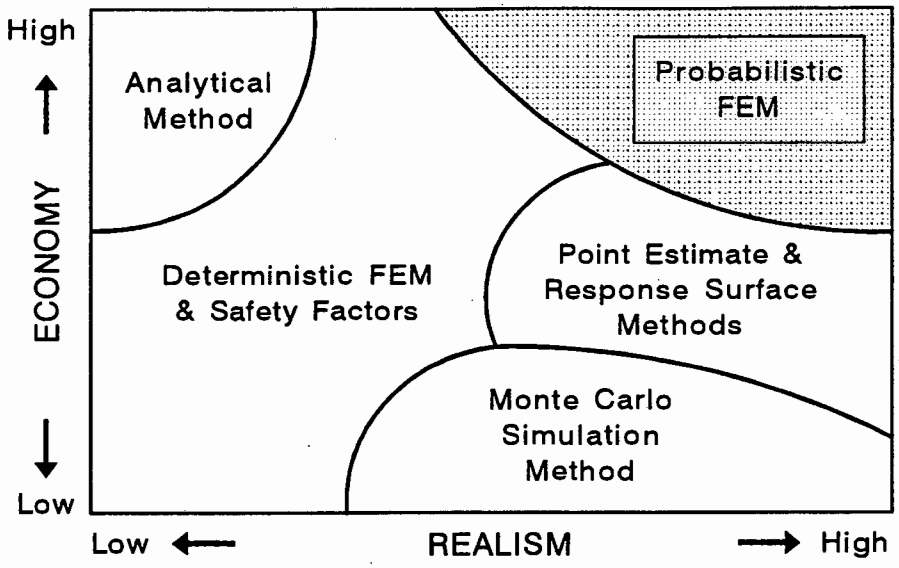

Figure 2.3: Schematic showing computational procedures for probabilistic methods

have been reviewed. The methods can be compared in terms of practical constraints on their utilisation as shown in the schematic diagram in Figure 2.3. Of these methods, the least realistic in terms of ability to include uncertainty and randomness in the solution of engineering problems are those to the left of the figure. The least economic in computational costs are at the bottom of the figure. As the methods approach the high right-hand corner of the diagram, so will the techniques become efficient as well as realistic in their ability to solve probabilistic problems. Analytical probabilistic techniques are high on economy but low on realism. Deterministic FEM combined with safety factors is limited in realism and spans the scope of economy depending on the efficiency of the model. Monte Carlo simulation techniques can be economical at the expense of realism but become costly if complex modelling is required. Probabilistic FEM and point estimate/response surface techniques allow complex modelling without sacrificing economy, with PFEM being the most economical of the three if the underlying modelling technique is FEM in all three cases.

2.4 Deterministic Finite Element Method

The objective of the finite element method is to describe the problem at hand by an appropriate model and to discretize this model into a number of *elements*, the behaviour under load of which can be described mathematically and analysed numerically using computers. An element stiffness matrix and load vector is calculated for each element. The stiffness matrix of a finite element can be evaluated from the volume integral (Zienkiewicz and Cheung, 1967):

$$\mathbf{K} = \int_{vol} \mathbf{R}^T \mathbf{B}^T \mathbf{D} \mathbf{B} \mathbf{R} \, dvol \tag{2.3}$$

where $\mathbf{R}$ is a rotation matrix, $\mathbf{B}$ is a strain-displacement matrix and $\mathbf{D}$ is a constitutive matrix. Numerical integration techniques are used to evaluate this integral. Similar techniques are used to evaluate the load vector. Chapter 3 describes how these techniques can be implemented in a finite element program. Appendix A describes the algorithms required for a three-dimensional beam element and a two-dimensional plane element.

The element stiffness matrices and load vectors are then assembled into a banded global stiffness matrix and load vector respectively, which can be illustrated as follows:

$$\mathbf{K} = \sum_{i=1}^{NELEM} \mathbf{K}_i = \begin{bmatrix} \mathbf{K}_1 & & & 0 \\ & \mathbf{K}_2 & & \\ & & \mathbf{K}_3 & \\ & sym & & \ddots \\ & & & \mathbf{K}_n \end{bmatrix} \quad \text{and} \quad \mathbf{f} = \sum_{i=1}^{NELEM} \mathbf{f}_i = \begin{Bmatrix} \mathbf{f}_1 \\ \mathbf{f}_2 \\ \mathbf{f}_3 \\ \vdots \\ \mathbf{f}_n \end{Bmatrix} \tag{2.4}$$

where the overlapping boxes indicate summation at joint element nodes. After assembly, the finite element model can be represented by a general finite element equation as:

$$\mathbf{K} \cdot \mathbf{u} = \mathbf{f} \tag{2.5}$$

where $\mathbf{K}$ is the stiffness matrix, $\mathbf{u}$ is the displacement vector and $\mathbf{f}$ is the load vector, and a solution for $\mathbf{u}$ is required. Strains, stresses and other solution variables can be calculated once the displacement vector is known. The problem is solved by calculating the inverse of $\mathbf{K}$ from which:

$$\mathbf{u} = \mathbf{K}^{-1} \cdot \mathbf{f} \tag{2.6}$$

Various algorithms can be used to calculate $\mathbf{K}^{-1}$, most prominent of which is the frontal solution algorithm (Hinton and Owen, 1977), although in principle any matrix inversion algorithm can be used. The frontal solution algorithm is preferred since in most problems it is robust as well as efficient, these criteria being the most important as the computing time spent in calculating the inverse of the stiffness matrix is usually a critical factor, especially if the problem involves many hundreds of elements. The frontal method can be considered as a particular technique for assembling element stiffness matrices and load vectors into a global stiffness matrix and load vector and solving for the unknown

displacements by means of a Gaussian elimination and backsubstitution process. The method was proposed by Irons (1970) and is used in many commercially available finite element programs. The main idea of the frontal solution technique is to *assemble the equations and eliminate the variables at the same time.* Therefore the complete stiffness matrix is never formed as such.

Equation (2.5) assumes that the load vector is applied in full. In problems where the load varies with time or when a solution is required at a fraction of the load (e.g. when an intermediate solution is required in a nonlinear problem), the problem is solved incrementally: the load is applied in increments and a solution is sought at the end of each increment as follows (Owen and Hinton, 1980):

$$\mathbf{u}^n = \mathbf{u}^{n-1} + \Delta\mathbf{u} \tag{2.7}$$

where $\mathbf{u}^n$ is the displacement vector at the end of the n^{th} increment and $\Delta\mathbf{u}$ is the incremental displacement calculated from:

$$\mathbf{K}\Delta\mathbf{u} = \Delta\mathbf{f} \tag{2.8}$$

where $\Delta\mathbf{f}$ is the load increment. Equations (2.5) and (2.8) are equivalent when the load is applied in full in one increment.

For a nonlinear problem involving, for instance, elastic-plastic material behaviour, an incremental solution procedure is unavoidable as convergence will be achieved only when small load increments are considered once the load level causes plastic strains. Convergence within a load increment will normally require an iterative procedure. The normal procedure for an elastic-plastic problem involving a Mises yield surface with an associative flow rule and linear hardening is to employ a Newton-Raphson elastic predictor-radial return method in deviatoric space. Two steps are involved: firstly the stresses for the current increment are calculated, assuming linear elastic behaviour, to give an elastic predictor. The stresses are then mapped onto a suitably updated yield surface to ensure that plastic flow consistency is maintained (Martin, 1975). Convergence is then checked by establishing whether equilibrium is reached between internal and external forces at the nodes. If convergence is not reached a further iteration is required. When predefined convergence criteria have been met, the increment is stopped and the solution is deemed to have converged. Some error will now exist between the "exact" solution and the numerical solution, which is dependent on the convergence criteria and the number of iterations that is economically feasible. The method is illustrated schematically in Figure 2.4, where the error between numerical and exact solution is exaggerated.

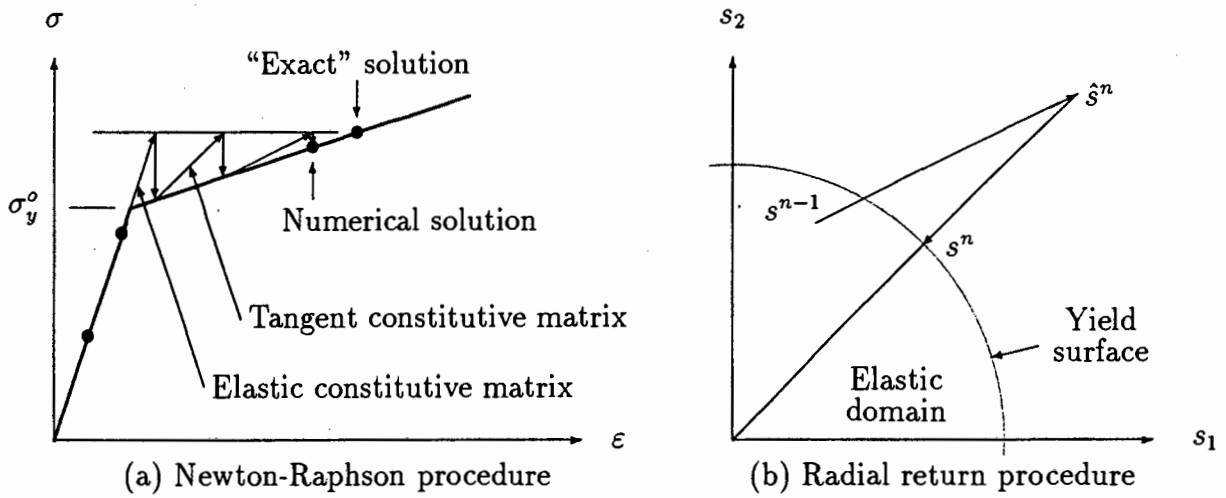

(a) Newton-Raphson procedure (b) Radial return procedure

Figure 2.4: Schematic of Newton-Raphson elastic predictor-radial return method

Simo and Taylor (1985) have shown that in elastic-plastic problems a quadratic rate of convergence of an incremental solution based on a Newton-Raphson iterative procedure can only be ensured if a *tangent constitutive matrix* and corresponding *tangent stiffness matrix* are derived in a manner consistent with the constitutive integration algorithm. This means that in a nonlinear analysis the stiffness matrix is adjusted at the end of an iteration for use in the next iteration. The first iteration in the procedure uses the elastic stiffness matrix. The procedure is illustrated in Figure 2.4. The tangent stiffness-radial return method has been found to be an accurate and robust procedure which generally performs better than other procedures such as secant stiffness methods (Krieg and Krieg, 1977). The derivation of the consistent tangent constitutive and stiffness matrices for a two-dimensional plane element is described in Appendix A.

It must be noted that it is possible to solve for elastic-perfectly plastic problems from the stationary state creep solution (Penny and Marriott, 1971). The number of increments required is usually larger than if the consistent tangent stiffness matrix is used, but the formulation is easier since the elastic stiffness matrix can be used. Even if elastic-plastic solution algorithms are available, the collapse load of a structure can often be calculated more efficiently from a reference stress-stationary state creep solution.

The overall finite element procedures for deterministic elastic-plastic problems are illustrated in Figure 2.5 which shows how first the element stiffness matrices and load vectors are formed for each element. The global stiffness matrix and load vector are then assembled and a solution for the global displacements is found. The elastic predictor strains and stresses are then calculated for each element from the displacements. If yield has occurred at any (integration) point within an element, the consistent tangent stiffness matrix is computed and the stresses and plastic strains at the end of the increment are calculated

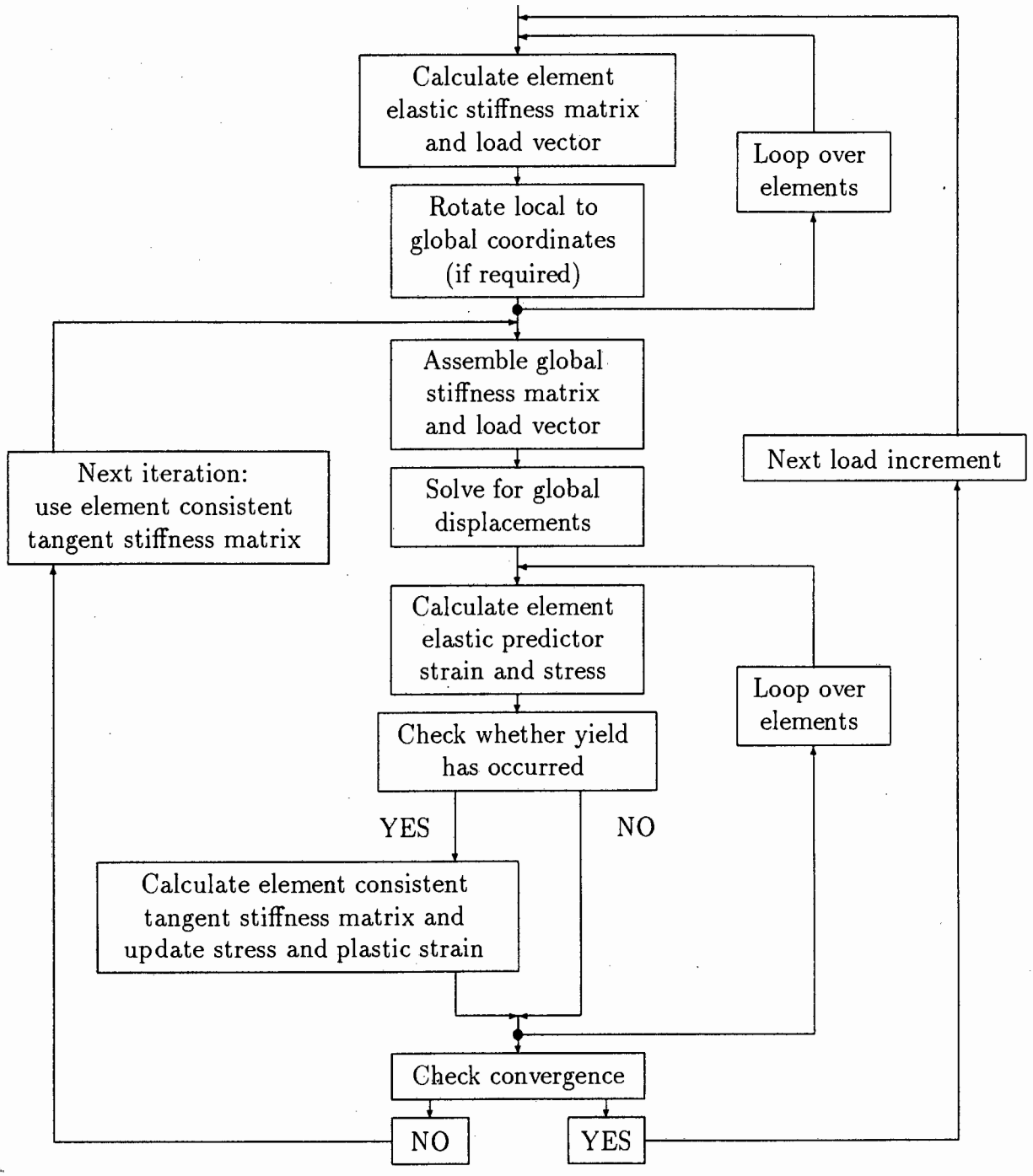

Figure 2.5: Schematic of elastic-plastic finite element procedure

using the radial return method. The residual vector is calculated and convergence of the increment is then checked. If the increment has not converged, another iteration is required, using the consistent tangent stiffness matrix for those elements in which yield has occurred (i.e. it is not necessary to recompute the load vector or the elastic stiffness matrix for non-yielded elements if that information is still available). If the increment has converged, the next load increment can commence.

2.5 Point Estimate Method

If a response function, which can be implicit (e.g. through a finite element analysis) or explicit, is represented by $Z = Z(\mathbf{x})$ where $\mathbf{x}$ is a set of n random variables $(x_1, x_2, \ldots, x_n)$, the point estimate method procedure consists of assembling a set of *point estimates* of Z through the repeated (essentially deterministic) evaluation of Z with parameters corresponding to all the possible permutations of positive and negative perturbations of the mean random variables by one standard deviation (Rosenblueth, 1975; Harr, 1987). The method will be illustrated by considering first the problem of a single random parameter and then extending this to multiple random parameters.

For a random function involving a single random parameter, $Z = Z(x)$, two point estimates are required:

$$\begin{aligned} Z_+ &= Z(\bar{x} + \sigma[x]) \\ Z_- &= Z(\bar{x} - \sigma[x]) \end{aligned} \tag{2.9}$$

From these two point estimates the probability moments are calculated as follows:

$$\begin{aligned} \mathrm{E}[Z] &= b_+ Z_+ + b_- Z_- \\ \mathrm{E}[Z^2] &= b_+ Z_+^2 + b_- Z_-^2, \quad \text{and in general the } M^{th} \text{ moment is:} \\ \mathrm{E}[Z^M] &= b_+ Z_+^M + b_- Z_-^M \end{aligned} \tag{2.10}$$

where M cannot be greater than the known moments of x and b_+ and b_- are weighting factors, equal to $\frac{1}{2}$. The mean and variance of the response are then calculated from:

$$\bar{Z} = \mathrm{E}[Z] \tag{2.11}$$

and

$$\sigma_Z^2 = \mathrm{E}[Z^2] - (\mathrm{E}[Z])^2 \tag{2.12}$$

The method can be extended to multiple random parameters with correlation between the parameters. In a problem involving n random parameters, 2^n point estimates are required, corresponding to the possible permutations of positive and negative perturbations:

$$Z_{\pm\pm\cdots\pm} = Z(\bar{x}_1 \pm \sigma[x_1], \bar{x}_2 \pm \sigma[x_2], \ldots, \bar{x}_n \pm \sigma[x_n]) \tag{2.13}$$

from which the probability moments can be evaluated using:

$$\mathrm{E}[Z^M] = b_{++\cdots+} Z^M_{++\cdots+} + b_{++\cdots-} Z^M_{++\cdots-} + \ldots + b_{--\cdots-} Z^M_{--\cdots-} \tag{2.14}$$

where the weighting functions are evaluated from:

$$b_{\pm\pm\cdots\pm} = \frac{1}{2^n}(1 + s_{12}\rho_{12} + s_{13}\rho_{13} + \ldots + s_{n-1,n}\rho_{n-1,n}) \tag{2.15}$$

where ρ_{ij} is the correlation coefficient between the random parameters x_i and x_j and the sign s_{ij} is obtained by multiplying the appropriate signs for the i^{th} and j^{th} parameters for the point estimate under consideration. As an example, consider a problem involving three random parameters and eight possible permutations:

$$\begin{aligned}
b_{+++} &= b_{---} = \frac{1}{2^3}(1 + \rho_{12} + \rho_{13} + \rho_{23}) \\
b_{++-} &= b_{--+} = \frac{1}{2^3}(1 + \rho_{12} - \rho_{13} - \rho_{23}) \\
b_{+-+} &= b_{+-+} = \frac{1}{2^3}(1 - \rho_{12} + \rho_{13} - \rho_{23}) \\
b_{+--} &= b_{-++} = \frac{1}{2^3}(1 - \rho_{12} - \rho_{13} + \rho_{23})
\end{aligned}$$

If the random parameters are all mutually independent, evaluation of the weighting factors becomes trivial, since all the ρ terms are zero and $b_{\pm\pm\cdots\pm} = 2^{-n}$.

To implement the point estimate method in a finite element scheme, the following general format of the finite element equations can be used:

$$\breve{\mathbf{K}}_{\pm}\breve{\mathbf{u}}_{\pm} = \breve{\mathbf{f}}_{\pm} \tag{2.16}$$

where the $\breve{}$ indicates a perturbed term and the subscript $\pm$ indicates the point estimate method type of perturbation. The point estimate required is a solution for $\breve{\mathbf{u}}_{\pm}$ (or its derivative such as stress or strain). The perturbed stiffness matrix and load vector are:

$$\begin{aligned}
\breve{\mathbf{K}}_{\pm} &= \mathbf{K}(\bar{r}_i \pm \sigma[r_i]) = \mathbf{K}_0 + \Delta\mathbf{K} \\
\breve{\mathbf{f}}_{\pm} &= \mathbf{f}(\bar{r}_i \pm \sigma[r_i]) = \mathbf{f}_0 + \Delta\mathbf{f}
\end{aligned} \tag{2.17}$$

where $\mathbf{K}_0$ and $\mathbf{f}_0$ are the deterministic stiffness matrix and load vector respectively. The format $\mathbf{K}(\bar{r}_i \pm \sigma[r_i])$ indicates the procedure to evaluate the stiffness matrix (i.e. evaluate as usual but use appropriate combinations of positively and negatively perturbed random parameters instead of the deterministic values). The perturbed stiffness matrix will in general change from point estimate to point estimate and each new stiffness matrix will have to be inverted in order to calculate a solution. This makes the point estimate method excessively computer intensive if the number of elements or number of random variables or both is large.

2.6 Stochastic Finite Element Method

2.6.1 Preamble

The stochastic finite element method is governed, for static structural problems, by general equations of the form (Nakagiri, 1987) :

$$\mathbf{K}(r) \cdot \mathbf{u}(r) = \mathbf{f}(r) \tag{2.18}$$

where the stiffness matrix $\mathbf{K}$, the load vector $\mathbf{f}$, and the deformation vector $\mathbf{u}$ are all dependent on the random parameters r (denoted by r_i; $i = 1, \ldots, n$). The random functions can be approximated as the sum of deterministic and random components (Benaroya and Rehak, 1988). In the simplest formulation of the problem, the stiffness matrix and load vector are expressed by a deterministic part $\mathbf{K}_0$ and $\mathbf{f}_0$ and a zero mean random part $\mathbf{K}_r$ and $\mathbf{f}_r$ as:

$$\begin{aligned} \mathbf{K}(r) &= \mathbf{K}_0 + \mathbf{K}_r \\ \mathbf{f}(r) &= \mathbf{f}_0 + \mathbf{f}_r \end{aligned} \tag{2.19}$$

In the probabilistic (and reliability) analysis of problems, the expectation of the response and an estimate of the sensitivity of the response to the random variables is required. The response can be displacement, stress level or any other characteristic quantity. Methods are now required which allow systematic inclusion of the random parts with the objective of calculating the probabilistic response of the structure.

2.6.2 Taylor series perturbation scheme

One such method is to expand the random functions by a Taylor series truncated at the second order from which the expressions for $\mathbf{u}, \mathbf{K}$ and $\mathbf{f}$ then become:

$$\mathbf{u}(r) = \mathbf{u}_0 + \sum_{i=1}^{n} \frac{\partial \mathbf{u}}{\partial r_i} \, \mathrm{d}r_i + \frac{1}{2} \sum_{i,j=1}^{n} \frac{\partial^2 \mathbf{u}}{\partial r_i \partial r_j} \, \mathrm{d}r_i \, \mathrm{d}r_j = \mathbf{u}_0 + \mathbf{u}_1 + \mathbf{u}_2 \tag{2.20}$$

$$\mathbf{K}(r) = \mathbf{K}_0 + \sum_{i=1}^{n} \frac{\partial \mathbf{K}}{\partial r_i} \, \mathrm{d}r_i + \frac{1}{2} \sum_{i,j=1}^{n} \frac{\partial^2 \mathbf{K}}{\partial r_i \partial r_j} \, \mathrm{d}r_i \, \mathrm{d}r_j = \mathbf{K}_0 + \mathbf{K}_1 + \mathbf{K}_2 \tag{2.21}$$

and

$$\mathbf{f}(r) = \mathbf{f}_0 + \sum_{i=1}^{n} \frac{\partial \mathbf{f}}{\partial r_i} \, \mathrm{d}r_i + \frac{1}{2} \sum_{i,j=1}^{n} \frac{\partial^2 \mathbf{f}}{\partial r_i \partial r_j} \, \mathrm{d}r_i \, \mathrm{d}r_j = \mathbf{f}_0 + \mathbf{f}_1 + \mathbf{f}_2 \tag{2.22}$$

The partial derivatives of the stiffness matrix and load vector terms are calculated directly or can be estimated by the effects of small perturbations about the mean values. The procedures involved are discussed in Section 2.6.4.

Substituting equations (2.20) - (2.22) into equation (2.18), equating terms of like order (Benaroya and Rehak, 1988) and neglecting the higher order cross-multiplication terms, three sets of equations are obtained from which $\mathbf{u}_0$, $\mathbf{u}_1$ and $\mathbf{u}_2$ can be solved:

$$\mathbf{K}_0\mathbf{u}_0 = \mathbf{f}_0 \tag{2.23}$$

$$\mathbf{K}_0\mathbf{u}_1 = \mathbf{f}_1 - \mathbf{K}_1\mathbf{u}_0 \tag{2.24}$$

and

$$\mathbf{K}_0\mathbf{u}_2 = \mathbf{f}_2 - \mathbf{K}_1\mathbf{u}_1 - \mathbf{K}_2\mathbf{u}_0 \tag{2.25}$$

and $\mathbf{K}_0, \mathbf{u}_0$ and $\mathbf{f}_0$ are evaluated at the mean of the random parameters. Equation (2.24) represents a system of n equations corresponding to the number of random variables and needs to be solved n times by considering the random parameters independently. Finally, these equations are used to obtain the response, $\mathbf{u}$ in terms of equation (2.20). The important feature here is that the inverse of the stiffness matrix $\mathbf{K}_0$ needed to solve equations (2.23), (2.24) and (2.25) needs to be evaluated only once during the solution procedure; $\mathbf{K}_0$ is the deterministic value of the stiffness matrix and, in linear elastic problems, depends only on the structural geometry and the elastic constitutive matrix. The perturbed parts of the stiffness and load matrices are implemented as *pseudo-elastic* components on the right-hand side of the finite element equation (Benaroya and Rehak, 1988) and equations (2.24) and (2.25) are linear. Thus the main advantage of the method is that it can follow all the techniques and algorithms of deterministic analyses. This is with the proviso that variations of uncertainties must be small in order that acceptable accuracy is obtained when the higher order cross-multiplication terms are neglected. It is then possible in principle to implement the stochastic finite element techniques in existing deterministic finite element programs.

Assuming that the covariance matrix $\sigma^2[r_i, r_j]$ is known, it is now possible to estimate the mean and covariance values of the response $\mathbf{u}$ (Liu et al., 1987):

$$\bar{\mathbf{u}} = \mathrm{E}[\mathbf{u}] = \int_{-\infty}^{\infty} \mathbf{u}(r) f(r)\, \mathrm{d}r = \mathbf{u}_0 + \frac{1}{2}\left\{ \sum_{i,j=1}^{n} \frac{\partial \mathbf{u}}{\partial r_i \partial r_j} \sigma^2[r_i, r_j] \right\} \tag{2.26}$$

and

$$\begin{aligned}\sigma^2[\mathbf{u}^i, \mathbf{u}^j] &= \int_{-\infty}^{\infty} (\mathbf{u}^i - \bar{\mathbf{u}}^i)(\mathbf{u}^j - \bar{\mathbf{u}}^j)\, f(r)\, \mathrm{d}r \\ &= \sum_{k,l=1}^{n} \frac{\partial \mathbf{u}^i}{\partial r_k} \frac{\partial \mathbf{u}^j}{\partial r_l} \sigma^2[r_k, r_l]\end{aligned} \tag{2.27}$$

When the random parameters are uncorrelated, equation (2.27) reduces to (Wong, 1985):

$$\sigma^2[\mathbf{u}] = \sum_{k=1}^{n} \left(\frac{\partial \mathbf{u}}{\partial r_k}\right)^2 \sigma^2[r_k] \tag{2.28}$$

Estimates of stress and strain values can be similarly made. It must be noted however that even though the deterministic stiffness matrix needs to be solved only once, nevertheless significant matrix manipulation is required to calculate the necessary quantities in the second moment representation of displacements, strains and stresses (Pearce, 1983).

The above derivation of the probabilistic finite element method is known as the *mean value second order method* or MVSO. The method can be simplified to a *mean value first order method* or MVFO by disregarding the second order terms. It has been noted by a number of workers (Yamazaki et al., 1988; Liu and Der Khiureghian, 1991; Teigen et al., 1991a) that in many engineering problems first order methods can give results comparable to second order methods without the additional complexities of second order terms. This is because the second order terms have an effect only on the mean response which can be seen from equation (2.26). Yamazaki et al. (1988) found that the second-order method results in an increase in computing cost not warranted by the marginal increase in accuracy when compared to first-order methods.

2.6.3 Iterative perturbation scheme

Dias et al. (1989) have presented a variation on the MVFO probabilistic finite element formulation discussed above. Here a first order approximation of the stiffness matrix and load vector are used, and the higher order cross-multiplication terms of the response are recovered by means of an iterative perturbation process. The method is also known as the Neumann series expansion method (Benaroya and Rehak, 1988). The solution algorithm is provided by the iterative expression:

$$\mathbf{K}_0\, \mathrm{d}\breve{\mathbf{u}}^n = \breve{\mathbf{f}} - \breve{\mathbf{K}}\breve{\mathbf{u}}^{n-1} \tag{2.29}$$

$$\breve{\mathbf{u}}^n = \breve{\mathbf{u}}^{n-1} + \mathrm{d}\breve{\mathbf{u}}^n \tag{2.30}$$

where $\breve{\mathbf{u}}^o = \mathbf{u}_0$ is used to start the iteration, $\mathbf{K}_0$ is the deterministic stiffness matrix, $\breve{\mathbf{K}}$ and $\breve{\mathbf{f}}$ are the perturbed stiffness matrix and load vector, and $\breve{\mathbf{u}}$ is the perturbed displacement. Equation (2.29) represents a system of n equations corresponding to the number of random variables and needs to be solved for the independent perturbations of the random parameters. The perturbation is achieved by calculating the stiffness matrix and load vector as in the deterministic manner but using for the random variable under consideration its mean plus a small fraction of the mean (usually one standard deviation), and keeping all the other variables at their mean value. The component $\breve{\mathbf{K}}\breve{\mathbf{u}}^{n-1}$ can then be considered as a *pseudo-inelastic* portion added to the right-hand side of the equation (2.29) which (in general) is nonlinear and has to be solved iteratively. The method has the advantage over methods involving Taylor series expansion techniques in that complex chain rule derivatives do not need to be evaluated, either numerically or explicitly (Dias et al., 1989). As such the method is easier to implement in finite element programs and can be used with more complex finite element formulations.

Dias and Nakazawa (1988) liken the method to a modified Newton-Raphson technique in which the deterministic stiffness matrix $\mathbf{K}$ is factorised only once and is used to precondition the iteration for all subsequent perturbed iterations. As modified Newton-Raphson techniques can suffer from poor convergence rates, Dias et al. (1989) propose a quasi-Newton iteration scheme which improves the convergence characteristics by replacing the stiffness matrix $\mathbf{K}$ in equation (2.29) by a different preconditioner $\breve{\mathbf{K}}^{n-1}$ and adding a relaxation term s^{n-1} (with $0 < s^{n-1} \leq 1$). Equations (2.29) and (2.30) then become:

$$\breve{\mathbf{K}}^{n-1}\, \mathrm{d}\breve{\mathbf{u}}^n = \breve{\mathbf{f}} - \breve{\mathbf{K}}\breve{\mathbf{u}}^{n-1} \tag{2.31}$$

$$\breve{\mathbf{u}}^n = \breve{\mathbf{u}}^{n-1} + s^{n-1}\, \mathrm{d}\breve{\mathbf{u}}^n \tag{2.32}$$

2.6.4 Discussion

Compared with the point estimate method, mean value methods using either the Taylor series perturbation scheme or the iterative perturbation scheme offer the advantage that the deterministic stiffness matrix needs to be inverted only once, whereas for the point estimate approach the perturbed stiffness matrix needs to be inverted for each calculation. The number of evaluations required is also smaller. In problems involving a large number of elements or a large number of random variables this means significant savings in computational effort which would offset increased computational complexity.

The computational difficulty in the Taylor series perturbation scheme lies in evaluating the derivatives of the stiffness matrix with respect to the random parameters. The stiffness

matrix is defined by a volume integral as follows:

$$\mathbf{K} = \int_{vol} \mathbf{R}^T \mathbf{B}^T \mathbf{D} \mathbf{B} \mathbf{R} \, dvol \tag{2.33}$$

Evaluating the first and second derivatives of the stiffness matrix with respect to the random parameters involves evaluating complex chain rule derivatives:

$$\frac{\partial \mathbf{K}}{\partial r_i} = \int_{vol} \mathbf{R}^T \left[\frac{\partial \mathbf{B}^T}{\partial r_i} \mathbf{D} \mathbf{B} + \mathbf{B}^T \frac{\partial \mathbf{D}}{\partial r_i} \mathbf{B} + \mathbf{B}^T \mathbf{D} \frac{\partial \mathbf{B}}{\partial r_i} \right] \mathbf{R} \, dvol \tag{2.34}$$

and, similarly

$$\begin{aligned} \frac{\partial^2 \mathbf{K}}{\partial r_i \partial r_j} = \frac{\partial}{\partial r_j} \frac{\partial \mathbf{K}}{\partial r_i} = \int_{vol} \mathbf{R}^T \Bigg[& \frac{\partial^2 \mathbf{B}^T}{\partial r_i \partial r_j} \mathbf{D} \mathbf{B} + \frac{\partial \mathbf{B}^T}{\partial r_i} \frac{\partial \mathbf{D}}{\partial r_j} \mathbf{B} + \dots \\ & \dots + \mathbf{B}^T \frac{\partial \mathbf{D}}{\partial r_j} \frac{\partial \mathbf{B}}{\partial r_i} + \mathbf{B}^T \mathbf{D} \frac{\partial^2 \mathbf{B}}{\partial r_i \partial r_j} \Bigg] \mathbf{R} \, dvol \end{aligned} \tag{2.35}$$

If the problem is a frame or shell structure where nodal positions are random, the chain rule derivatives need to include also the rotation matrix $\mathbf{R}$. While evaluation of these chain rule derivatives is in principle possible, programming these in a general yet systematic way is difficult.

Two simplifications can be considered: firstly it can be specified that the combination of random nodal positions and random material parameters is not allowed. This is often not an unreasonable specification, since in many problems some geometric parameters can be lumped with material parameters through geometric section parameters (e.g. cross-sectional dimensions of a beam, thickness of a plate or shell), and it is often the section parameters which are random or uncertain. A second simplification is to disregard the second order effects. As discussed previously, first order methods can give comparable results to second order methods and can make significant improvements in computational efficiency.

In this thesis random geometry in the sense nodal position was not considered, although some geometric section parameters were included in the set of random parameters. Second order effects were not included in the probabilistic finite element analysis. The problem is then essentially reduced to finding the first derivatives of the constitutive matrix and load vector with respect to the random parameters. The load vector derivative will in most cases be zero, except when the load itself is the random parameter (and then the stiffness matrix derivative will be zero). Each such derivative needs to be evaluated independently and implemented in the probabilistic finite element program.

Rather than implementing the partial derivatives explicitly, it is more convenient to obtain the first order term through a small perturbation about the mean value. For a random parameter r_j the first order stiffness term required in equation (2.24) is:

$$\mathbf{K}_{1_j} = \frac{\partial \mathbf{K}}{\partial r_j} \mathrm{d}r_j \tag{2.36}$$

which, providing small perturbations are used, can be approximated by:

$$\mathbf{K}_{1_j} \simeq \frac{\Delta \mathbf{K}}{\Delta r_j} \Delta r_j = \Delta \mathbf{K}_j \tag{2.37}$$

It should be noted that the above finite difference based method is approximate and other approaches have been used to implement the Taylor series expansion, the most common of which is the adjoint variable approach which originates in structural sensitivity analysis. A detailed discussion is found in Hien and Kleiber (1989). These methods can be more efficient under certain conditions but are more difficult to implement (Tortorelli, 1991).

The $\Delta \mathbf{K}$ term is sometimes denoted by $\epsilon \mathbf{K}$ in the literature and is usually obtained by calculating the deterministic stiffness matrix using one standard deviation of the random parameter under consideration instead of the mean value, keeping the other parameters at the mean value. For a random parameter r_j equations (2.20) - (2.22) then become:

$$\begin{array}{lllll} \mathbf{u}(r_j) & = \mathbf{u}_0 + \Delta \mathbf{u}_j & = \mathbf{u}_0 + \mathbf{u}_{1_j} & & \\ \mathbf{K}(r_j) & = \mathbf{K}_0 + \Delta \mathbf{K}_j & = \mathbf{K}_0 + \mathbf{K}(\bar{r}_{i \neq j}; \delta[r_j]) & = \mathbf{K}_0 + \mathbf{K}_{1_j} & \\ \mathbf{f}(r_j) & = \mathbf{f}_0 + \Delta \mathbf{f}_j & = \mathbf{f}_0 + \mathbf{f}(\bar{r}_{i \neq j}; \delta[r_j]) & = \mathbf{f}_0 + \mathbf{f}_{1_j} & \end{array} \tag{2.38}$$

where $\mathbf{K}(\bar{r}_{i \neq j}; \delta[r_j])$ represents the procedure to evaluate the $\Delta \mathbf{K}_j$ term corresponding to random parameter r_j and the perturbation amount $\delta[\cdot]$ represents a small fraction of the mean of the random parameter, usually one standard deviation. From this equations (2.23) and (2.24) then become:

$$\mathbf{K}_0 \mathbf{u}_0 = \mathbf{f}_0 \tag{2.39}$$

and

$$\mathbf{K}_0 \Delta \mathbf{u} = \Delta \mathbf{f} - \Delta \mathbf{K} \mathbf{u}_0 \tag{2.40}$$

Obtaining the perturbations of the stiffness matrix and load vector is conceptually much simpler than evaluating the derivatives directly, and is easier to program in a systematic way. Any inaccuracy will in general be small when the perturbation amount is small.

If the probabilistic FEM is geared to a fast probability integration scheme, the gradient of the response with respect to the individual random variables is required to be evaluated. Equation (2.40) is "solved" for each of the independent random parameters. In linear problems only matrix manipulations are involved if the inverse of $\mathbf{K}_0$ can be stored from the solution of equation (2.39). It must be noted that in this procedure either the $\Delta\mathbf{f}$ or the $\Delta\mathbf{K}$ term will be zero, depending on whether the random variable is a load or stiffness parameter.

When equations (2.39) and (2.40) are added, the following expression is obtained:

$$(\mathbf{K}_0 + \Delta\mathbf{K})(\mathbf{u}_0 + \Delta\mathbf{u}) - \Delta\mathbf{K}\Delta\mathbf{u} = \mathbf{f}_0 + \Delta\mathbf{f} \tag{2.41}$$

or

$$\check{\mathbf{K}}\check{\mathbf{u}} - \Delta\mathbf{K}\Delta\mathbf{u} = \check{\mathbf{f}} \tag{2.42}$$

indicating that the higher order cross-multiplication terms are neglected in the solution of the full perturbation problem. Comparing with equation (2.16) it can be noted that equations (2.39) and (2.40) can be used as an approximation to the point estimate method if the $\Delta\mathbf{f}$ and $\Delta\mathbf{K}$ are achieved through the combined perturbation of the random variables. The $\Delta\mathbf{f}$ and $\Delta\mathbf{K}$ terms will then usually both be non-zero. Upon solution of equation (2.40) for $\Delta\mathbf{u}$ an approximate point estimate $\check{\mathbf{u}}_\pm$ is obtained by adding $\mathbf{u}_0$ and $\Delta\mathbf{u}$. The $\Delta\mathbf{f}_\pm$ and $\Delta\mathbf{K}_\pm$ terms must be evaluated from the difference between the perturbed and the deterministic load vector and stiffness matrix, not as in equation (2.38), otherwise first order cross-multiplication terms are neglected, and:

$$\begin{aligned} \Delta\mathbf{K}_\pm &= \check{\mathbf{K}}_\pm - \mathbf{K}_0 = \mathbf{K}(\bar{r}_i \pm \sigma[r_i]) - \mathbf{K}_0 \\ \Delta\mathbf{f}_\pm &= \check{\mathbf{f}}_\pm - \mathbf{f}_0 = \mathbf{f}(\bar{r}_i \pm \sigma[r_i]) - \mathbf{f}_0 \end{aligned} \tag{2.43}$$

and $\sigma[\cdot]$ represents the standard deviation of the random parameter. The method approximates the conventional point estimate method because the higher order cross-multiplication terms are neglected, as shown in equation (2.42). In many problems this approximation can be justified by the increased numerical efficiency of a single inversion of the deterministic stiffness matrix.

A similar approach to the Taylor series perturbation scheme is used in the iterative perturbation scheme: the perturbed stiffness matrix and load vector are obtained by adding a small fraction of the mean, usually one standard deviation, to the random parameter under consideration, keeping the other parameters at their mean levels, and evaluating the stiffness matrix and load vector as in the deterministic procedure. The perturbed

stiffness matrix for a random parameter r_j is denoted $\breve{\mathbf{K}}_j$, the perturbed load vector is denoted $\breve{\mathbf{f}}_j$ and are defined as:

$$\begin{aligned} \breve{\mathbf{K}}_j &= \mathbf{K}(\bar{r}_{i\neq j}; \bar{r}_j + \delta[r_j]) = \mathbf{K}_0 + \Delta\mathbf{K}_j \\ \breve{\mathbf{f}}_j &= \mathbf{f}(\bar{r}_{i\neq j}; \bar{r}_j + \delta[r_j]) = \mathbf{f}_0 + \Delta\mathbf{f}_j \end{aligned} \tag{2.44}$$

where the $\mathbf{K}(\bar{r}_{i\neq j}; \bar{r}_j + \delta[r_j])$ represents the procedure to evaluate $\breve{\mathbf{K}}_j$.

The solution procedure for the iterative perturbation scheme is as follows. First the deterministic system is solved for the deterministic displacement $\mathbf{u}_0$ (from which other solution quantities can be derived). The stiffness matrix and load vector are then perturbed as described above and the perturbed system is solved iteratively for the perturbed displacement $\breve{\mathbf{u}}$ (from which other perturbed solution quantities can be derived). The solution procedure is repeated below:

$$\begin{aligned} \mathbf{K}_0\, \mathrm{d}\breve{\mathbf{u}}^n &= \breve{\mathbf{f}} - \breve{\mathbf{K}}\breve{\mathbf{u}}^{n-1} \\ \breve{\mathbf{u}}^n &= \breve{\mathbf{u}}^{n-1} + \mathrm{d}\breve{\mathbf{u}}^n \end{aligned} \tag{2.45}$$

where $\breve{\mathbf{u}}^o = \mathbf{u}_0$ is used to start the iteration. Depending on which random variable is being perturbed, either the $\breve{\mathbf{f}}$ term or $\breve{\mathbf{K}}$ term reverts to the deterministic one. If the inverse of the deterministic stiffness matrix is still available, the procedure requires iterative matrix manipulation until the $\mathrm{d}\breve{\mathbf{u}}^n$ term becomes negligible. Some rearranging of equation (2.45) indicates that this is equivalent to solving:

$$(\mathbf{K} + \Delta\mathbf{K})(\mathbf{u} + \Delta\mathbf{u}) = \mathbf{f} + \Delta\mathbf{f} \tag{2.46}$$

or

$$\breve{\mathbf{K}}\breve{\mathbf{u}} = \breve{\mathbf{f}} \tag{2.47}$$

This means that the iterative perturbation scheme is equivalent to solving the full perturbation problem without neglecting the higher order cross-multiplication terms which were dropped in the Taylor series scheme. Comparing with equation (2.16) it can be noted that the procedures in equation (2.45) are the same as for the point estimate method if the $\breve{\mathbf{K}}$ and $\breve{\mathbf{f}}$ term are achieved by a combination of the perturbation of all the random variables rather than of one individual random variable (i.e. not as in equation (2.44). The required $\breve{\mathbf{K}}_\pm$ and $\breve{\mathbf{f}}_\pm$ terms are:

$$\begin{aligned} \breve{\mathbf{K}}_\pm &= \mathbf{K}(\bar{r}_i \pm \sigma[r_i]) = \mathbf{K}_0 + \Delta\mathbf{K} \\ \breve{\mathbf{f}}_\pm &= \mathbf{f}(\bar{r}_i \pm \sigma[r_i]) = \mathbf{f}_0 + \Delta\mathbf{f} \end{aligned} \tag{2.48}$$

The iterative perturbation scheme can thus provide a full solution procedure for the point estimate method in a way which incorporates the advantages of the probabilistic finite element method (i.e. inversion of only the deterministic stiffness matrix is required), thereby reducing the numerical effort required in the point estimate method.

For problems involving material nonlinearity, the derivations based on Taylor series expansions are limited by the fact that they cannot cope with the differentiation of discontinuous random variables such as initial yield strength and yield surface (Nakagiri, 1987; Hisada and Noguchi, 1989). Taylor series expansions approximated by small perturbations and iterative perturbation schemes do not suffer from the same problem since explicit differentiation of the perturbed variables is not required.

These perturbation schemes cannot cope with the load path dependent characteristics of most nonlinear materials. The nonlinear material models require incremental analyses. If the deterministic results for a particular increment are now used to calculate the perturbed response, firstly, the information from a previously perturbed increment is lost (i.e. one perturbs the current deterministic response) (Harren, 1989) and, secondly, the level of permanent displacement calculated for the deterministic response, $\mathbf{u}_0$, cannot be reduced during the perturbation increment (i.e. it is not possible to derive numerically a negative plastic strain perturbation) and physical meaning would be lost if the parameters involved in calculating the constitutive matrix are perturbed (Cruse et al., 1990).

The iterative perturbation scheme and the Taylor series scheme will give incorrect results if the problem involves random parameters which are used to calculate the nonlinear stiffness matrix. The methods can in principle deal with perturbations in the load if the perturbation is positive, but not if the perturbation is negative. In any case, for problems involving significant plasticity, the above methods are numerically unstable and do not converge easily since the consistent tangent stiffness matrix derived in the deterministic problem is not the correct tangent matrix to solve the perturbed problem, and even small deviations from the consistent tangent stiffness matrix exert considerable influence on the convergence characteristics of the problem (Simo and Taylor, 1985).

Hisada and Noguchi (1989) have proposed an iterative perturbation scheme which apparently can cope with load path dependence if the load is the random parameter. It is not clear how the method deals with random material parameters. However, since the method is equivalent to a modified Newton-Raphson technique, the method can suffer from a tendency to diverge if the unbalanced force (the right-hand side of equation (2.29)) increases during an iteration (Ryu et al., 1985).

In problems involving elastic-plastic behaviour and random parameters other than loading, the correct approach in the continuum mechanics sense is to repeat the analysis

completely. It is often also more convenient to re-analyse since the time taken to fine-tune the problem in order to achieve convergence can be considerable, even if the load is perturbed. The advantage of re-using the deterministic stiffness matrix is then lost.

The perturbation schemes described above can now be distinguished into two main categories: schemes which require complete re-analysis of the perturbed problem (i.e. where the stiffness matrix in the deterministic problem would change throughout the deterministic analysis; e.g. elastic-plastic problems, or where information from previous converged increments is required) and schemes where the inverse of the deterministic stiffness matrix can be used to solve the perturbed problem (i.e. linear problems).

The first category follows the same computational procedures as deterministic problems, and the re-analysis procedure is required to be implemented in the finite element code. The second category can be further subdivided into Taylor series perturbation schemes and iterative perturbation schemes. The Taylor series scheme results in a linear problem requiring a single iteration to reach convergence. This is possible because the method neglects the higher-order cross-multiplication terms. Consequently the full perturbation problem is not recovered. When the perturbations are small the effect can be considered negligible, while the computational savings are high. The iterative perturbation scheme normally requires a number of iterations to converge (perturbation of the load results in a single iteration). The full perturbation problem is recovered since the higher-order cross-multiplication terms are included.

Although the second category of methods was developed for mean value first order methods involving the individual perturbation of the random parameters it has been shown that the concept of re-using the inverse of the deterministic stiffness matrix can be applied to the point estimate method involving the combined perturbation of the random parameters. The Taylor series perturbation scheme remains linear in this case, still requiring only one iteration to converge.

Both probabilistic methods (i.e. PEM and MVFO) and the different perturbation schemes (i.e. full, Taylor series and iterative perturbation) all result in finite element expressions which are similar in format to the deterministic expression. Both probabilistic methods require a systematic sequence of perturbed evaluations to be performed, and the purpose of the probabilistic finite element program is to track through this sequence.

Because of the similarity with the deterministic finite element method, these probabilistic methods can be integrated in standard finite element program structure. To achieve this a control module needs to be added to the existing program structure which controls the perturbation sequence, calculates the perturbed terms, and solves these according to one of the perturbation schemes.

2.7 Fast Probability Integration Method

2.7.1 Derivation

The methods discussed in Section 2.6 calculate the perturbed response when the random parameters are perturbed by a prescribed amount. While this information will suffice to make design decisions regarding the ranking of the more sensitive design variables, it is not sufficient to calculate reliability of the component. One technique which is suited to the MVFO methods described above is known as the *fast probability integration* method. The method was first proposed by Hasofer and Lind (1974), was further developed by Rackwitz and Fiessler (1978). It has been incorporated in some design codes (NBS Special Publication 577, 1980) and was adapted to MVFO-type probabilistic finite element methods by Wu and co-workers (Wirsching and Wu, 1987; Wu, 1987; Wu et al., 1987; Wu and Wirsching, 1987; Wu et al., 1989; Wu and Wirsching, 1989; Wu et al., 1990).

The calculation of reliability in static structural problems requires the definition of a *limit state* function such that the event of failure is (Ditlevsen, 1981):

$$g(\mathbf{x}) \leq 0 \tag{2.49}$$

where $\mathbf{x} = (x_1, x_2, \ldots, x_n)$ are the random parameters which are assumed to be mutually independent. The term *failure* is used in a generalised context and can include exceedance of a serviceability or safety limit. The probability of failure is then:

$$p_f = p_f[g(\mathbf{x}) < 0] \tag{2.50}$$

An exact solution for the probability of failure requires the solution of a joint probability integral. The exact solution of this integral is prohibitively complicated in most engineering problems. An alternative approach involves the definition of an approximate response function $Z(\mathbf{x})$. Failure is then defined as:

$$Z_f - Z(\mathbf{x}) \leq 0 \text{ or } Z(\mathbf{x}) \geq Z_f \tag{2.51}$$

where Z_f is the limit state or failure criterion. For this limit state, the *most probable point* can be defined as the point at a minimum distance from the origin, $\mathbf{u} = 0$, to the limit state, $g(\mathbf{u}) = 0$, where $\mathbf{u}$ are the standard, normal variables transformed from the non-normal, independent variables $\mathbf{x}$ through (Rackwitz and Fiessler, 1978):

$$\mathbf{x} = F_{\mathbf{x}}^{-1}[\Phi(\mathbf{u})] \text{ or } \mathbf{u} = \Phi^{-1}[F_{\mathbf{x}}(\mathbf{x})] \tag{2.52}$$

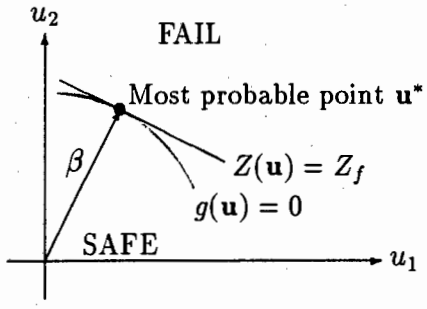

Figure 2.6: Most probable point and reliability index

where $\Phi(\cdot)$ is the standard normal CDF and $F_{\mathbf{x}}(\mathbf{x})$ is the CDF of $\mathbf{x}$. A method for computing the standard normal CDF is given in Appendix B. If the random parameters are non-normal and dependent a Rosenblatt transformation is required (Rosenblatt, 1952). The minimum distance is denoted β and is known as the *reliability* or *safety index.* The probability of failure is estimated from (Der Khiureghian and Moghtaderi-Zadeh, 1982):

$$p_f = \Phi(-\beta) \tag{2.53}$$

The reliability index β is often used as a comparative measure of reliability. The most probable point is the most likely combination of the random variables for $g(\mathbf{x}) = 0$ to hold and is illustrated in Figure 2.6 for a problem involving two random parameters which have been transformed to standard normal variables (i.e. the limit state is $g(\mathbf{u}) = 0$ and the approximation is $Z(\mathbf{u}) = Z_f$). The minimum distance can be estimated from the mean and standard deviation of the response Z (Ditlevsen, 1982):

$$\beta = \frac{Z_f - \bar{Z}}{\sigma_Z} \tag{2.54}$$

The approximate response function can be estimated from the results of the perturbed analysis by assuming that Z is "smooth" or can be smoothed, and that the Taylor series expansion of Z exists at the mean values $\boldsymbol{\mu}_x$ of the random parameters $\mathbf{x}$. If the random parameters are normal and mutually independent, the response function can be expressed as follows (Wu et al., 1990):

$$\begin{aligned} Z(\mathbf{x}) &= Z(\boldsymbol{\mu}_x) + \sum_{i=1}^{n} \left(\frac{\partial Z}{\partial x_i} \right) \cdot (x_i - \mu_{x_i}) + H(\mathbf{x}) \\ &= Z(\boldsymbol{\mu}_x) - \sum_{i=1}^{n} \left(\frac{\partial Z}{\partial x_i} \right) \mu_{x_i} + \sum_{i=1}^{n} \left(\frac{\partial Z}{\partial x_i} \right) x_i + H(\mathbf{x}) \\ &= a_o + \sum_{i=1}^{n} a_i x_i + H(\mathbf{x}) \\ &= Z_1(\mathbf{x}) + H(\mathbf{x}) \end{aligned} \tag{2.55}$$

where the derivatives (or gradients) are evaluated at the mean values and $H(\mathbf{x})$ represents the higher order terms of the expansion.

The following derivation is in terms of independent normal random parameters $\mathbf{x}$. These can be transformed to standard normal variables $\mathbf{u}$ using:

$$u_i = \frac{x_i - \mu_{x_i}}{\sigma_{x_i}} \tag{2.56}$$

If the x_i terms are non-normal the transformation of equation (2.52) must be used. If the x_i terms are non-normal and correlated, which is the general case, the correlated terms have to be transformed to uncorrelated standard normal terms using techniques described by Rosenblatt (1952), Hasofer and Lind (1974), Hohenbichler and Rackwitz (1981) and Wu et al. (1989). These methods are based on an orthogonal transformation of the covariance matrix $\mathbf{C}$ to a diagonal matrix of uncorrelated variables.

Neglecting at this stage the higher order terms $H(\mathbf{x})$, the mean $\bar{Z}$ and standard deviation σ_Z of the response can be estimated from:

$$\bar{Z} = a_o + \sum_{i=1}^{n} a_i \mu_{x_i} = Z(\boldsymbol{\mu}_x) \tag{2.57}$$

and

$$\sigma_Z^2 = \sum_{i=1}^{n} a_i^2 \sigma_{x_i}^2 \tag{2.58}$$

An initial estimate of the reliability index β can be made for the limit state Z_f as follows (Wu et al., 1989):

$$\beta = \frac{Z_f - \bar{Z}}{\sigma_Z} \tag{2.59}$$

Evaluating the minimum distance β at a number of target level values of Z_f, and using equation (2.53), a first estimate of the cumulative distribution function of Z can be made. This first estimate is usually referred to as the mean value first order (MVFO) method and is (Wu et al., 1989):

$$\Phi(-\beta) = p_f\,[Z < Z_f] \tag{2.60}$$

A more accurate estimate of the CDF is obtained by including the higher order terms $H(\mathbf{x})$. This can be achieved by estimating the most probable point from the linear approximation $Z_1(\mathbf{x})$ (Wu et al., 1990):

$$x_i^* = \beta \cdot \frac{a_i \sigma_{x_i}^2}{\sigma_Z} + \mu_{x_i} \tag{2.61}$$

It is now possible to re-analyse the structure at the most probable point and to estimate the higher order terms $H(\mathbf{x})$ from:

$$H(\mathbf{x}) = Z(\mathbf{x}^*) - Z_f \tag{2.62}$$

When the H-term is included, the probability statement becomes:

$$\Phi(-\beta) = p_f\,[Z < Z(\mathbf{x}^*)] \tag{2.63}$$

This procedure is known as the advanced mean value first order (AMVFO) method and can be summarised by the following steps:

1. Obtain the linear approximation $Z_1(\mathbf{x})$ to the response function based on perturbations about the mean value.
2. Estimate the most probable point $\mathbf{x}^*$ for selected CDF values.
3. Recalculate $Z(\mathbf{x}^*)$ to correct Z_f for the same CDF as in step 2.

The AMVFO procedure is convenient in building up a CDF plot, even if the actual response function is nonlinear. However, the most probable points calculated from the MVFO results are, in general, not the exact probable points, and therefore there will still be some error in the CDF (Cruse et al., 1988b; Wu et al., 1989). This is because the a_i coefficients at the most probable points are not the same as those used to estimate the most probable points. However the AMVFO method is able to increase significantly the accuracy of the CDF using only one computation of the response gradients (i.e. one probabilistic analysis). The number of re-analyses (at the most probable points) depends on the range of the CDF which is of interest.

The fast probability integration method for estimating the cumulative density function can be adapted to the point estimate method by the use of equation (2.54): the mean and standard deviation can be estimated directly by the point estimate method. By varying Z_f in equation (2.54) and using equation (2.53) to calculate the probability of failure, the cumulative density function can be built up from the point estimate results. It is not possible to calculate the most probable points.

When the probability of exceeding a specific failure criterion is required (i.e. not the entire CDF), a repeated AMVFO method (Wu and Wirsching, 1989) can be used: the MVFO

results about the deterministic values of the random parameters are obtained as usual. The most probable points for a range of responses can then be predicted and better estimates can be obtained by the AMVFO method. The specific most probable point which results in a response closest to the failure criterion is used to generate a better estimate of the linearised failure surface. This is achieved by performing another probabilistic perturbation analysis to calculate the response gradients at this most probable point. This procedure is repeated until convergence is reached (i.e. until the response gradients are stationary). This algorithm is also known as advanced mean value iteration or AMV$^+$ (Wu et al., 1990).

The repeated AMVFO procedure can, in principle, be automated if a search algorithm can be implemented in the probabilistic finite element program in order to converge to and find the most probable point which best matches the failure criterion. The procedure can be formulated to converge to a probability given a fixed failure criterion (z-level algorithm) or to converge to a failure criterion given a fixed probability (p-level algorithm) (Wu et al., 1990; Millwater et al., 1992). In this thesis such a search algorithm was not developed, and manual z-level searches were carried out in each instance. It was found that with some experience of, and insight to the problem, the number of search evaluations ranged between two and four. It is unlikely that a search algorithm could improve on that.

If the failure criterion is a random parameter with mean and standard deviation, the randomness of the failure criterion can be included in the fast probability integration: the expression for the reliability index is modified to (Hasofer and Lind, 1974):

$$\beta = \frac{\bar{Z}_f - \bar{Z}}{\sqrt{\sigma_Z^2 + \sigma_{Z_f}^2}} \tag{2.64}$$

The most probable points are now calculated by including the standard deviation of the failure criterion and a most probable failure point is also calculated:

$$\begin{aligned} x_i^* &= \beta \cdot \frac{a_i \sigma_{x_i}^2}{\sqrt{\sigma_Z^2 + \sigma_{Z_f}^2}} + \mu_{x_i} \\ Z_f^* &= -\beta \cdot \frac{\sigma_{Z_f}^2}{\sqrt{\sigma_Z^2 + \sigma_{Z_f}^2}} + \bar{Z}_f \end{aligned} \tag{2.65}$$

The object of the repeated AMVFO procedure is now to find that most probable point which results in a response closest to the most probable failure point. When this point has been established, the response gradients at it are established using another perturbation analysis. The procedure is repeated until convergence is reached.

2.7.2 Discussion

The procedures described above require that the gradients of the response with respect to the random parameters are available. When the techniques described in Section 2.6.4 are used, it is possible to approximate these gradients by:

$$\frac{\partial Z}{\partial x_i} \simeq \frac{\Delta Z_i}{\Delta x_i} = \frac{\breve{Z}_i - Z(\boldsymbol{\mu}_x)}{\breve{x}_i - \mu_{x_i}} \tag{2.66}$$

which can be substituted into equation (2.55) to approximate the response function. Most of the papers dealing with perturbation methods perturb the random parameters by one standard deviation. The mixed-iterative perturbation scheme of Dias et al. (1989) perturbs by a fraction of a standard deviation to improve the convergence characteristics.

None of the papers on fast probability integration discuss whether perturbation is by a positive or negative amount. In some problems it does not matter whether a positive or negative perturbation is used, since the ratio in equation (2.66) is insensitive to that. In others this is not so: if, for instance, the initial yield stress is perturbed and the equivalent plastic strain is the required response, the gradient of equation (2.66) will be different for positive and negative perturbations. The linear response function of equation (2.55) does not allow for this, and the following amendment is proposed: consider linear response functions Z_1^+ and Z_1^- due to positive and negative perturbations respectively. A better approximation of the response function is then the mean of Z_1^+ and Z_1^-:

$$\begin{aligned}
Z_1^+ &= Z(\boldsymbol{\mu}_x) + \sum_{i=1}^{n} \left(\frac{\partial Z}{\partial x_i^+} \right) \cdot (x_i - \mu_{x_i}) \\
Z_1^- &= Z(\boldsymbol{\mu}_x) + \sum_{i=1}^{n} \left(\frac{\partial Z}{\partial x_i^-} \right) \cdot (x_i - \mu_{x_i}) \\
\hline
Z_1^+ + Z_1^- &= 2Z(\boldsymbol{\mu}_x) + \sum_{i=1}^{n} \left(\frac{\partial Z}{\partial x_i^+} \right) \cdot (x_i - \mu_{x_i}) + \sum_{i=1}^{n} \left(\frac{\partial Z}{\partial x_i^-} \right) \cdot (x_i - \mu_{x_i}) \\
Z_1 &= Z(\boldsymbol{\mu}_x) - \sum_{i=1}^{n} \frac{1}{2} \left(\frac{\partial Z}{\partial x_i^+} + \frac{\partial Z}{\partial x_i^-} \right) \mu_{x_i} + \sum_{i=1}^{n} \frac{1}{2} \left(\frac{\partial Z}{\partial x_i^+} + \frac{\partial Z}{\partial x_i^-} \right) x_i \\
Z_1 &= a_o + \sum_{i=1}^{n} a_i x_i
\end{aligned} \tag{2.67}$$

2.8 Discussion and Concluding Remarks

In the probabilistic methods for structural analysis described above, two main strategies can be distinguished, namely mean value first order methods based on the individual perturbation of the random parameters and point estimate methods based on the combined perturbation of the random parameters. The specific strategy determines the method to post-process the perturbed response.

The perturbation schemes available to calculate the perturbed response can be assigned to two main categories, namely full perturbation (i.e. the problem is resolved completely) and perturbation schemes which re-use the inverse of the deterministic stiffness matrix (i.e. perturbed values are obtained using the inverted deterministic stiffness matrix which is already available). The second category is not compatible with elastic-plastic material models and is limited to linear problems.

To achieve probabilistic finite element procedures within the scope of existing deterministic finite element codes one option is to implement a point estimate perturbation method in a deterministic finite element program by perturbing the random model parameters following the point estimate procedures (i.e. all the possible permutations of negative and positive perturbations of the random parameters by one standard deviation) and by collecting the necessary point estimates of the response. The probability moments can then be calculated using equation (2.14) from which the mean and standard deviation can be calculated using equations (2.11) and (2.12). A CDF of the response can be built up through the combination of equations (2.54) and (2.53).

Deterministic finite element programs need to be modified to track systematically through the required point estimates and to sum equation (2.14) internally. If only the first and second moment are required, the storage requirements compared with deterministic analyses is trebled (i.e. deterministic results, expectation of first moment and expectation of the second moment). This is independent of the number of random variables since the number of random variables only affects the number of point estimates.

If the material model is linear considerable savings in analysis time can be achieved by implementing the solution algorithms for the iterative or Taylor series perturbation schemes as described in Section 2.6.4. The deterministic stiffness matrix then needs to be inverted only once, and the point estimates can be obtained from (essentially) matrix manipulations. The solution will require some iteration in the iterative perturbation scheme, but is linear in the Taylor series perturbation scheme.

Since the point estimate method allows assessment of mean and standard deviation of the response within the finite element program and allows relatively simple inclusion of corre-

lation between the random parameters, it seems an ideal procedure to be implemented in the smaller finite element programs which are mainly PC or workstation based and may have storage limitations.

The advantages of the point estimate method are:

- Evaluation of mean and standard deviation is robust. Correlation between random parameters can be included directly in the probabilistic finite element analysis.
- The CDF of the response can be simply constructed.
- The reliability index and probability of failure at any point of the structure can be estimated directly from the analysis output. The failure criterion can involve randomness.
- Implementation on the user's side is simple since input of only mean, standard deviation and correlation between the random parameters is required.
- No post-processing is required to evaluate mean and standard deviation of essentially all the normal solution variables (i.e. stress, strain, displacement, and so on).
- Storage requirements for the probabilistic information is limited (at most trebled).
- Considerable savings can be made in the analysis time if the material model is linear by implementing Taylor series and/or iterative perturbation schemes.

The point estimate method has the following limitations:

- The number of perturbed evaluations increases exponentially with the number of random parameters.
- It is not possible to calculate most probable points for failure and therefore it is not possible to improve the estimates of reliability.
- It is not possible to consider partial spatial correlation of the random parameters.

A second option to achieve probabilistic finite element methods is to implement a mean value first order method in the finite element program. The deterministic finite element code should be modified to track through the required perturbations systematically. The perturbed results of all individual perturbations need to be stored for later post-processing and this can pose considerable storage requirements when the number of random parameters is large or if many elements are involved.

Once the perturbed results have been calculated, fast probability integration procedures can be used to obtain estimates of the mean and standard deviation of the response, and to build up a CDF. The fast probability integration procedures allow the calculation of the most probable points of failure. Re-analysis at these most probable points will result in better estimates of the CDF. If response function is nonlinear it may be necessary to perturb both negatively and positively to obtain a good approximate response function and a procedure is proposed in Section 2.7.2.

Savings in analysis time can be made in linear problems by utilising Taylor series or iterative perturbation schemes. These schemes are not compatible with nonlinear problems.

Mean value first order methods linked to fast probability integration procedures are more suited to large finite element programs installed on large computers, where the temporary storage of large files can be accommodated. Through advanced mean value first order methods good estimates of the response in the tails of the probability can be obtained. Good estimates of the reliability index corresponding to a specific failure criterion can be found through repeated AMVFO procedures.

The mean value first order method discussed here assumes independent random parameters, each of which is fully correlated through the structure. While the concept of independent random parameters is consistent with many engineering problems (e.g. elastic modulus, moment of area and loading are all independent), the concept of full correlation throughout a structure does not always make sense. For instance, for a structure consisting of a number of beams, there is no reason why the moment of area of one beam should be fully correlated to the moment of area of another. Similarly, a wind load is not necessarily fully correlated along the length of a beam. In problems involving welds, the weld material is not related to the parent metal and usually has different material properties (Price and Alberry, 1988).

Since the MVFO method linked to fast probability integration requires individual perturbation of the random parameters, it seems reasonable to deal with problems involving these independent "zones" by perturbing the independent zones individually. For example, in a structure consisting of two beams for which the elastic modulus and moment of area are independent parameters and for which the two beams are statistically independent, it would be necessary to perform two separate probabilistic finite element analyses: in the one analysis the elastic modulus and moment of area is perturbed in one beam while the other beam is not perturbed. In the next analysis the other beam is perturbed. The results of the two analyses are stored for the entire structure. The fast probability integration program then processes the results of both analyses. While this procedure may not be mathematically elegant, it is simple. The procedure has been used in some verification problems and produces results which compare well with more advanced methods.

The advantages of the mean value first order method linked to fast probability integration procedures are:

- Evaluation of mean and standard deviation is robust.
- The CDF of the response can be directly constructed. Better estimates of the CDF can be obtained by AMVFO procedures.
- The reliability index and probability of failure at any point of the structure can be estimated. The failure criterion can involve randomness. Better estimates of the reliability index can be obtained through repeated AMVFO procedures.
- Random parameters which are statistically independent for different parts of the structure can be considered.
- Implementation on the user's side is simple since input of only mean and standard deviation is required.
- Considerable savings can be made in the analysis time if the material model is linear by implementing Taylor series and/or iterative perturbation schemes.
- The number of perturbed evaluations increases linearly with the number of random parameters. Additional evaluations are required for the AMVFO procedures.

The mean value first order method has the following limitations:

- Correlation between random parameters cannot be included in a simple manner.
- The procedures involve considerable post-processing of the results of the probabilistic analysis.
- The result storage requirements relative to a deterministic analysis are multiplied by the number of random parameters. This storage is temporary until the fast probability integration procedures have been completed.

It has been shown in this review of the literature that the mean value first order and point estimate method procedures can be integrated into a finite element program. Full perturbation, Taylor series perturbation and iterative perturbation schemes can also be integrated within the same program. These probabilistic procedures can be added to standard deterministic programs without significantly changing existing routines. The following changes are required:

- The solution algorithms must be able store the inverse of the deterministic stiffness matrix and use it to calculate a perturbed displacement vector when the Taylor series or iterative perturbation schemes are used.
- A perturbation control module must be added to the program to control the perturbation sequence. This module must incorporate the features of the point estimate method and the mean value first order method. This module will affect only individual element calculations.
- The perturbation control module must also control the perturbation scheme and appropriate finite element calculations.
- A database file system must be integrated with the program to store the perturbed response of the mean value first order method.

3 Deterministic Finite Element Subroutines

3.1 Preamble

The program structure of a commercially available finite element program normally involves a set of subroutines and sub-units dealing exclusively with element operations and calculations. If standard deterministic element subroutines developed in this way can be converted to probabilistic element subroutines without having changed the other sub-units of the deterministic finite element program (e.g. the mesh development and matrix assembly routines, the solution algorithms), it should be straightforward to implement this conversion in an existing deterministic finite element program.

In order to simulate the structure of a standard deterministic finite element program, a deterministic three-dimensional beam element and a deterministic two-dimensional plane element have been developed. These have been implemented within the general purpose finite element program ABAQUS as two separate user element subroutines. The ABAQUS user element subroutine facility requires that those subroutines necessary to perform the element calculations and operations be coded by the user. All the other features of the standard ABAQUS program remain: problem input file specifications are nominally the same as for standard elements, except for some minor differences in the input card format. The ABAQUS mesh generation and refinement, matrix assembly and inversion routines are used and convergence is checked within the main ABAQUS program.

The development of the deterministic finite element subroutines and the structure and algorithms by which they were implemented follow closely the standard finite element programming format found in the literature, on the premise that commercially available finite element programs are implemented along the same format. The overall program structure used in this thesis follows the proposals of Hinton and Owen (1977) and Owen and Hinton (1980). The algorithms for the plasticity calculations in the plane elements are based on commercially available finite element programs: ABAQUS for the plane strain and axisymmetric formulations (ABAQUS Theory Manual, 1989) and LUSAS for the plane stress formulation (FEA Report No. FEAL807, 1988). These algorithms correspond almost exactly to algorithms proposed in the literature: they are simplified to allow easier implementation in program code.

The element formulations are identical to those found in standard finite element programs: iso-parametric shape functions and Gaussian quadrature numerical integration are used and the element types (Timoshenko beam, plane strain, plane stress and axisymmetric) are standard in many programs. Node numbering and load specification follow the conventions used in ABAQUS.

The reasons for following these standard formats are:

- The object of this thesis **is not** to optimise or improve existing deterministic finite element programs;
- The object of this thesis **is** to show that deterministic finite element routines as implemented in standard finite element programs can be converted to probabilistic routines without requiring significant additional coding.

Different element formulations, in respect of element type, number of nodes, integration order, and load type have been implemented in these routines. They can be accessed through option flags specified by the user in the problem input file. For example, the plane element involves three element types, two node number options, three integration order options and two distributed load types, all available within the same program.

The element routines developed in this thesis are, in all likelihood, not at the optimum in efficiency. Nevertheless they should resemble the routines found in standard finite element programs. The finite element theory on which these elements are based is described in Appendix A. A brief description of the ABAQUS user element subroutine interface is given in Appendix C.

The routines have been verified and found to produce results which compare well with analytical calculations and with results predicted by standard finite element programs. The main verification problems are discussed in Section 6.1. This chapter will discuss the program structure of the deterministic user element subroutines developed in this thesis. As a convention in this thesis, any programming variables and operations described in the text are printed in a different typeface to the main text.

3.2 User Element Subroutine Structure

The user element subroutines developed in this thesis for the three-dimensional beam element and the two-dimensional plane element are similar in structure and the following discussion will cover the program structure for both subroutines. The routines consist of a number of smaller, specific purpose subroutines which correspond to the main calculations described in Appendix A and are described below:

`UEL` The main subroutine which interprets the information passed by ABAQUS, calls further subroutines and returns the residual vector `RHS`, the element stiffness matrix `AMATRX` and the solution state variable array `SVARS` to ABAQUS.

LOAD	Main subroutine called by UEL which calculates the load vector ELOAD containing the consistent nodal forces for the distributed loads acting on the element.
RESID	Main subroutine called by UEL which updates the solution state variable array SVARS to its values at the end of the current increment, calculates the element stiffness matrix AMATRX, and calculates the residual vector RHS by subtracting the internal forces at the nodes from the load vector ELOAD.
GAUSS	Sets up the Gaussian quadrature points.
SHAPE, JACOB	Evaluate the iso-parametric shape functions and shape function derivatives and the Jacobian matrix $\mathbf{J}$ and its determinant.
BMATX, DMATXE	Evaluate the strain-displacement matrix $\mathbf{B}$ and the elastic constitutive matrix $\mathbf{D}^{el}$.
LINEAR	Evaluates the elastic predictor strains and stresses.
PLAST	Evaluates the equivalent plastic strain increment using a Newton iteration method and updates the yield surface if the previous value of the yield surface has been exceeded by the elastic predictor stresses.
DMATXP	Evaluates the consistent tangent constitutive matrix $\mathbf{D}^{pl}$ if the previous value of the yield surface has been exceeded by the elastic predictor stresses.
ROTAT	Evaluates the rotation matrix $\mathbf{R}$ to transform from local to global coordinates.

Figure 3.1 shows the overall user element subroutine structure and indicates the relationship of the various subroutines.

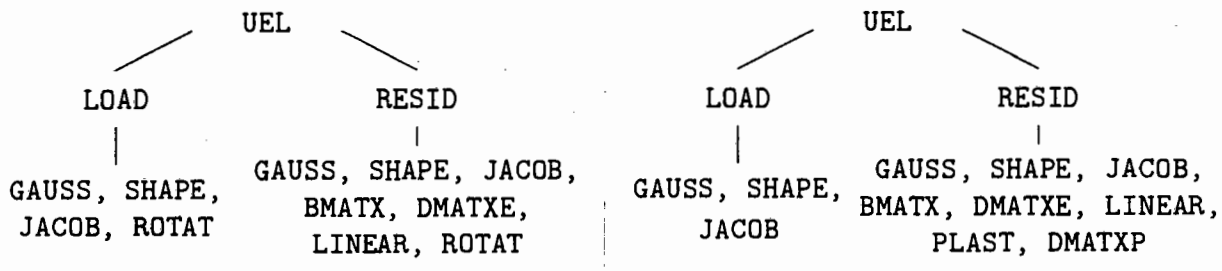

(a) Beam element (b) Plane element

Figure 3.1: Overall deterministic user element subroutine structures

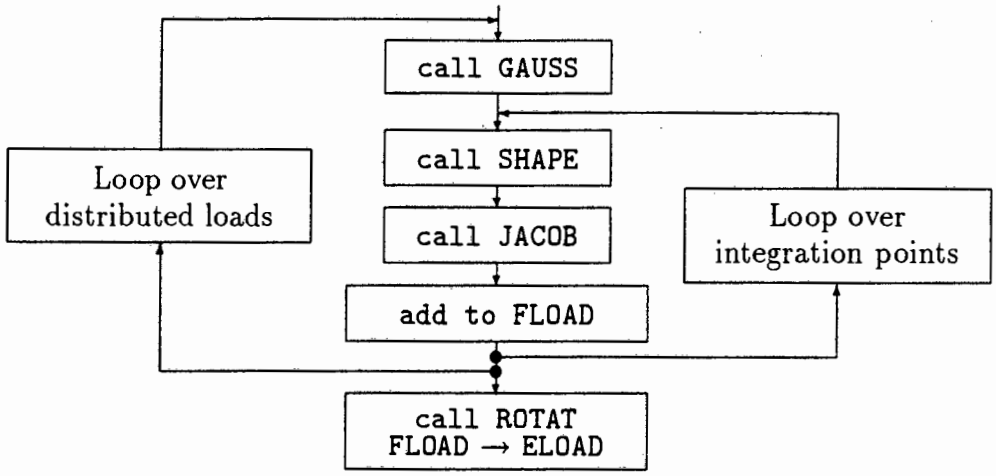

(a) Beam element

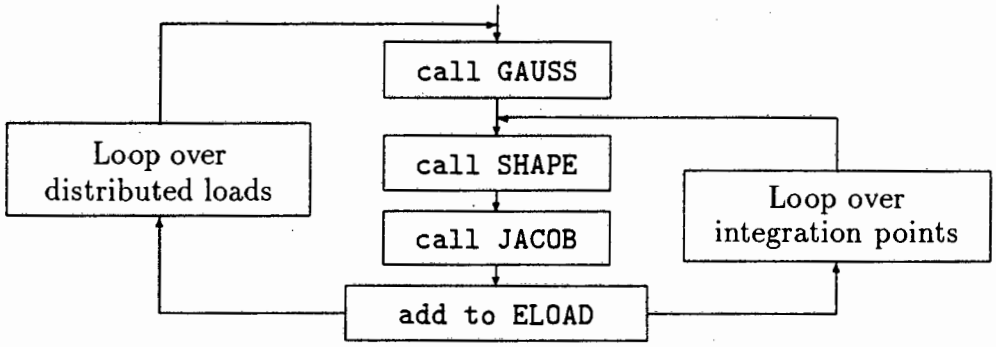

(b) Plane element

Figure 3.2: Structure of LOAD subroutine

Subroutine LOAD performs the calculations described in Section A.10. If a distributed load is active on the element, its magnitude is supplied by ABAQUS through an array of active loads ADLMAG. An integer flag is used to determine the type and direction of this distributed load (e.g. in the plane element routine this flag determines whether the distributed load is normal or tangential and on which element face it acts). The distributed load applied to an element edge is transformed by numerical integration to a vector of consistent nodal forces, named ELOAD. This procedure is repeated for each distributed load active on the element. The structure of the main calculations and operations performed in the LOAD subroutine is illustrated in Figure 3.2. FLOAD is the load vector in the local directions.

The distributed load types implemented in the beam element can act transverse to the beam in either of the principal axis directions or in the global directions. In the latter case consistent nodal forces are integrated over the projected length of the element and transformation from local to global coordinates is not required. The distributed loads implemented in the plane element can act normal or tangential to the element face.

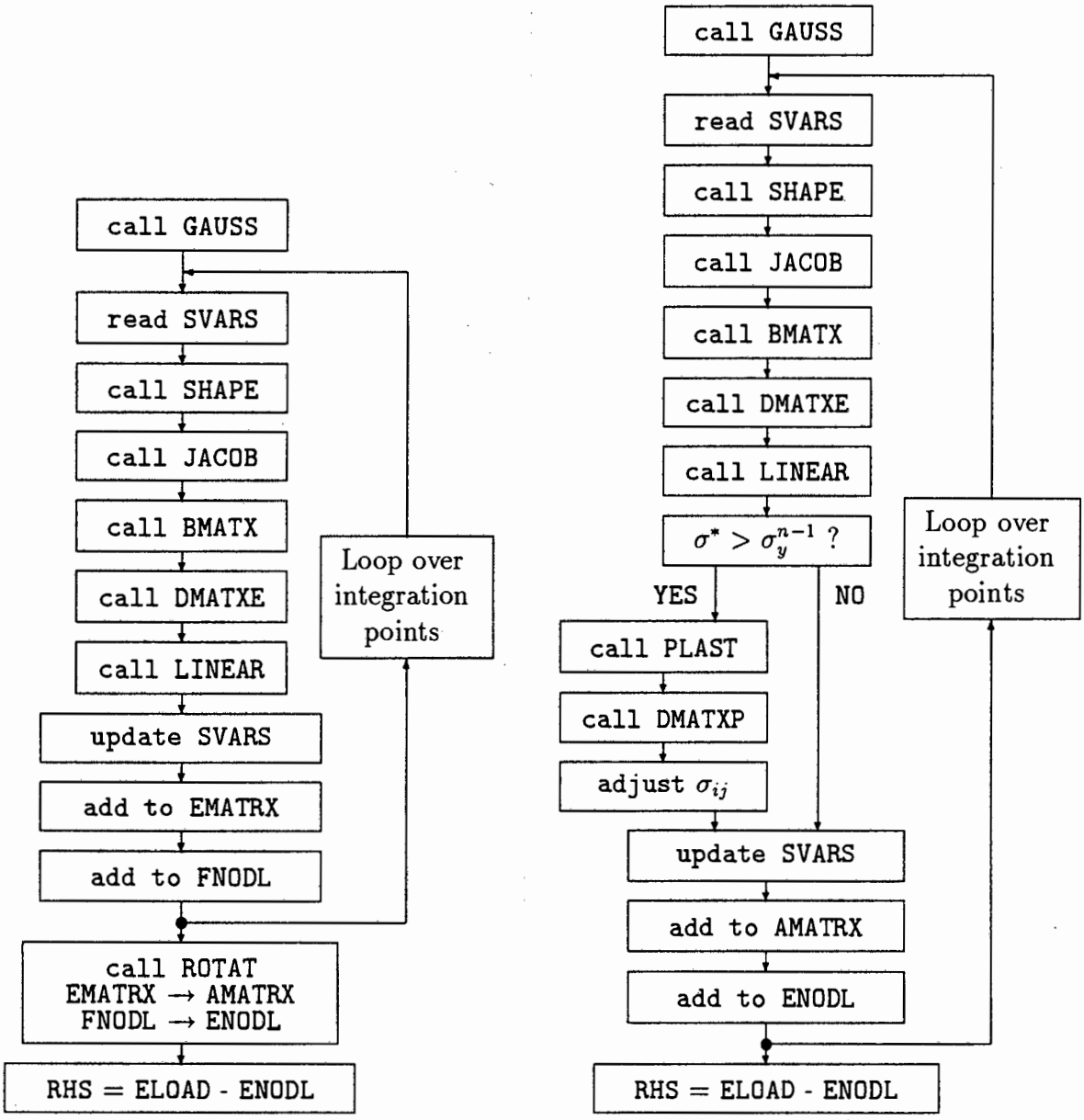

(a) Beam element (b) Plane element

Figure 3.3: Structure of RESID subroutine

Subroutine RESID performs three functions: it updates the element solution state variable array SVARS using the displacement increment DU, it evaluates the element stiffness matrix AMATRX, and it calculates the residual vector RHS. The structure of the main calculations and operations performed in the RESID subroutine is shown in Figure 3.3. EMATRX and FNODL are the stiffness matrix and internal force vector in the local coordinate system.

The solution state variables evaluated in the beam element are the axial force, shear forces, bending moments and torque at each integration point. The solution state variables eval-

uated in the plane element are the total direct strains, the direct stresses, the equivalent plastic strain, the Mises stress and the maximum principal stress at each integration point.

The stiffness matrix is evaluated by numerical integration and the required algorithms are described in Appendix A. If the displacement increment results in elastic predictor stresses which exceed the current value of the yield surface, these predictor stresses have to be brought back to a suitably updated yield surface. The elastic predictor-radial return procedures are discussed in Section 2.4 and solution algorithms are described in Section A.9. In general the adjusted stresses will not result in a converged residual vector at the end of the first iteration, and further iterations, which use the consistent tangent stiffness matrix, are required until convergence is reached.

The residual vector is obtained by evaluating the vector of internal forces at the nodes corresponding to the updated stresses and by subtracting these from the vector of consistent nodal forces. Any point loads acting on the element are added to the residual vector within the main ABAQUS program. Reaction forces occurring at constrained nodes are also taken care of within the main ABAQUS program.

3.3 Element Features

The main element features are summarised in Table 3.1. The beam element and, in particular, the plane element routines developed in this thesis incorporate a number of possible configurations. The beam element routine allows either two-noded or three-noded elements. No choice is allowed regarding the integration order: both configurations are implemented with reduced integration to avoid locking problems.

The beam element can be reduced to a truss element by releasing the rotational degrees of freedom at the boundary conditions and pin-joints of the trusses. In this way rigid frame systems, truss systems and combined beam-truss systems can be analysed. This involves no additional coding within the user element subroutines. The release of rotational degrees of freedom is specified within the program input file and is taken care of within the main ABAQUS program.

Only linear elastic material behaviour is implemented in the beam element and the required material properties and section parameters are listed in Table 3.1.

The plane element routine allows the choice between four-noded and eight-noded elements. Standard and reduced integration is implemented for both elements. The plane element gives the user the choice between plane stress, plane strain and axisymmetric behaviour.

Element type	**3D Beam element**	**2D Plane element**
Element formulation	Timoshenko beam Truss	Plane stress, Plane strain or Axisymmetric
Node number	2 (linear interpolation) or 3 (quadratic interpolation)	4 (linear interpolation) or 8 (quadratic interpolation)
Degrees of freedom	6 per node	2 per node
Integration order	1 or 2	1, 2 or 3
Integration type	Gaussian quadrature	Gaussian quadrature
Shape functions	Iso-parametric	Iso-parametric
Material behaviour	Linear elastic	Elastic-plastic
Material/section parameters	Elastic modulus Poisson's ratio Cross-sectional area Second moment of area (about y and z axes) Polar moment of area Shear correction factor (in y and z directions) Beam principal axes rotation	Elastic modulus Poisson's ratio Initial yield stress Plastic hardening modulus Element thickness (req. for plane stress)
Load types	Concentrated loads and moments and distributed loads in global directions Transverse distributed loads Axial thermal expansion/misfit	Concentrated loads Distributed normal and tangential loads
Solution variables	Displacement at nodes Stress (axial force, shear force, bending moment, torque)	Displacement at nodes Total strain and stress Mises equivalent stress Maximum principal stress Equivalent plastic strain

Table 3.1: Element features

General elastic-plastic material behaviour is implemented in the plane element (i.e. linear elastic behaviour can be achieved by specifying a high value for the initial yield stress). The plasticity model followed is based on a Mises yield surface and isotropic hardening. The required material properties are listed in Table 3.1.

The user element subroutines deal with these different configurations through option flags. These flags are either specified by the user in the element property array `PROPS` or are passed through directly by ABAQUS (e.g. the option flag `NTYPE`, part of the plane element properties, determines whether plane stress, plane strain or axisymmetric behaviour is used; the option flag `NNODE`, passed through by ABAQUS directly, determines the number of nodes on an element).

Apart from a number of option flags, the element property array `PROPS` also passes through the required element material and section properties. These are supplied by the user in the problem input file and follow a specified order. The amount of axial thermal expansion or misfit in, and the rotation of the beam principal axes of a beam element are also specified in the element property array.

4 Probabilistic Finite Element Subroutines

4.1 Preamble

This chapter describes the conversion of the deterministic finite element subroutines to probabilistic finite element subroutines. This has been achieved within the limitations of the ABAQUS user element interface described in Appendix C. The deterministic finite element program structure described in Chapter 3 was maintained.

The conversion should in principle be possible for all deterministic finite element programs without affecting the entire program structure: if the element calculations are performed in separate sub-units of the overall program structure, only these sub-units are affected significantly by the conversion. The conversion affects the program input routines, but this will be minimal, as only additional element properties and control options need to be defined. The finite element solution algorithms must be able to store and re-use the inverse of the deterministic stiffness matrix in order to benefit from the time-saving features of the Taylor series and iterative perturbation schemes in linear problems.

The conversion was performed for the deterministic three-dimensional beam and two-dimensional plane elements described in Chapter 3 but this conversion can be achieved for any type of element since the probabilistic analysis is independent of the finite element features (e.g. number of nodes, integration order). Procedures which control the probabilistic analysis have to be added but this can be achieved separate to, but integrated with, the deterministic program structure. The existing program structure can be maintained. Subroutines used to define components in the deterministic element (e.g. a subroutine to define the elastic constitutive matrix or the load vector) can be modified to be used in both the deterministic and probabilistic routines.

Two different methods of probabilistic analysis can be implemented in the same program: the point estimate method (PEM) and the mean value first order method (MVFO). These differ mainly in the systematic sequence of perturbed evaluations from which the probabilistic response is calculated. The purpose of the probabilistic finite element routines is to track through the appropriate perturbation sequence. The operation of the probabilistic routines depends on the probabilistic analysis method chosen:

- if the point estimate method is chosen, the subroutines evaluate the necessary point estimates and record the expectation of the first and second moments of the response parameters. These are stored within the solution state variable array. It is not necessary to store the results of each point estimate, since the probability moments can be evaluated within the probabilistic finite element analysis using equation

(2.10). The mean and standard deviation at a point can be evaluated using equations (2.11) and (2.12).

- if the mean value first order method is chosen, the subroutines evaluate the perturbed response corresponding to each individual random parameter and store these in an external database file for access by the fast probability integration programs.

4.2 Conversion Procedure

The subroutines developed in this thesis track a probabilistic finite element analysis through a systematic sequence consisting of a deterministic analysis followed by a number of perturbed analyses. This perturbation sequence corresponds to the standard pseudo-time incrementation schemes implemented in commercially available finite element programs: each analysis is considered to be an increment, with an elastic-plastic analysis further subdivided into load increments. The number of perturbation increments depends on the probabilistic analysis method and the number of random parameters. The random parameters which can be perturbed in the probabilistic routines developed in this thesis are listed in Table 4.1. It is possible to increase this range of random parameters.

A systematic perturbation sequence has been instituted in order to be able to link perturbation to increment number and to link perturbation to position in the database file. As a convention the random parameters are perturbed in the order in which they are listed in Table 4.1. A particular perturbation increment can be by-passed if the perturbation amount specified for a specific random parameter is zero throughout the structure (i.e. the parameter is considered random only if a non-zero perturbation amount has been specified by the user). The user cannot alter the perturbation sequence once it has been implemented in the program code. This is not considered a problem since the perturbation sequence can be transparent to the user.

Beam element	Plane element
Elastic modulus	Elastic modulus
Moment of area	Poisson's ratio
Thermal expansion	Initial yield stress
Distributed load 1	Hardening modulus
Distributed load 2	Distributed load 1
Point load	Distributed load 2

Table 4.1: Random parameters

It is necessary also to institute a fixed format in which the random parameters and perturbation control parameters are specified. This should not lead to problems for the user: if a program uses an interactive input module, the program can institute the format internally. If a separate input file is used (and most interactive programs still incorporate this as an option), this input file must be in some fixed format anyway.

The conversion of the deterministic finite element routines to probabilistic routines involves three main steps:

1. algorithms have to be written which assign the correct perturbation amount to the correct random parameter during the correct increment. These algorithms differ between the MVFO and PEM methods, but are independent of the perturbation scheme (i.e. full, Taylor series or iterative perturbation).

2. algorithms have to be written for the solution of the finite element expressions corresponding to the different perturbation schemes. The different schemes available are: full perturbation involving re-analysis, iterative perturbation and Taylor series perturbation. These algorithms are independent of the probabilistic method (i.e. MVFO or PEM). The deterministic solution procedure has to be maintained.

3. algorithms have to be written to write the perturbed response to an external database file for access by the fast probability integration programs.

The key to the conversion lies in the fact that the finite element expressions required to solve the perturbed problems are similar in format to those required to solve the deterministic problem: only the arrays involved differ. Table 4.2 lists the finite element expressions involved in the different perturbation schemes. These expressions have been derived earlier in Chapter 2. The different expressions have in common that they all require the definition of an element stiffness matrix and a right-hand side vector from which a solution for a displacement (or displacement increment) vector is derived.

The solution of a general, nonlinear deterministic finite element expression involves the iterative convergence of a residual vector: the inverse of the stiffness matrix is multiplied with the residual vector to give an estimate of the displacement (or displacement increment) vector. The residual vector is then updated and checked for convergence. If the problem is linear, convergence will be reached after one iteration. If the problem is nonlinear further iterations will be required. If the problem is plastic, the stiffness matrix will change throughout the iterative procedure.

Table 4.2 shows that the finite element expressions corresponding to the perturbation schemes display the characteristics of the deterministic expression. What is required

Perturbation scheme	Finite element expression	Definitions
Deterministic	$\mathbf{K}_0\mathbf{u}_0 = \mathbf{f}_0$	
Full perturbation	$\breve{\mathbf{K}}\breve{\mathbf{u}} = \breve{\mathbf{f}}$	$\breve{\mathbf{K}} = \mathbf{K}_0 + \Delta\mathbf{K}$ $\breve{\mathbf{f}} = \mathbf{f}_0 + \Delta\mathbf{f}$
Iterative perturbation	$\mathbf{K}_0 d\breve{\mathbf{u}}^n = \breve{\mathbf{f}} - \breve{\mathbf{K}}\breve{\mathbf{u}}^{n-1}$ $\breve{\mathbf{u}}^n = \breve{\mathbf{u}}^{n-1} + d\breve{\mathbf{u}}^n$ $\breve{\mathbf{u}}^o = \mathbf{u}_0$	$\breve{\mathbf{K}} = \mathbf{K}_0 + \Delta\mathbf{K}$ $\breve{\mathbf{f}} = \mathbf{f}_0 + \Delta\mathbf{f}$
Taylor series perturbation	$\mathbf{K}_0\Delta\mathbf{u} = \Delta\mathbf{f} - \Delta\mathbf{K}\mathbf{u}_0$ $\breve{\mathbf{u}} = \mathbf{u}_0 + \Delta\mathbf{u}$	$\Delta\mathbf{K} = \breve{\mathbf{K}} - \mathbf{K}_0$ $\Delta\mathbf{f} = \breve{\mathbf{f}} - \mathbf{f}_0$

Table 4.2: Finite element expressions for different perturbation schemes

Perturbation scheme	Stiffness matrix	Residual vector	Solution vector
Deterministic	$\mathbf{K}_0$	$\mathbf{f}_0 + \mathbf{r}_0 - \mathbf{f}_0^{INT}$	$\mathbf{u}_0$ or $\Delta\mathbf{u}_0$
Full perturbation	$\breve{\mathbf{K}}$	$\breve{\mathbf{f}} + \breve{\mathbf{r}} - \breve{\mathbf{f}}^{INT}$	$\breve{\mathbf{u}}$ or $\Delta\breve{\mathbf{u}}$
Iterative perturbation	$\mathbf{K}_0$	$\breve{\mathbf{f}} + \breve{\mathbf{r}} - \breve{\mathbf{K}}\breve{\mathbf{u}}^{n-1}$	$\breve{\mathbf{u}}$
Taylor series perturbation	$\mathbf{K}_0$	$\Delta\mathbf{f} + \Delta\mathbf{r} - \Delta\mathbf{f}^{INT} - \Delta\mathbf{K}\mathbf{u}_0$	$\Delta\mathbf{u}$

Table 4.3: Solution procedures for different perturbation schemes

then to convert the deterministic routines to probabilistic routines is that the appropriate stiffness matrix and residual vector are returned to the assembly and solution routines of the finite element program. This can be achieved by perturbation control flags.

The stiffness matrix and residual vector required by the different perturbation schemes are listed in Table 4.3. It is important to note that the finite element expression given in the literature (and in this thesis) for the iterative perturbation scheme is in fact the iterative expression and the solution is in terms of the perturbed displacement vector. The Taylor series perturbation scheme solves for the displacement increment and the perturbed displacement is calculated by adding this increment to the (known) deterministic displacement. The deterministic and full perturbation schemes solve either for the full displacement if the load is applied in full or for a displacement increment corresponding to a load increment.

The full perturbation problem is essentially the same as the deterministic problem except that the perturbed stiffness matrix and load vector are used. The iterative perturbation and Taylor series perturbation problems involve the same stiffness matrix as the deter-

MVFO			PEM		
$\breve{\mathbf{K}}_j$	=	$\mathbf{K}(\bar{r}_{i\neq j}; \bar{r}_j + \delta[r_j])$	$\breve{\mathbf{K}}_{\pm}$	=	$\mathbf{K}(\bar{r}_i \pm \sigma[r_i])$
$\breve{\mathbf{f}}_j$	=	$\mathbf{f}(\bar{r}_{i\neq j}; \bar{r}_j + \delta[r_j])$	$\breve{\mathbf{f}}_{\pm}$	=	$\mathbf{f}(\bar{r}_i \pm \sigma[r_i])$

Table 4.4: Definition of perturbed stiffness matrix and load vector

ministic problem, but differ in the formulation of the residual vector. This determines whether stiffness matrix inversion is required: matrix inversion is required for the full perturbation scheme, but not for the iterative perturbation and Taylor series perturbation schemes if the inverse of the deterministic stiffness matrix is available.

The latter problems can therefore be solved by re-using the inverse of the deterministic stiffness matrix. The ABAQUS V4.8 release incorporates an option which specifies that the same (linear) stiffness matrix can be used throughout a step (i.e. a series of increments) (ABAQUS User's Manual, 1989). The ABAQUS V5.2 release no longer supports this option although the same effect is available through the linear perturbation option (ABAQUS User's Manual, 1992).

The probabilistic analysis method (i.e. PEM or MVFO) does not affect the perturbation scheme. The probabilistic method affects only the definition of the perturbed stiffness matrix and load vector. The definitions of the perturbed arrays given in Table 4.2 are generic ones and are defined more fully in Table 4.4 for the two methods. The perturbed stiffness matrix involves only a perturbed constitutive matrix (which may be the perturbed tangent constitutive matrix in the plane element). The perturbed load vector involves only a perturbed load magnitude.

The procedures to calculate the perturbed stiffness matrix and load vector are essentially the same as for the deterministic stiffness matrix and load vector and the subroutines developed for the deterministic elements can be adapted for this purpose. The only modification required is that whenever a random parameter needs to be perturbed, a small amount must be added to it, otherwise it should maintain its deterministic (mean) value. This can be achieved through perturbation control flags.

4.3 Perturbation Control Module

The perturbation sequence and the actual perturbation of the random parameters are controlled by a number of control flags and arrays and a control module is added to the existing program structure. The modified structure is shown in Figure 4.1.

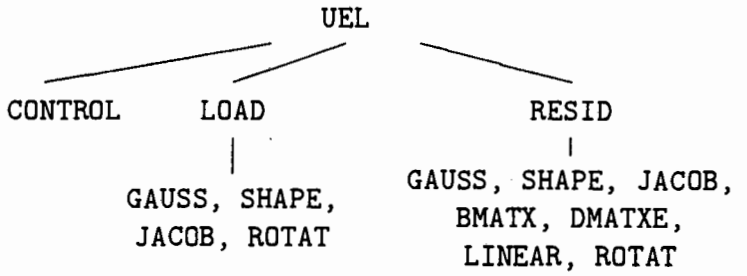

(a) Beam element

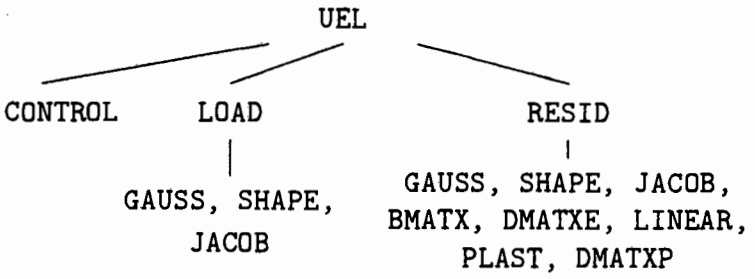

(b) Plane element

Figure 4.1: Overall probabilistic user element subroutine structures

The CONTROL module is the first module called by the main subroutine UEL and initialises the perturbation control flags and arrays which are passed to all the subroutines affected by the perturbation. The control flags and arrays required are defined below.

MTYPE — A scalar control flag which is zero when the increment is deterministic and one when the increment is perturbed and differentiates between deterministic and perturbed parameter evaluations.

LTYPE — A scalar control flag which determines the probabilistic method. Options are: MVFO method with single perturbation (either positive or negative), MVFO method with double perturbation (both positive and negative) and point estimate method. It is defined by the user in the problem input file.

LSCEM — A scalar control flag which determines the perturbation scheme. Options are: full perturbation (implemented in the plane element), iterative perturbation and Taylor series perturbation (both implemented in the beam element). It is in principle possible to combine all three in the same element routine, as long as the iterative perturbation and Taylor series perturbation schemes are restricted to linear elastic analyses. This flag is defined by the user in the problem input file.

PTVAL — A control array which is defined at the start of each perturbation increment. Each entry of the array corresponds to a specific random parameter and contains the perturbation amount relevant to the current perturbed increment. The order of the array corresponds to the sequence of random parameters in Figure 4.1. At the start of each increment each entry of the array is set, either to zero if the corresponding entry should not be perturbed during that increment, or to the perturbation amount if the corresponding random parameter should be perturbed during that increment. The perturbation amount for each possible random parameter is specified by the user in the element properties in the problem input file.

The algorithm used to initialise PTVAL depends on the probabilistic method chosen:

- If the MVFO perturbation with single perturbation is chosen, the entries of PTVAL are all set to zero except for the entry corresponding to the perturbation increment. That entry contains the perturbation amount specified by the user.
- If the MVFO perturbation with double perturbation is chosen, the entries of PTVAL are all set to zero except for the entry corresponding to the perturbation increment. This perturbation increment now consists of two sub-increments. During the first sub-increment the entry in PTVAL contains the positive perturbation amount specified by the user. During the second sub-increment, the entry contains the negative perturbation amount.
- If the point estimate method is used, all entries in PTVAL contain the perturbation amount specified by the user. The signs of each entry depend on the perturbation increment as the increment is linked to the combination of positive and negative perturbations. The algorithm which determines the sign is based on the following: the sign of the first random parameter with non-zero perturbation amount changes after every perturbation increment. The sign of the second random parameter changes after every second perturbation increment. The sign of the third parameter changes after every fourth increment. The algorithm is illustrated in Table 4.5. If less than six parameters are random, the same sequence is used but involving only the columns up to the number of random parameters. This algorithm is also used to evaluate the point estimate weighting factors if correlation between random parameters is included.

Perturbation	Random parameter						Perturbation	Random parameter					
increment	1	2	3	4	5	6	increment	1	2	3	4	5	6
1	+	+	+	+	+	+	33	+	+	+	+	+	−
2	−	+	+	+	+	+	34	−	+	+	+	+	−
3	+	−	+	+	+	+	35	+	−	+	+	+	−
4	−	−	+	+	+	+	36	−	−	+	+	+	−
5	+	+	−	+	+	+	37	+	+	−	+	+	−
6	−	+	−	+	+	+	38	−	+	−	+	+	−
7	+	−	−	+	+	+	39	+	−	−	+	+	−
8	−	−	−	+	+	+	40	−	−	−	+	+	−
9	+	+	+	−	+	+	41	+	+	+	−	+	−
10	−	+	+	−	+	+	42	−	+	+	−	+	−
11	+	−	+	−	+	+	43	+	−	+	−	+	−
12	−	−	+	−	+	+	44	−	−	+	−	+	−
13	+	+	−	−	+	+	45	+	+	−	−	+	−
14	−	+	−	−	+	+	46	−	+	−	−	+	−
15	+	−	−	−	+	+	47	+	−	−	−	+	−
16	−	−	−	−	+	+	48	−	−	−	−	+	−
17	+	+	+	+	−	+	49	+	+	+	+	−	−
18	−	+	+	+	−	+	50	−	+	+	+	−	−
19	+	−	+	+	−	+	51	+	−	+	+	−	−
20	−	−	+	+	−	+	52	−	−	+	+	−	−
21	+	+	−	+	−	+	53	+	+	−	+	−	−
22	−	+	−	+	−	+	54	−	+	−	+	−	−
23	+	−	−	+	−	+	55	+	−	−	+	−	−
24	−	−	−	+	−	+	56	−	−	−	+	−	−
25	+	+	+	−	−	+	57	+	+	+	−	−	−
26	−	+	+	−	−	+	58	−	+	+	−	−	−
27	+	−	+	−	−	+	59	+	−	+	−	−	−
28	−	−	+	−	−	+	60	−	−	+	−	−	−
29	+	+	−	−	−	+	61	+	+	−	−	−	−
30	−	+	−	−	−	+	62	−	+	−	−	−	−
31	+	−	−	−	−	+	63	+	−	−	−	−	−
32	−	−	−	−	−	+	64	−	−	−	−	−	−

Table 4.5: Perturbation sign sequence - point estimate method

4.4 Perturbation of Random Parameters

The method used to perturb the random variables is standard throughout the program and is best described by an example. In the routines developed in this thesis, the elastic modulus is assigned the programming variable `YOUNG` and its mean and perturbation amount are defined in the first and second entry of the element property array `PROPS`. The first entry of the perturbation array `PTVAL` is linked to the perturbation of the elastic modulus. If the elastic modulus needs to be perturbed during the current perturbation increment (and this can be during all increments if the point estimate method is chosen), the `CONTROL` module assigns the first entry of `PTVAL` with the necessary perturbation amount. For example, if the MVFO method with positive perturbation is chosen:

```
PTVAL(1) = PROPS(2)
```

when the elastic modulus should be perturbed during the current increment and

```
PTVAL(1) = 0
```

when the elastic modulus should not be perturbed. PROPS(2) contains the perturbation amount appropriate to the elastic modulus and can be zero when the elastic modulus is deterministic or when the elastic modulus of that element should not be perturbed when multiple independent zones are analysed separately. The control flags and control arrays are now passed to each subroutine involved in the perturbed analysis. For instance, the elastic modulus is required in the subroutine DMATXE in which the linear elastic constitutive matrix is evaluated. As a first step in this subroutine the programming variable YOUNG is defined:

```
YOUNG = PROPS(1) + MTYPE*PTVAL(1)
```

where PROPS(1) contains the mean value of the elastic modulus. This formulation is now repeated each time a random parameter is defined in the program code. It is obvious that the value of the random parameters will be their mean whenever a deterministic analysis is carried out (MTYPE = 0 in this case), when another random parameter should be perturbed, when the parameter is deterministic, or when the parameter should not be perturbed for that element (PTVAL(2) = 0 in these cases). The only additional coding required is that the control flags and control array need to be passed to each subroutine involved in the perturbation analysis and that the expression + MTYPE*PTVAL(i) needs to be added to the definition of each random parameter r_i.

4.5 Database File

The database file is required for a number of purposes:

- The database file is accessed to read the deterministic displacement required to initiate the iterative perturbation scheme and in the Taylor series perturbation scheme.
- The database file is accessed to read the perturbed displacement of the previous iteration in the iterative perturbation scheme.
- The database file is accessed by the fast probability integration and other post-processing programmes.

The structure and format of the database file is dependent on the finite element program in which it is implemented and on the post-processing programmes which access it. It is therefore preferable to integrate the database file with existing result storage file structures if possible. In this thesis however the database file had to be implemented independent of the standard ABAQUS results storage files since the user element interface does not allow modification of the storage file structure. In principle though, the storage structure implemented in an existing finite element program can be adapted. Two options are available:

1. An extra dimension is added to the deterministic storage structure. This extra dimension corresponds to the perturbation sequence. This option results in some complicated read and write algorithms in the program code as the position in the database file must be linked to the position in the perturbation sequence. This makes it difficult to increase the number of random parameters or to change the perturbation sequence.

   On the other hand, this option makes it easy to perform a number of probabilistic analyses, each involving perturbation of different (independent) zones of the finite element model. Each time the probabilistic analysis is performed the storage file is given a different (but characteristic) name. It gives the user the capability to deal with complex problems involving independent zones of the same random parameter. This is important to deal with, for instance, complex beam structures, where each beam may need to be considered independent of the others.

2. The storage system is duplicated for each random parameter. The results of each perturbed analysis are written to a separate storage file (with a characteristic name). This option results in simpler read and write algorithms as only the file unit specifier and the filename need to be linked to the perturbation sequence. The read and write statements and storage file format implemented in an existing finite element program code can be used for the probabilistic program. It is also easier to increase or alter the random parameters and change the perturbation sequence.

   On the other hand, it becomes complex to deal with multiple independent zones, not so much in the probabilistic finite element program as long as results are not overwritten, but in the post-processing programs because of the large number of files that may be required.

Since a database had to written from start in this thesis, the first option was used. However the second option is more suitable if an existing deterministic finite element program is adapted to include probabilistic analyses since it involves only limited additional code development.

4.6 Program Features

The main program features implemented in the probabilistic routines developed in this thesis are summarised in Table 4.6. Both the beam and the plane element involve up to six independent random parameters. This number can be increased, but the parameters implemented here are the most likely parameters to be random in practice (if randomness of the geometry is not considered). The user can consider two independent random distributed loads active on an element.

The number of random parameters active in a structure can be increased by considering more than one independent zones. This is achieved by defining the zones as different element sets in the problem input file and setting the perturbation amount in the inactive zones to zero. More than one probabilistic analysis is then carried out, the total number corresponding to the number of independent zones.

Element	**3D Beam element**	**2D Plane element**
Random parameters	Elastic modulus Moment of area Thermal expansion Distributed load 1 Distributed load 2 Point load	Elastic modulus Poisson's ratio Initial yield stress Hardening modulus Distributed load 1 Distributed load 2
Number of load increments	1	User specified
Material behaviour	Linear elastic	Elastic-plastic
Probabilistic method	MVFO (single or double) PEM	MVFO (single or double) PEM
Perturbation scheme	Iterative perturbation Taylor series perturbation	Full perturbation
Response variables	Displacement (u_x, u_y, u_z) Rotation (θ_x, θ_y, θ_z) Axial force (F_x) Shear force (S_y, S_z) Bending moment (M_y, M_z) Torsion (T_x) Effective moment ($M_y + M_z$)	Equivalent plastic strain Mises equivalent stress Max. principal stress

Table 4.6: Probabilistic element program features

Both elements incorporate the mean value first order method and the point estimate method. The user can specify whether single (i.e. positive or negative) or double (i.e. positive and negative) perturbation should be performed in an MVFO analysis. The user can choose between the iterative and Taylor series perturbation scheme in the beam element. Only full perturbation is allowed in the plane element.

The response variables are written to the database file in MVFO analyses and to the ABAQUS solution state variable array in PEM analyses. The number of response variables which is written to file is limited in order to limit the file size, and the user specifies in the problem input file which response variables are stored.

5 Fast Probability Integration Programs

5.1 Preamble

The purpose of the fast probability integration (FPI) programs is to post-process the results of an MVFO perturbation finite element analysis and to calculate the probabilistic response of the structure. Two types of fast probability integration can be distinguished:

1. MVFO-FPI analysis of the whole model with the objective of calculating the mean, standard deviation, coefficient of variance, reliability index and probability of failure for all the elements in the model. These results can then be presented graphically in contour plots. This would be the first step in a probabilistic finite element analysis and would enable the user to evaluate the overall probabilistic behaviour of the structure and identify regions which need closer attention.

2. AMVFO-FPI analysis with the objective of obtaining better estimates of the probability of failure at discrete points corresponding to specific elements. These discrete points are typically the points of maximum mean response, maximum coefficient of variance or minimum strength. The position of these points can be identified from the results of the whole model MVFO-FPI analysis.

The output from the two types of fast probability integration differs: whole model MVFO-FPI analysis output must be integrated with the graphical post-processing routines of the finite element program. Discrete point AMVFO-FPI analysis output must be in file format: what is required is a table of CDF response levels, the reliability index and probability of failure corresponding to them and the most probable points for re-analysis at each CDF response level.

Whole model MVFO-FPI analysis should therefore be integrated within the post-processing procedures of a finite element program, while discrete point AMVFO-FPI analysis can be achieved best by a program separate from the finite element program but which can access the probabilistic database files.

The numerical procedures to calculate the probabilistic response at a point are similar for the two types of fast probability programs and many algorithms are used in both. These algorithms are based on the equations derived in Section 2.7. This chapter describes the program structure in which these have been implemented.

5.2 Program Structures

The structure of the whole model MVFO-FPI analysis program is shown in Figure 5.1. It has been implemented in this thesis within an ABAQUS user material subroutine which is called at each integration point. This technique and the reasons for using it are briefly described in Appendix C. The advantage of this is that the standard ABAQUS post-processing features to create contour plots are available.

For each evaluation point the MVFO-FPI program reads the deterministic and perturbed response from the database file into an internal array. If the perturbation analysis was performed for a number of independent zones, the program reads in the results from a number of files corresponding to these independent zones. The database structure and filenaming convention used by the probabilistic finite element program must be integrated into the MVFO-FPI analysis program.

Two options are available to calculate the response function coefficients a_i, depending on whether perturbation was performed in one direction (i.e. positive or negative – equation (2.55)) or in both directions (i.e. positive and negative – equation (2.67)). The mean, standard deviation, reliability index and probability of failure is then calculated for each evaluation point (using equations (2.57), (2.58), (2.64), and (2.60) respectively). The program incorporates the ability to deal with random failure criteria through the use of equation (2.64) rather than (2.59) to calculate the reliability index. The probability of failure is calculated using the routines described in Appendix B. The most probable points to cause failure are not calculated in the whole model MVFO-FPI analysis program.

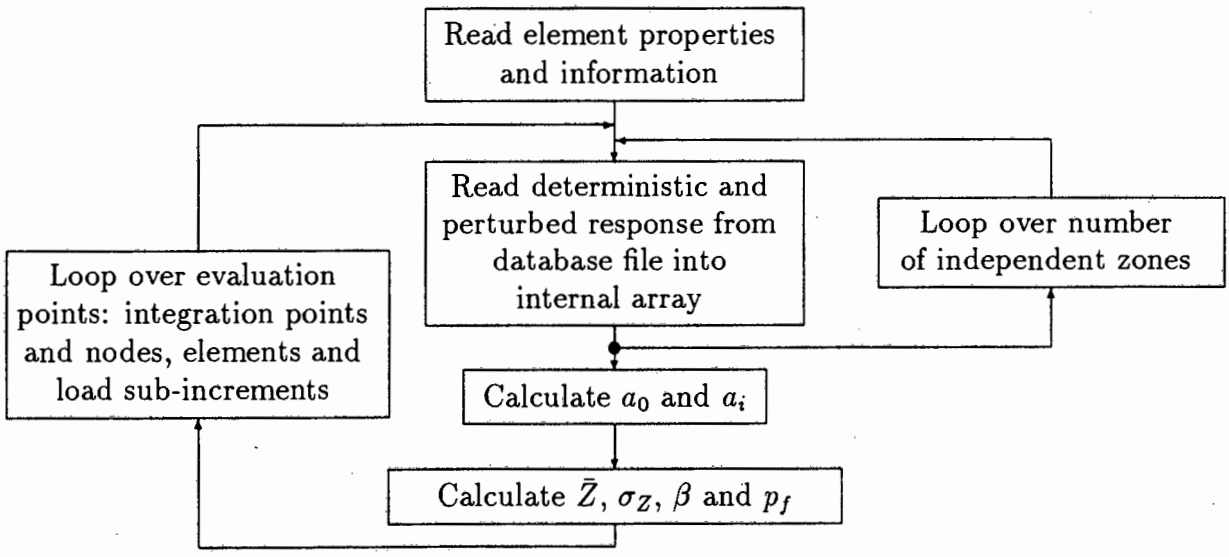

Figure 5.1: Whole model MVFO-FPI analysis program structure

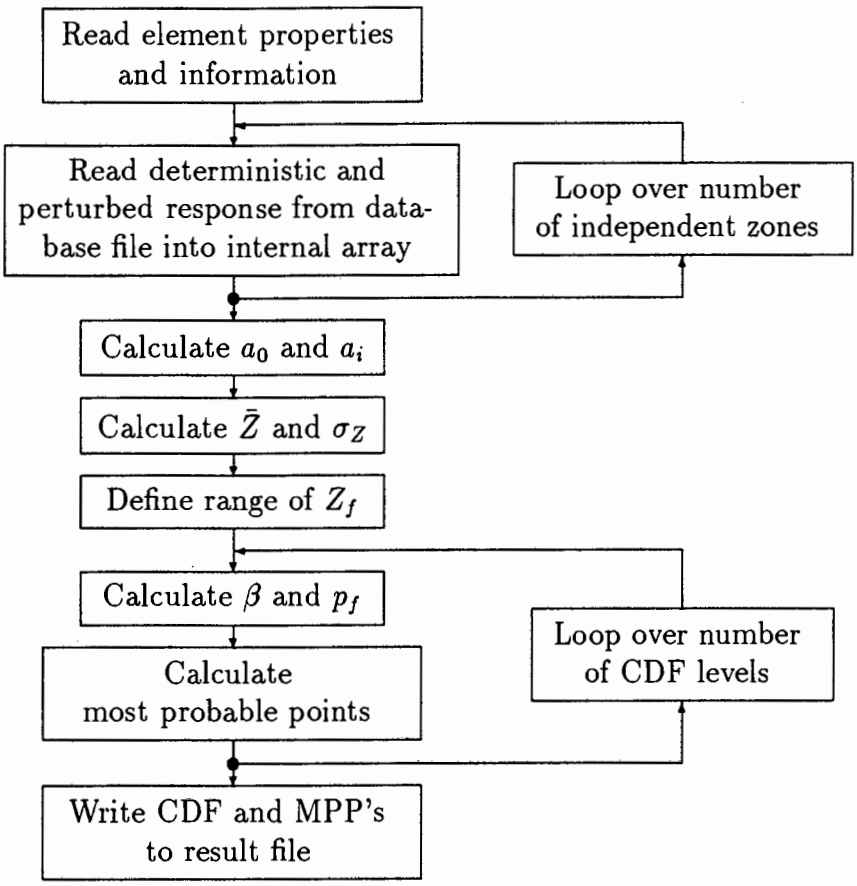

Figure 5.2: Discrete point AMVFO-FPI analysis program structure

The structure of the discrete point AMVFO-FPI analysis program is similar to that of the whole model MVFO-FPI analysis program and is shown in Figure 5.2. In this program however, the user specifies the element number corresponding to the point of interest and the program reads the appropriate deterministic and perturbed response from the database file (or files if a number of independent perturbed analyses were performed). The object of program is to calculate the most probable points to cause failure for a series of CDF response levels. The user must specify a range of failure states Z_f for the CDF levels. The program defaults to a range from $\bar{Z} - 4\sigma_Z$ to $\bar{Z} + 4\sigma_Z$ which is convenient to create CDF plots, but for repeated AMVFO this range should center more closely around the expected failure point in order to search for the most probable point resulting in a response closest to the most probable failure point.

The reliability index, probability of failure and most probable points are calculated for each CDF level. Randomness of the failure criterion is included through equations (2.64) and (2.65). A table of results is written to file which can then be used to re-analyse the structure at the most probable points. The re-analysis results can be used to construct a CDF plot or to find a better estimate of the reliability index through repeated AMVFO.

6 Verification Problems Analysed and Results

This chapter describes the some of the problems that were analysed in order to verify the finite element subroutines and fast probability integration programs developed in this thesis. The performance of the subroutines and programs was continually tested and evaluated as these were being developed and the programs were tested in many more problems than can be presented here. The problems which are presented here were chosen because they span a range of typical applications and because comparative results are available.

Section 6.1 presents results for deterministic problems and verifies that the finite element routines produce numerically accurate results in the continuum mechanics sense. Section 6.2 presents results for probabilistic problems and verifies that the finite element routines and fast probability programs produce numerically accurate results in the stochastic sense.

In each problem the results obtained are verified against at least one other method. These methods include analytical derivations, results of commercially available finite element programs, Monte Carlo simulations and the published work of other authors.

6.1 Deterministic Finite Element Programs

6.1.1 Three-dimensional beam element

The deterministic beam element was verified against analytically derived results in a number of different configurations. A first set of tests involved one-dimensional beams with determinate and indeterminate boundary conditions. The material properties and section geometry are the same for all tests in this set and are listed in Table 6.1. A square cross-section is used in all tests and the beams are modelled using ten three-noded elements.

The main results of these tests are shown in Table 6.2 where they are compared with analytical results obtained from Young (1989). The results presented are the maximum absolute values along the beam. The signs and distribution of deflection, rotation, shear force, bending moment and torque along the length of the beam were also verified against the analytical solutions and found to correspond. The minor differences between the analytical and FEM deflections when a transverse load is applied is due to the fact that shear effects have been neglected in the analytical solutions (which are based on conventional beam theory).

Parameter	Term	Value
Elastic modulus	E	200GPa
Poisson's ratio	ν	0.3
Coefficient of thermal expansion	α_t	$18\text{x}10^{-6}/°\text{C}$
Length of beam	l	2m
Cross-section side	a	0.04m
Cross-sectional area	A	$1.6\text{x}10^{-3}\text{m}^2$
Second moment of area	$I_y = I_z$	$2.133\text{x}10^{-7}\text{m}^4$
Polar moment of area	J	$3.60\text{x}10^{-7}\text{m}^4$
Shear correction factor	α	1.177

Table 6.1: Beam element test properties

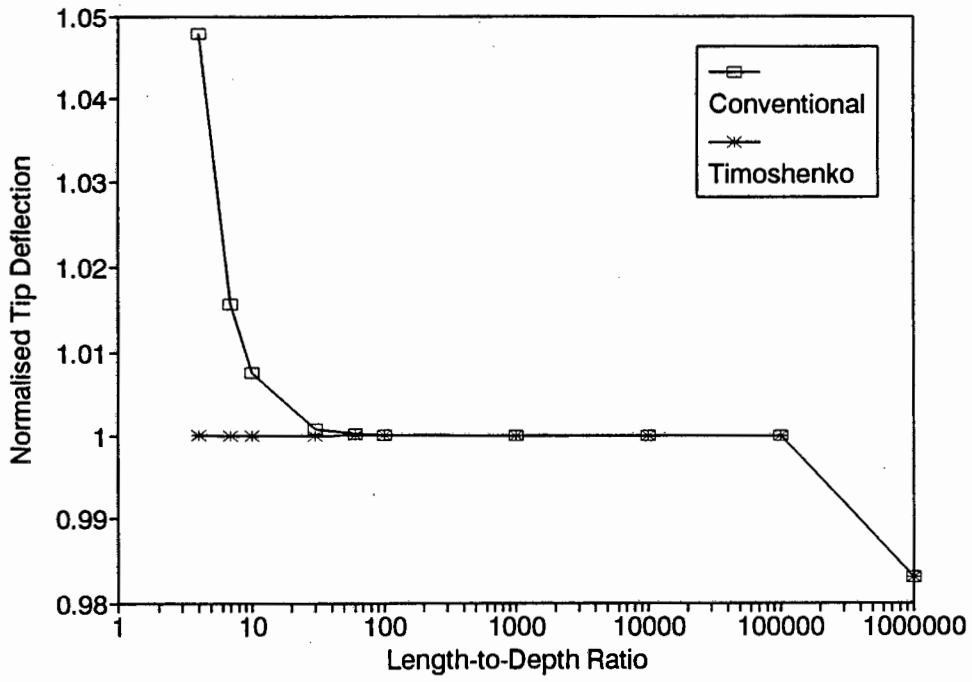

Figure 6.1: Beam element locking test results

A locking test was performed to verify that the beam element would not produce overstiff results for thin beams. A cantilever beam with a transverse point load at the free end was modelled by ten three-noded elements. A wide range of length-to-depth ratios was considered. Figure 6.1 shows the results of this test where the tip deflections are normalised with respect to analytical conventional and Timoshenko beam results. The figure shows that the element does not produce any stiffening for length-to-depth ratios up to 10^5. A length-to-depth ratio of 10^6 does produce some stiffening but this is beyond ratios found in practice. The figure also shows that the element performs well for thick beams

Structure	Load Type	Solution Variable	Analytical Solution	FEM Solution
Cantilever beam	Point load at free end (500N)	δ_{max} θ_{max} M_{max} S_{max}	31.255mm 0.0234rad 1000Nm 500N	31.264mm 0.0234 rad 1000Nm 500N
Cantilever beam	Moment at free end (500Nm)	δ_{max} θ_{max} M_{max}	23.441mm 0.0234rad 500Nm	23.441mm 0.0234rad 500Nm
Cantilever beam	Torque at free end (500Nm)	θ_{max} T_{max}	0.0361rad 500Nm	0.0361rad 500Nm
Cantilever beam	Distributed load (500N/m)	δ_{max} θ_{max} M_{max} S_{max}	23.441mm 0.0156rad 1,000Nm 1,000N	23.451mm 0.0156rad 1,000Nm 1,000N
Simply supported beam	Point load at mid-point (5,000N)	δ_{max} θ_{max} M_{max} S_{max}	19.534mm 0.0293rad 2,500Nm 2,500N	19.558mm 0.0293rad 2,500Nm 2,500N
Simply supported beam	Distributed load (5,000N/m)	δ_{max} θ_{max} M_{max} S_{max}	24.418mm 0.0391rad 2,500Nm 5,000N	24.442mm 0.0391 2,500Nm 5,000N
Built-in beam	Point load at mid-point (50,000N)	δ_{max} M_{max} S_{max}	48.836mm 12,500Nm 25,000N	49.075mm 12,500Nm 25,000N
Built-in beam	Distributed load (50,000N/m)	δ_{max} M_{max} S_{max}	48.836mm 16,667Nm 50,000N	49.075mm 16,667Nm 50,000N

Table 6.2: Verification results for one-dimensional beams

where shear effects are important. The limiting length-to-depth ratio for which conventional beam formulations are valid is ten in the case of the cantilever beam (less than 1% difference). Below this ratio conventional beam assumptions can lead to errors of up to 5%. The limiting ratio is a function of the boundary conditions and the cross-section geometry.

The beam element was further verified in more complex structures which involved the interaction of multiple beams fastened together. Analytical solutions were derived for seven different structures and are included in Appendix D. The material properties and section geometry are listed in Table 6.1, except for the appropriate beam lengths which are given in Appendix D. Three-noded beams were used in all tests.

Structure	Load Type	Solution Variable	Analytical Solution	FEM Solution
Angle bracket (Appendix D.1)	In-plane load (500N)	M_A^Y	1,000Nm	1,000Nm
Angle bracket (Appendix D.1)	Out-of plane load (500N)	T_A M_A^Z	1,000Nm 1,000Nm	1,000Nm 1,000Nm
Crossed beam structure (Appendix D.2)	Overhanging point load (10,000N)	δ_E	21.705mm	21.786mm
Three bar link (Appendix D.3)	Axial end load (50,000N)	F_1 F_2 F_3 δ_D	23,077N 11,538N 15,385N 72.116μm	23,077N 11,538N 15,385N 72.115μm
Two bar truss system (Appendix D.4)	Downward load (50,000N)	F_1 F_2 u_B v_B	70,711N -50,000N -312.5μm -1.196mm	70,711N -50,000N -312.5μm -1.196mm
Combined beam-truss system (Appendix D.5)	Downward load	u_B u_B θ_{max}	-312.4μm -1.196mm -0.897mrad	-312.4μm -1.196mm -0.897mrad
Rectangular plane frame (Appendix D.6)	Distributed load on horizontal beam (1,000N/m)	M_A M_B M_{max}	2,032Nm -4,064Nm 3,936Nm	2,031Nm -4,074Nm 3,930Nm
Rectangular plane frame (Appendix D.6)	Distributed load on left vertical beam (1,000N/m)	M_A M_B M_C M_D	-6,044Nm 1,397Nm -1,893Nm 3,166Nm	-6,044Nm 1,390Nm -1,900Nm 3,167Nm
Rectangular plane frame (Appendix D.6)	Uniform temperature change (10°C)	M_A M_B	4.564Nm -1.755Nm	4.563Nm -1.755Nm
Gable plane frame (Appendix D.7)	Distributed load acting vertically on gable beams (1,000N/m)	M_A M_B M_C	2,595Nm -3,251Nm 1,241Nm	2,595Nm -3,262Nm 1,249Nm

Table 6.3: Verification results for complex beam structures

The main results for these structures are given in Table 6.3. The distributions of the solution variables along the beams were also verified where possible using the analytical solutions and found to correspond. The analytical derivations are based on conventional beam theory and this results in some discrepancy between the analytical and FEM deflections. In the plane frame structures, the discrepancy between the analytical and FEM moments is also affected by the extrapolation of values at the integration points to the nodes. The maximum discrepancy is 0.6% and is considered acceptable.

6.1.2 Two-dimensional plane element

The deterministic plane element was verified using the verification test problems included in the ABAQUS Verification Manual (1992). To test the plane strain and plane stress elements, a rectangular shape is subjected to distributed normal and tangential loads as shown in the schematic diagram below.

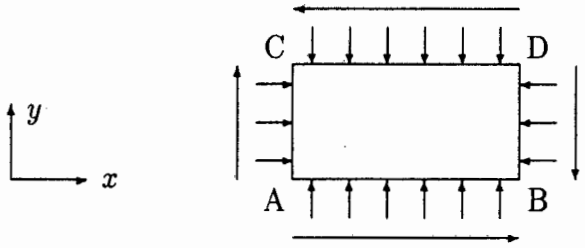

$E = 30\text{x}10^6$

$\nu = 0.3$

$u_x^A = u_y^A = 0$

$u_y^B = 0$

The rectangle is 2x1 units in size and the loading is 1,000 units/length for both the normal and tangential loads. Elastic material behaviour is assumed. The rectangle was modelled by four eight-noded plane elements using standard integration. The results obtained are listed in Table 6.4 and match the ABAQUS verification results exactly. The nodal displacements also follow the ABAQUS results (i.e. $u_x = x\varepsilon_{xx} + y\gamma_{yy}$ and $u_y = y\varepsilon_{yy}$).

To test the axisymmetric element, a ring with rectangular cross-section is subjected to distributed normal loads as shown in the schematic diagram below.

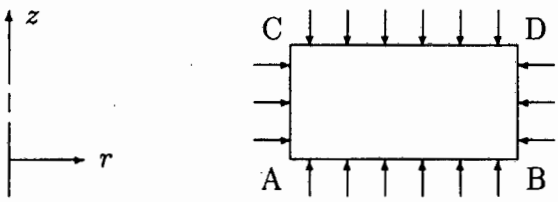

$E = 30\text{x}10^6$

$\nu = 0.3$

$u_z^A = u_z^B = 0$

The rectangular cross-section is 2x1 units and the internal radius is 1000 units. The distributed loads are 1000 units/length. Elastic material behaviour is assumed. The ring was modelled by four eight-noded axisymmetric elements using standard integration. The results are listed in Table 6.4 and match the ABAQUS verification results exactly. The nodal displacements along AC also match the ABAQUS results (i.e. $u_r = \text{-}1.33\text{x}10^{-2}$ and $u_z = \text{-}1.33\text{x}10^{-5}z$).

To verify the numerical accuracy of the plane elements in more complex geometries and under stresses which cause elastic-plastic behaviour, three further tests were performed and compared with the results predicted by equivalent standard ABAQUS elements. The material properties for the three tests are listed in Table 6.5. The three tests are briefly described below:

Formulation	Variable	Value
Plane strain	$\sigma_{xx} = \sigma_{yy} = \tau_{xy}$	-1,000
	σ_{zz}	-600
	$\varepsilon_{xx} = \varepsilon_{yy}$	-1.7333x10^{-5}
	γ_{xy}	-8.6667x10^{-5}
Plane stress	$\sigma_{xx} = \sigma_{yy} = \tau_{xy}$	-1,000
	$\varepsilon_{xx} = \varepsilon_{yy}$	-2.3333x10^{-5}
	γ_{xy}	-8.6667x10^{-5}
Axisymmetric	$\sigma_{rr} = \sigma_{\theta\theta} = \sigma_{zz}$	-1,000
	τ_{xy}	0
	$\varepsilon_{rr} = \varepsilon_{\theta\theta} = \varepsilon_{zz}$	-1.3333x10^{-5}
	γ_{rz}	0

Table 6.4: Verification results for two-dimensional plane elements

1. The plane stress element was used to model a square perforated plate under uni- and equibiaxial tension. The geometry of the plate and the applied loading is shown schematically below. The ratio of the hole diameter to the width of the plate is 1/10. The width of the plate is 200mm. The distributed loading is chosen to cause elastic behaviour and the σ_{yy} stress at the hole and along the x-axis are of interest. Analytical derivations for an infinite plate with a hole indicate that for a uniaxial distributed load p the σ_{yy} stress at the hole is $3p$ and for equibiaxial distributed load p the σ_{yy} stress at the hole is $2p$ (Timoshenko and Goodier, 1970).

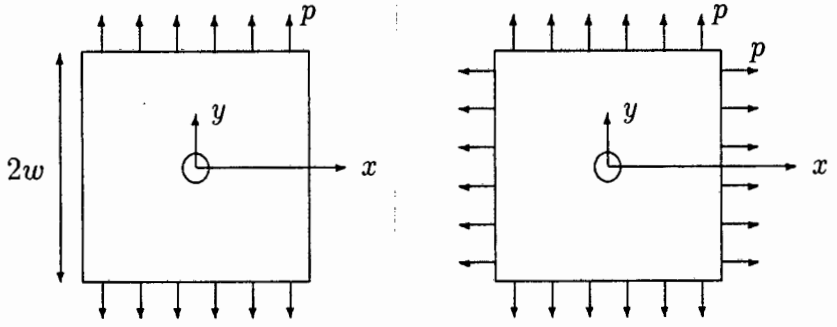

A distributed load of $p = 25$MPa was applied to a model of a quarter of the plate, consisting of 96 eight-noded elements. Standard integration was used. The results were compared with standard ABAQUS results for the same mesh and found to correspond exactly. The stress concentration at the hole matches the analytically derived values for both load cases.

2. The plane strain element was used to model a thick pipe of infinite length subjected to an internal pressure of 40MPa. The thickness is 3/10 of the external radius, R_o,

Property	Value
Elastic modulus	200GPa
Poisson's ratio	0.3
Initial yield stress	100MPa
Hardening modulus	20GPa

Table 6.5: Material parameters – plane element tests

which is 100mm. A quarter of the pipe was modelled using 148 eight-noded plane strain elements. An analysis involving four load increments was performed. The Mises stresses and equivalent plastic strains through the thickness were compared at the integration points with standard ABAQUS results and found to correspond exactly. Convergence of the problem was monitored and found to be quadratic and identical to the standard ABAQUS convergence.

3. The axisymmetric element was used to model a notched rod pulled in tension. The geometry of the rod is shown schematically below. The radius of the notch a is 3/10 of the radius of the rod R which is 30mm. The axial force P was applied as a distributed load of 40MPa. A quarter of the notched rod was modelled using 128 eight-noded axisymmetric elements and solved using four load increments. The Mises stress and equivalent plastic strain along the r-axis were compared with standard ABAQUS results and found to correspond exactly, as did the convergence characteristics.

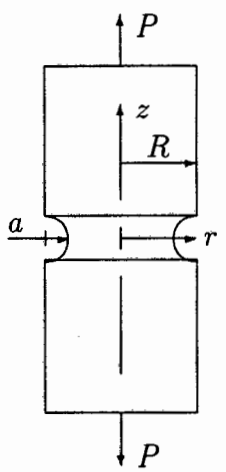

6.2 Probabilistic Finite Element Programs

6.2.1 Crossed beam structure

A schematic diagram of a crossed beam structure involving a built-in beam supporting a cantilever beam is shown below. A point load is applied at the free end of the cantilever. The deflection at point E is of interest. The two beams have the same length, cross-section and elastic modulus. The elastic modulus, moment of area and load are independent random parameters, the stochastic data for which is given in Table 6.6.

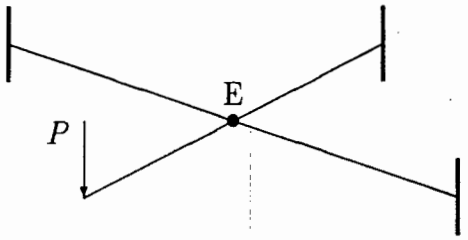

Parameter	Length l	Elastic modulus E	Moment of area I	Load P
Mean	2m	200GPa	1.333×10^{-8}m^4	500N
STD	-	10GPa	1.333×10^{-9}m^4	75N
COV	-	5%	10%	15%

Table 6.6: Problem parameters – crossed beam structure

An analytical expression for the deflection at point E is derived in Appendix D.2. This expression was implemented in a Monte Carlo simulation program involving 20,000 trials. This program is described in Appendix E. From this program the mean, standard deviation and coefficient of variance of the deflection at E was estimated. The simulation process was stable with less than 0.3% difference between the minimum and maximum estimates of four sets of simulations, indicating that the number of trials is sufficient.

The structure was modelled using 20 three-noded beam elements. A probabilistic analysis was performed using the different perturbation methods and schemes available. The MVFO method involved both iterative perturbation and Taylor series perturbation. In both cases the random parameters were perturbed positively and negatively as well as in the direction which would cause the highest deflection at E (i.e. positively for the load and negatively for the stiffness terms). The point estimate method involved both iterative perturbation and Taylor series perturbation.

Probabilistic method	Mean (mm)	STD (mm)	COV (%)
MVFO - iterative perturbation			
P, E, I: positive and negative	17.378	3.261	18.77
P: positive; E, I: negative	17.378	3.269	18.81
MVFO - Taylor series perturbation			
P, E, I: positive and negative	17.378	3.251	18.71
P: positive; E, I: negative	17.378	3.251	18.71
Point estimate method			
Iterative perturbation	17.597	3.301	18.76
Taylor series perturbation	17.378	3.251	18.71
Monte Carlo Simulation	17.604	3.327	18.90

Table 6.7: Deflection results at point E – crossed beam structure

The results for the different probabilistic methods are shown in Table 6.7. The results show that there is no difference between the two types of MVFO-Taylor series perturbation and the point estimate-Taylor series perturbation. This is because the change in deflection is a function of the stiffness of the beams (i.e. the elastic modulus and the moment of area), and the change in deflection caused by a decrease in stiffness is higher than that caused by an equal increase in stiffness. This aspect is neglected by the Taylor series perturbation scheme as it neglects the multiplication of the change in deflection and the change in stiffness (i.e. the $\Delta\mathbf{K}\Delta\mathbf{u}$ term). The iterative perturbation scheme does take this effect into account and gives a higher estimate for the standard deviation.

There is good agreement between the different methods: although all finite element results underestimate the standard deviation when compared with the Monte Carlo results, the largest difference is 2.5% (the Taylor series results). The iterative perturbation results correspond best to the Monte Carlo results.

The MVFO method gives the deterministic result as an estimate for the mean. The mean deflection is expected to be slightly higher than the deterministic deflection for the reasons given above (decreases in stiffness affect the deflection more than increases). This is reflected in the point estimate method involving iterative perturbation and the Monte Carlo method.

The results of the Monte Carlo simulation were used to construct a plot of the cumulative distribution (CDF) of the deflection at E, shown in Figure 6.2. The figure also shows plots which were constructed from the MVFO and point estimate method results. Iterative perturbation schemes were used in both cases. AMVFO results were derived by re-analysing the structure at the most probable points predicted by the MVFO method for

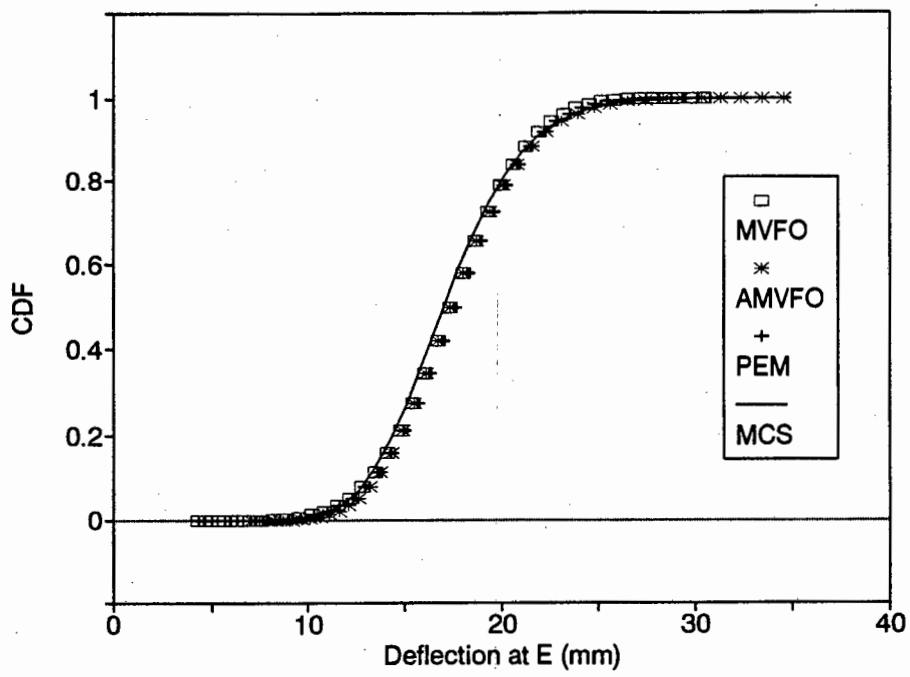

Figure 6.2: Cumulative distribution plot of deflection – crossed beam structure

each deflection level. Good agreement with the Monte Carlo simulation results is achieved by all three perturbation methods. The AMVFO results give the best agreement at the extreme tails, but require re-analysis at each deflection level, which can be computationally significant. The point estimate results follow the shape of the curve better than the MVFO results, but are not representative in the extreme tails.

6.2.2 Plane strain element

A schematic diagram of a square plane strain element subjected to distributed biaxial loading is shown below. The elastic modulus, Poisson's ratio, initial yield stress, hardening modulus and distributed loads are independent random parameters and their stochastic values are listed in Table 6.8. The problem was modelled by a single eight-noded element involving two equal load increments. The distributed loads were chosen to cause mild plastic behaviour in the deterministic problem at full load but to cause only elastic behaviour at half load. Of interest is the Mises stress at half load, the Mises stress at full load and the equivalent plastic strain at full load.

The problem was analysed 250 times with randomly varying properties and loads using the deterministic version of the plane element subroutines. This does not constitute a proper Monte Carlo simulation but computational facilities limited the extent of this. However this limited Monte Carlo simulation was considered sufficient to characterise the probabilistic behaviour of the problem. The problem was devised such that not all trials

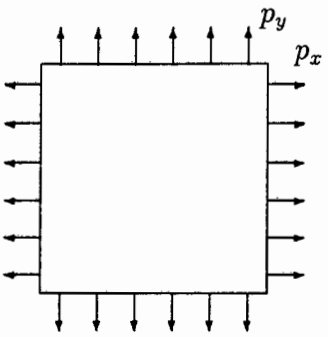

Parameter	Mean	STD	COV
Elastic modulus	200GPa	20GPa	10%
Poisson's ratio	0.3	0.03	10%
Initial yield stress	100MPa	10MPa	10%
Hardening modulus	20GPa	2GPa	10%
Distributed load p_y	150MPa	15MPa	10%
Distributed load p_x	25MPa	2.5MPa	10%

Table 6.8: Problem parameters – plane strain element

would result in plastic behaviour and this was reflected in the Monte Carlo results: in 62 out of 250 trials the Mises stress at full load did not exceed the initial yield stress and zero plastic strain was recorded. The Mises stress results of the Monte Carlo simulation were further analysed using Weibull techniques (Ang and Tang, 1975).

The problem was analysed using the MVFO perturbation method and the point estimate method. Both methods involved full perturbation re-analysis in view of the elastic-plastic behaviour. All random parameters were perturbed both positively and negatively. The mean and standard deviation of the response parameters were calculated using the three methods and are listed in Table 6.9. Good agreement between the three methods is found for the mean and standard deviation of the Mises stress. This appears not to be the case for the equivalent plastic strain. However it must be realised that the Monte Carlo results for the equivalent plastic strain span several orders of magnitude. The feature that the standard deviation of plastic strain is of the same magnitude (PEM) or even larger (MVFO, Monte Carlo simulation) than the mean is also of interest: this confirms that the spread of plastic strain around the mean is large.

The results were used to plot the cumulative distribution (CDF) of the response parameters. The cumulative distribution of the Mises stress at half and full load are plotted

	Mises stress Half load (MPa)		Mises stress Full load (MPa)		Plastic strain ($x10^{-4}$m/m)	
Probabilistic method	Mean	STD	Mean	STD	Mean	STD
MVFO - full perturbation	56.89	6.76	109.82	11.15	4.909	6.955
Point estimate method	56.95	6.76	110.54	11.95	6.508	6.065
Monte Carlo simulation	56.18	7.18	109.34	12.80	6.297	8.462

Table 6.9: Mean and standard deviation of response parameters – plane strain element

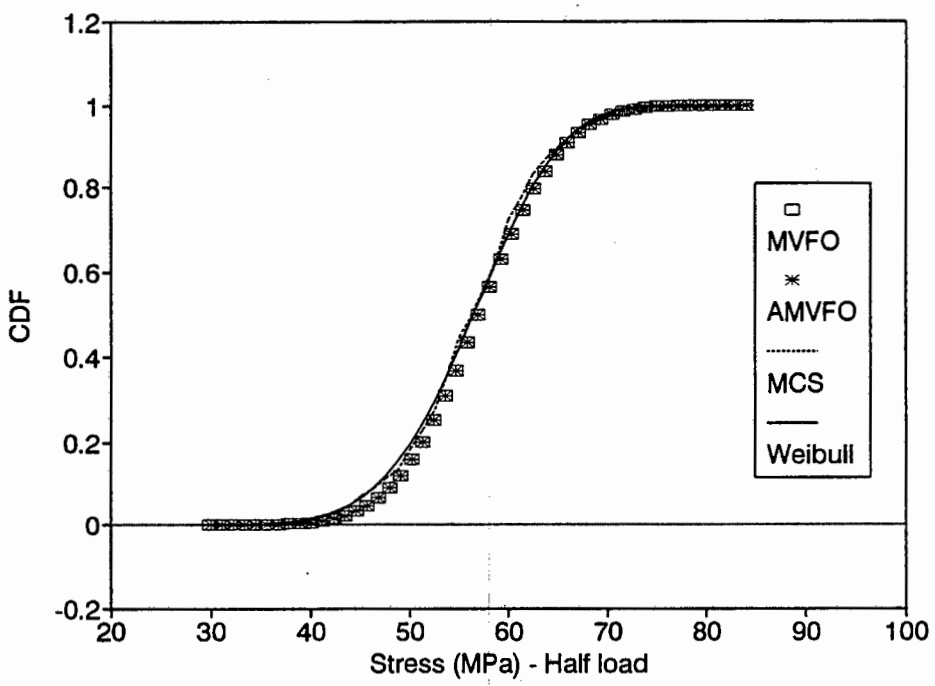

Figure 6.3: Cumulative distribution plot of Mises stress at half load

in Figures 6.3 and 6.4 respectively. In both figures the CDF obtained directly from the Monte Carlo results (MCS) is shown as is the CDF obtained from a Weibull analysis of these results. It can be seen that the Weibull analysis smoothens the original curve.

The MVFO and AMVFO curves follow the Weibull curve except in the bend of the lower tail. The improvement achieved by the re-analysis at the most probable points of the AMVFO method in Figure 6.3 is minimal. This is because the dominant random parameter is the load, to which the Mises stress is linearly related (since the material is still linear elastic at half load). Consequently the error term in the linearised response function is negligible and re-analysis at the most probable points will give little improvement. The re-analysis at the most probable points of the AMVFO method in Figure 6.4 leads to better representation of the upper tail since the stress in this region involves increasing

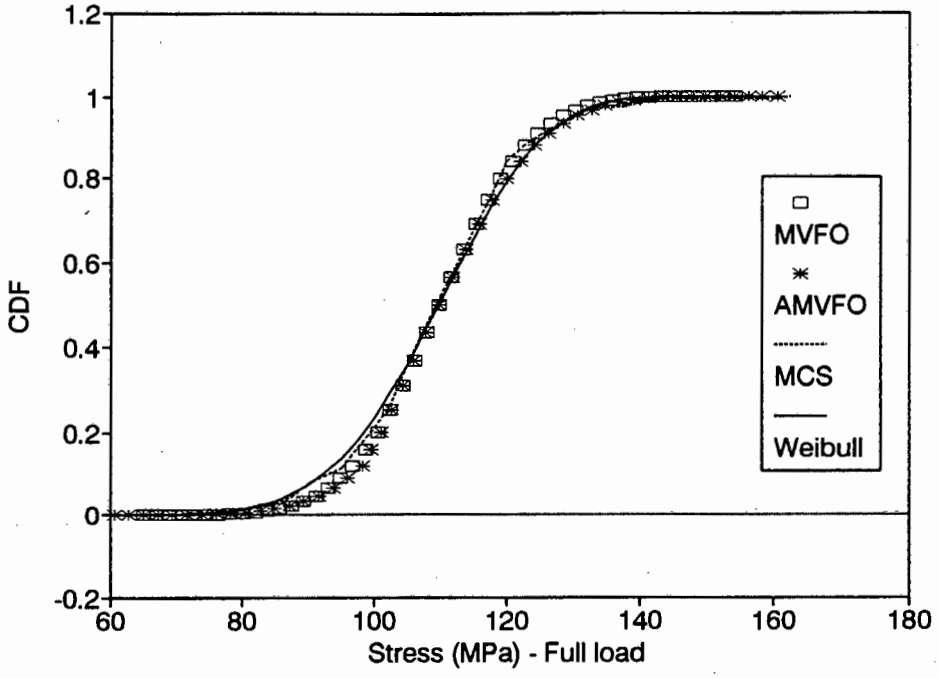

Figure 6.4: Cumulative distribution plot of Mises stress at full load

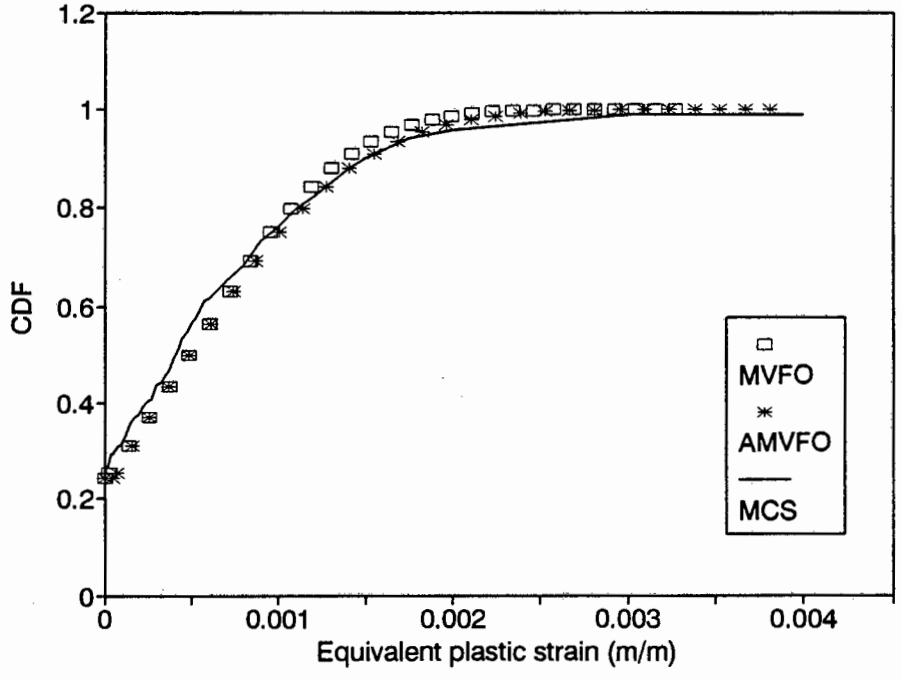

Figure 6.5: Cumulative distribution plot of equivalent plastic strain

amounts of plastic strain which are not fully accounted for by the MVFO results.

The cumulative distribution of the equivalent plastic strain at full load is shown in Figure 6.5. Meaningful Weibull analysis is not possible since this would involve logarithms of zero (zero plastic strain occurred for 62 trials). The CDF obtained directly from the

Monte Carlo results is not smooth but definite trends can nevertheless be seen. Both the MVFO and AMVFO results represent the Monte Carlo results well. The AMVFO is able to make significant improvements in the upper tail region. It is also significant that both the MVFO and AMVFO methods can estimate the probability of zero plastic strain accurately. This is important for (supposedly) linear problems where mild plasticity is acceptable provided the probability of this occurring is low.

6.2.3 Propped cantilever

Lawrence (1986, 1987) analysed a propped cantilever which is shown schematically below. The left cantilever consists of a single component and the right cantilever consists of two components welded together for which the stiffness is statistically independent. A point load is applied at the free end. The tip deflection is of interest.

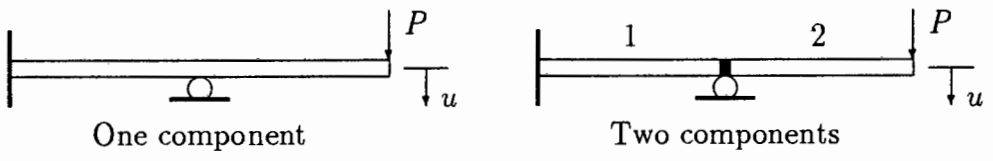

One component Two components

The random parameters considered by Lawrence are the stiffness $k = EI$ and the load P. This formulation was adapted to one consistent with the present one (i.e. involving a separate elastic modulus and moment of area). The original and representative stochastic values are shown in Table 6.10.

Lawrence (1986, 1987) specifies that the stiffness has a correlation decay factor of 44.75. The effect of correlation on the standard deviation as a function of the distance between two points on the beam is plotted in Figure 6.6 (data from other sources in the figure will be considered later). It is argued here that the correlation decay length is such that the cantilever can be considered almost fully correlated along the length. Similar results to those of Lawrence should therefore be obtained by neglecting the effects of correlation.

Parameter	Length l	Stiffness $k = EI$	Load P	Elastic modulus E	Moment of area I
Mean	24	10	$1\text{x}10^{-2}$	$1.2\text{x}10^{6}$	$8.33\text{x}10^{-6}$
STD	-	1	$1\text{x}10^{-3}$	$1.2\text{x}10^{5}$	-
COV	-	10%	10%	10%	-

Table 6.10: Problem parameters – propped cantilever

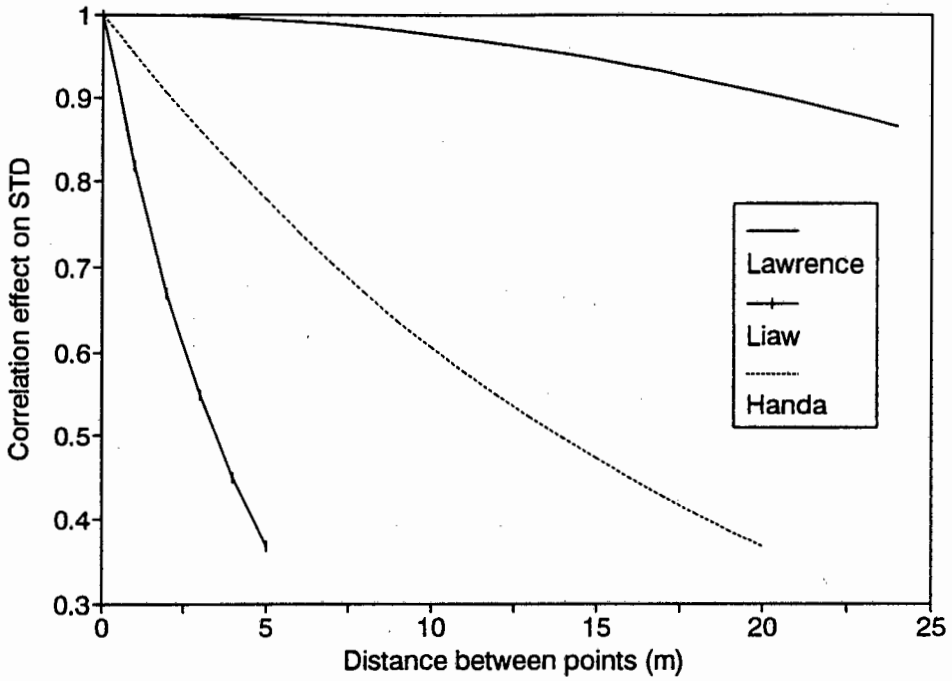

Figure 6.6: Effect of partial correlation on standard deviation

Problem	Probabilistic method	Mean	STD	COV (%)
One component	MVFO - iterative perturbation			
	P, E: positive and negative	1.0081	0.1433	14.21
	P: positive; E: negative	1.0081	0.1508	14.96
	MVFO - Taylor series perturbation			
	P, E: positive and negative	1.0081	0.1426	14.15
	P: positive; E: negative	1.0081	0.1426	14.15
	Point estimate method			
	Iterative perturbation	1.0180	0.1472	14.46
	Taylor series perturbation	1.0081	0.1426	14.15
	Lawrence (1986, 1987)	1.0186	0.1410	13.84
Two component	MVFO - iterative perturbation			
	P, E: positive and negative	1.0081	0.1243	12.33
	P: positive; E: negative	1.0081	0.1288	12.78
	MVFO - Taylor series perturbation			
	P, E: positive and negative	1.0081	0.1239	12.29
	P: positive; E: negative	1.0081	0.1239	12.29
	Lawrence (1986, 1987)	1.0209	0.1289	12.63

Table 6.11: Tip deflection results – propped cantilever

The propped cantilever was modelled by ten three-noded elements. For the one component beam all elements were perturbed together. For the two component beam the elements corresponding to the two components were perturbed separately (i.e. two independent zones were considered and two separate probabilistic analyses were performed). The results from different perturbation methods are listed in Table 6.11. Good agreement is found between the results of Lawrence (1986, 1987) and the results of the present methods, although the present methods tend to underestimate the mean tip deflection.

6.2.4 Simply-supported beam

Liaw and Yang (1989) considered a simply-supported beam with distributed load as shown schematically below. The midspan deflection is of interest. The distributed load is a random parameter. The problem parameters are listed in Table 6.12.

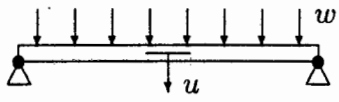

Parameter	Length l	Elastic modulus E	Moment of area I	Load w
Mean	5m	210GPa	$26.72\text{x}10^{-6}\text{m}^4$	2,000N/m
STD	-	-	-	200N/m
COV	-	-	-	10%

Table 6.12: Problem parameters – simply-supported beam

Liaw and Young considered three cases of correlation: full, partial and zero correlation. Full correlation can be dealt with directly by the present method. The effect of partial correlation on the standard deviation as a function of the distance between two points on the beam is plotted in Figure 6.6. The correlation effect reaches 0.5 at slightly more than half the beam distance. It is argued here that by modelling the beam to consist of two independent zones, the effect of partial correlation can be approximated. Similarly, zero correlation is estimated by considering ten independent zones.

Liaw and Yang (1989) present results achieved from mean value second order methods (MVSO) which include correlation directly in the analysis. They also present an analytical solution. Their results and those predicted by the present MVFO method are shown in

Correlation type	Mean deflection (mm)			STD deflection (mm)		
	MVFO	MVSO	Analytical	MVFO	MVSO	Analytical
Full correlation	2.939	2.901	2.901	0.294	0.290	0.290
Partial correlation	2.939	2.901	2.901	0.208	0.233	0.233
Zero correlation	2.939	2.901	2.901	0.103	0.0457	0.0457

Table 6.13: Midspan deflection results – simply-supported beam

Table 6.13. The MVFO results are achieved from Taylor series perturbation involving positive perturbation of the load. The mean midspan deflections predicted by MVFO differ from the MVSO and analytical results as the latter are based on conventional beam formulation. The length-to-depth ratio is approximately 25 and shear effects will increase the deflections (albeit to a small extent). All methods predict a coefficient of variance of 10% for the full correlation case. This is expected since the deflection is linearly related to the distributed load. The MVFO results for the partially correlated load agree reasonably with the MVSO and analytical results. The MVFO results for zero correlation do not compare well, although they show that the coefficient of variance is significantly reduced by zero correlation of the load.

6.2.5 Cantilever tube

Handa and Andersson (1981) analysed a cantilever tube subjected to a distributed load as shown schematically below. The elastic modulus, moment of area and distributed load are independent random parameters. The problem parameters are listed in Table 6.14. The coefficient of variance of the deflection along the tube length is of interest for the cases of full correlation along the length, partial correlation and zero correlation. The effect of partial correlation on the standard deviation as a function of the distance between two points on the beam is plotted in Figure 6.6. The effect reaches 0.5 for a distance between points of slightly more than half the tube length. To approximate the effects of partial correlation, the tube was modelled as two independent zones. The effect of zero correlation was estimated by modelling the tube as ten independent zones.

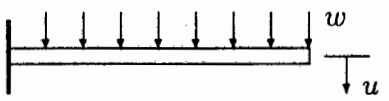

Parameter	Length l	Diameter D	Moment of area I	Elastic modulus E	Load w
Mean	20m	1m	$3.8\text{x}10^{-3}\text{m}^4$	210GPa	100N/m
STD	-	-	$3.8\text{x}10^{-4}\text{m}^4$	10.5GPa	25N/m
COV	-	-	10%	5%	25%

Table 6.14: Problem parameters – cantilever tube

Probabilistic method	Mean (mm)	STD (mm)	COV (%)
MVFO - iterative perturbation			
w, E, I: positive and negative	2.522	0.691	27.4
w: positive; E, I: negative	2.522	0.702	27.8
MVFO - Taylor series perturbation			
w, E, I: positive and negative	2.522	0.691	27.4
w: positive; E, I: negative	2.522	0.691	27.4
Point estimate method			
Iterative perturbation	2.553	0.702	27.5
Taylor series perturbation	2.522	0.691	27.4
Handa and Andersson (1981)			
MVFO - Taylor series perturbation	-	-	27.6
Liaw and Yang (1989)			
MVSO - Taylor series perturbation	-	-	27.0
Monte Carlo Simulation	2.539	0.703	27.7

Table 6.15: Cantilever tube tip deflection results – full correlation

Table 6.15 shows the results for the tip deflection in the case of full correlation. The MVFO and PEM results are very similar. This is because the randomness of the distributed load dominates in this problem. The results agree well with the original results of Handa and Andersson (1981) and later results of Liaw and Young (1989). These results were scaled from graphs in their respective papers. The results also correlate with a Monte Carlo simulation involving 20,000 trials of an analytical expression for the deflection of a cantilever beam.

Figure 6.7 shows a plot of the coefficient of variance along the beam length for the three levels of correlation. The results of Handa and Andersson (1981) are reproduced here, having been scaled from a graph in their paper. There is good agreement between the present results and those of Handa and Andersson for the case of full correlation. The

Parameter	Length l	Cross-section A	Moment of area I	Elastic modulus E	Load P
Mean	20in	3in x 1in	2.25in^4	30x10^{6}psi	1000lbs
STD	-	-	-	3x10^{6}psi	200lbs
COV	-	-	-	10%	20%

Table 6.16: Problem parameters – cantilever beam

The problem was solved by the repeated AMVFO method: the MVFO results about the deterministic values of the random parameters are obtained as usual. The most probable points for a range of responses can then be predicted and better estimates can be obtained by the AMVFO method. The specific most probable point which, when the structure is re-analysed at it, results in a response closest to the failure criterion is used to generate a better estimate of the linearised failure surface. This is achieved by performing another probabilistic perturbation analysis to calculate the response gradients at this most probable point. This procedure is repeated until convergence is reached (i.e. response gradients are stationary).

In the first iteration of the problem, the perturbation amounts used were one standard deviation of the random parameters. In further iterations, 10% of the values of the most probable point were used to perturb the random parameters. The problem was solved using the Timoshenko beam formulation implemented in the finite element subroutines. Different perturbation methods and types were used. The results are listed in Table 6.17. The results predicted by the different methods are similar since the loading is the dominant parameter and any differences are smoothed by the repeated AMVFO process. The results are independent of the perturbation type used for the Taylor series perturbation method. In all cases convergence was achieved by the third iteration.

The above approach predicted a probability of failure higher than predicted by Gopalakrishna and Donaldson (1991). Their approach used a conventional beam formulation. The length to depth ratio of the beam is approximately 7. Figure 6.1 shows that in this case shear effects are important and will increase the deflection of the beam. To check the repeated AMVFO method against the results of Gopalakrishna and Donaldson (1991), the repeated AMVFO procedure was performed manually using the analytical expression for a conventional cantilever beam and a full perturbation scheme. The converged results are included in Table 6.17 and match the results of Gopalakrishna and Donaldson (1991) and an analytical solution based on conventional beam theory.

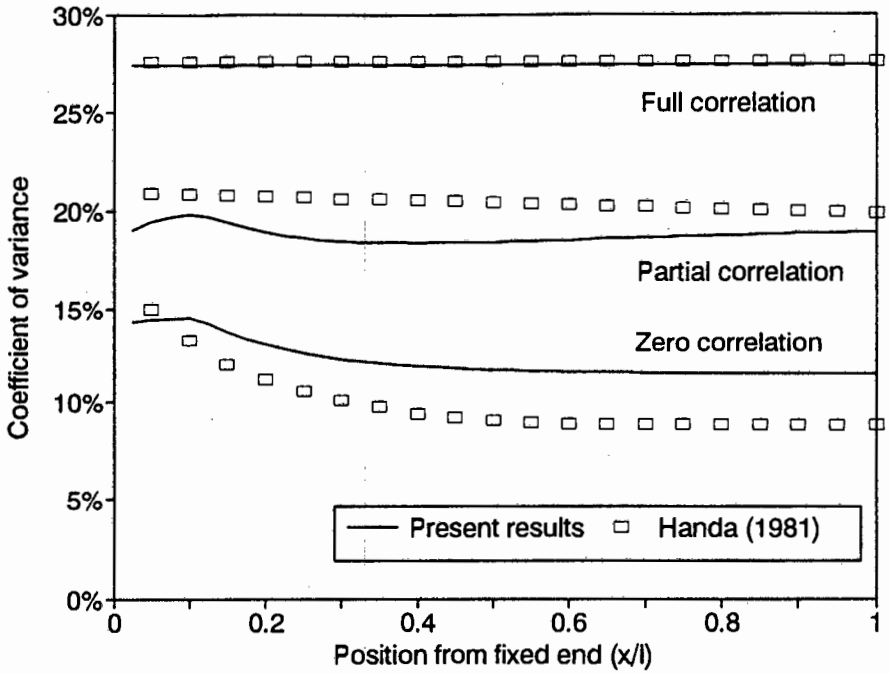

Figure 6.7: Coefficient of variance along cantilever tube length

present methods can also give reasonable approximations for the partial and zero correlation. The cause for the kink in the curve of the present results is unknown, but it is expected that it is due to the interaction of loading and stiffness: a local change in stiffness will have a bigger influence on the overall deflection of the tube if it occurs at the fixed end. On the other hand, a local change in distributed load will have a bigger influence on the tube deflection if it occurs at the free end. It is possible to hypothesise that the kink will continue to move to the left as more and more independent zones are used, and vanish as zero correlation is reached (using infinitely many independent zones).

6.2.6 Cantilever beam

Gopalakrishna and Donaldson (1987, 1991) have analysed a cantilever beam with a point load at the free end as shown schematically below. The deflection at the free end is of interest when the load and elastic modulus are random parameters. The problem parameters are listed in Table 6.16. The probability that the tip deflection exceeds 0.08in must be estimated.

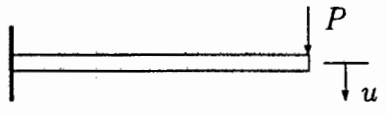

Probabilistic method	E^* (x10^6psi)	P^* (lbs)	β	p_f (x10^{-3})
Repeated AMVFO - iterative perturbation				
P, E: positive and negative	22.59	1497.1	3.505	0.2283
P: positive; E: negative	22.22	1474.6	3.509	0.2249
Repeated AMVFO - Taylor series perturbation				
P, E: positive and negative	22.59	1496.0	3.501	0.2318
P: positive; E: negative	22.59	1496.0	3.501	0.2318
Conventional beam formulation				
Repeated AMVFO - full perturbation				
P, E: positive and negative	22.28	1503.3	3.599	0.1597
Gopalakrishna and Donaldson (1991)				
ANSYS optimisation scheme	22.13	1495.5	3.608	0.1543
Analytical solution (Figure 6.8)	22.32	1506	3.601	0.1591
Monte Carlo Simulation				
Conventional beam formulation	-	-	-	0.113
Timoshenko beam formulation	-	-	-	0.172

Table 6.17: Resultant most probable points and reliability indices – cantilever beam

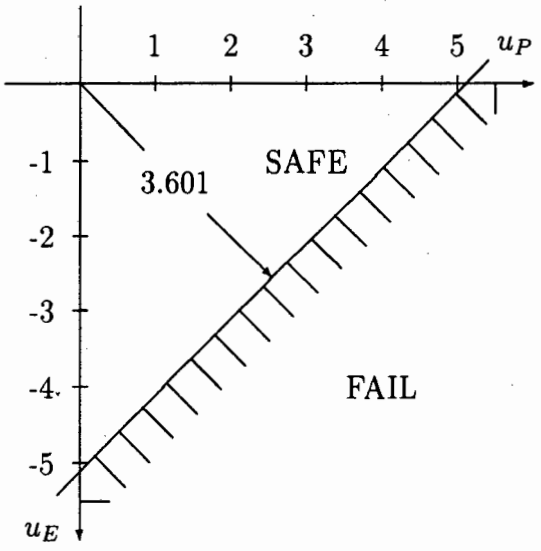

Figure 6.8: Schematic representation of failure function in transformed coordinates

This analytical solution can be obtained by representing the failure function in terms of transformed standard normal coordinates u_E and u_P. This failure function is drawn in Figure 6.8 and the minimum distance from the origin to the failure function is the exact reliability index from which the probability of failure can be found.

The problem was also solved using Monte Carlo simulation involving an analytical expression for the deflection of a cantilever beam. Both conventional beam and Timoshenko beam formulations were considered. As the probability of failure was low, one million trials were involved since it was found that for a lower number of trials the results were not stable. The simulations predict a lower failure probability than the analytical (exact) solution indicates. This is probably because the numerical random number generator is unable to generate random values accurately in the extreme tails of the distribution. However, the Monte Carlo results are of the same order of magnitude, and display the same characteristics for the conventional and the Timoshenko formulation as the finite element solutions.

6.2.7 Plane frame

Hisada and Nakagiri (1985) analysed a plane frame subjected to a side load as shown schematically below. The moments of area of the beams, the load and the failure deflection are independent random parameters, listed in Table 6.18. The moments of area of the vertical and horizontal beams are statistically independent. The probability that the deflection at the load exceeds the failure deflection is of interest.

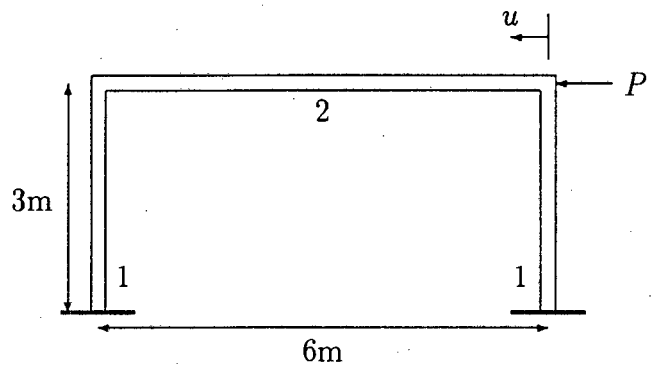

Parameter	Elastic modulus	Moment of area		Side load	Deflection
	E	I_1	I_2	P	u_{fail}
Mean	2,500kgf/mm^2	3.0x10^{-4}m^4	4.0x10^{-4}m^4	2,000kgf	12mm
STD	-	7.5x10^{-5}m^4	1.0x10^{-4}m^4	600kgf	1.5mm
COV	-	25%	25%	30%	12.5%

Table 6.18: Problem parameters – plane frame

The problem was solved by the repeated AMVFO method involving two independent zones: the MVFO results about the deterministic values of the random parameters are

Probabilistic method	I_1^* (x10^{-4}m^4)	I_2^* (x10^{-4}m^4)	P^* (kgf)	u^* (mm)	β
Repeated AMVFO - iterat. perturb.					
P, I: positive and negative	1.55	3.65	2,700	10.91	2.398
P: positive; I: negative	1.50	3.66	2,650	11.00	2.396
Repeated AMVFO - Taylor perturb.					
P, I: positive and negative	1.56	3.66	2,700	10.88	2.383
Hisada and Nakagiri (1985)					
Repeated AMVFO - Taylor perturb.	1.56	3.67	2,670	10.98	2.345
Repeated AMVFO - full perturb.	1.51	3.68	2,700	10.92	2.429

Table 6.19: Resultant most probable points and reliability indices – plane frame

obtained by perturbing the vertical and horizontal beams in separate analyses. The most probable points for a range of structural responses can then be predicted. The randomness of the failure deflection was included in the fast probability integration and most probable points for failure for a range of structural responses were obtained. Better estimates of the structural response were obtained by the repeated AMVFO method by re-analysing at the most probable points. The specific most probable point which, when the structure is re-analysed at it, results in a response closest to the corresponding most probable point of failure is used to generate a better estimate of the linearised failure surface. This is achieved by performing another probabilistic perturbation analysis to calculate the response gradients at this most probable point. This procedure is repeated until convergence is reached (i.e. response gradients are stationary).

In the first iteration of the problem, the perturbation amount used was one standard deviation of the random parameters. In further iterations, 10% of the values of the most probable point were used to perturb the random parameters. Different perturbation schemes and types were used. The results are listed in Table 6.19.

The results compare well with those of Hisada and Nakagiri (1985). The difference between the various perturbation schemes is minimal although there appears to be a correspondence in reliability index between the present Taylor series perturbation results and those of Hisada and Nakagiri and the present iterative perturbation results and the full perturbation results of Hisada and Nakagiri. The number of iterations to reach convergence is between five and eight which is consistent with the findings of Hisada and Nakagiri (1985). The iterative perturbation scheme involving positive and negative perturbations reached convergence in the least number of iterations.

7 Case Studies

To illustrate the application of the probabilistic finite element routines that were developed in this thesis, two case studies are presented in this chapter. The first analyses a four-story, two-bay plane frame structure with random wind and floor loads, elastic moduli and moments of area. The second case study analyses a reactor pressure vessel nozzle with random internal pressure, piping system reaction moments and material properties.

7.1 Plane Frame Structure

A four-story building can be modelled as a four-story, two-bay plane frame structure by "collapsing" the depth of the building. The resulting plane frame structure is shown schematically in Figure 7.1. The distributed loads acting on the building are similarly modelled: the wind pressures on the side wall and roof, self-weight and floor loads are represented by equivalent loads distributed along the length of the frame members.

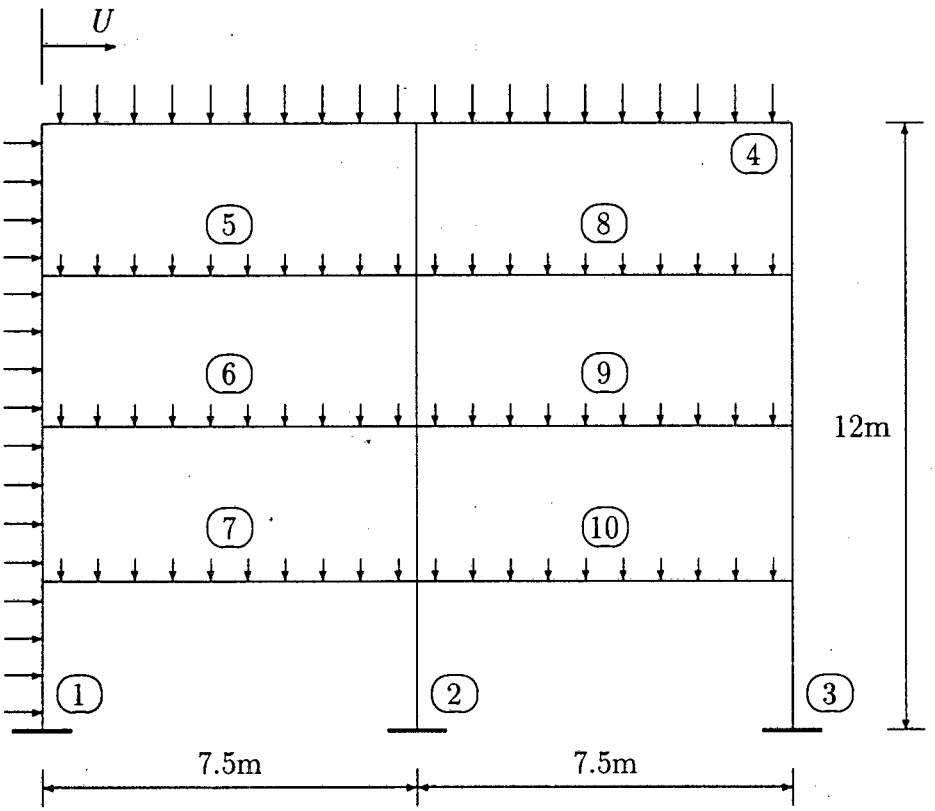

Figure 7.1: Four-story, two-bay frame structure

Parameter	Description	Mean	STD	COV
w_1	Side load due to wind (kN/m)	15	3	20%
w_4	Roof load due to wind (kN/m)	5	1	20%
	Self-weight (kN/m)	5	-	-
w_5 - w_{10}	Floor loads (kN/m)	2.5	0.375	15%
	Self-weight (kN/m)	2.5	-	-
E_1 - E_4	Elastic modulus (GPa)	200	20	10%
E_5 - E_{10}		180	18	10%
I_1 - I_4	Moment of area (10^{-6}m^4)	800	80	10%
I_5 - I_{10}		600	60	10%

Table 7.1: Problem parameters – frame structure

Parameter	Description	Mean	STD	COV	p_f
U	Limiting horizontal drift (mm)	20	4	20%	$1x10^{-2}$
M_1 - M_4	Limiting bending moment (kNm)	240	18	7.5%	$5x10^{-4}$
M_5 - M_{10}	Limiting bending moment (kNm)	150	9	6%	$5x10^{-4}$

Table 7.2: Failure criteria and design reliability specifications – frame structure

Ten frame members form the structure: three vertical columns, a roof beam and six floor beams. The beams and columns are constructed from reinforced concrete. The model parameters associated with the problem are listed in Table 7.1. The variance of the wind and floor loads correspond to fluctuations with time and the variance of the elastic modulus and moment of area of the beams correspond to differences from design and construction specifications. The self-weight of the beams is considered deterministic since any variation will be small compared to the wind and floor loads. The wind loads acting on beams 1 and 4 are correlated and their magnitudes correspond to mean maximum wind-gust speeds with a one year return period (i.e. a wind load of this magnitude is likely to occur once a year). The floor loads acting on beams 5 to 10 are considered statistically independent as are the stiffness properties of all the beams. The random parameters are assumed to be normally distributed.

Two types of failure criteria are considered: limiting horizontal drift or sway of the structure and limiting bending moment in a beam. The failure criteria are listed in Table 7.2. The horizontal drift constraint corresponds to a comfort criterion and a structural failure criterion, since if excessive horizontal drift occurs building fixtures and cladding will fail.

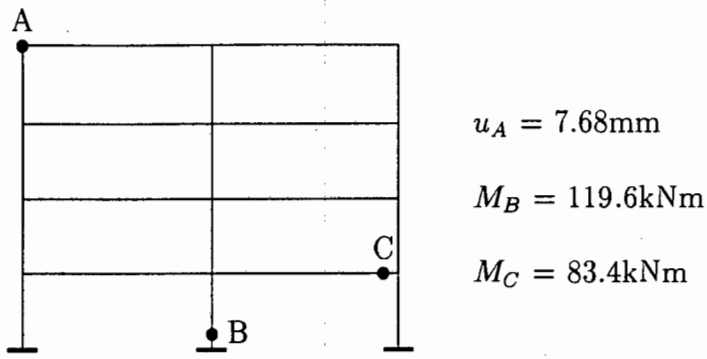

Figure 7.2: Points of maximum deflection and bending moment

The limiting bending moment corresponds to a failure criterion for the structural members since an excessive bending moment will lead to excessive tensile stresses and cracking in the concrete. The limiting bending moment criteria depend on the cross-section of the structural members. The consequences of failure due to excessive bending moment are more severe than failure due to excessive drift.

The object of the probabilistic analysis is to evaluate the mean and standard deviation of the response of the structure and to estimate the probability of exceeding the limiting drift criterion and the limiting bending moment criterion in order to ensure that they are less than the design specifications of $1\text{x}10^{-2}$ and $5\text{x}10^{-4}$ respectively.

The first step in the analysis is to calculate the deterministic response of the structure and determine where in the structure the maxima of horizontal deflection and bending moment occur. A finite element model involving 128 three-noded beam elements was used to analyse the structure at the mean values of the random parameters. The magnitudes and positions of the maximum horizontal deflection and bending moments were obtained and these are indicated in Figure 7.2. Since the limiting bending moment is different for beams 1-4 and beams 5-10, the maximum for each set was found.

The probabilistic structural analysis concentrates on the points at which maximum response occurs. Since the stiffness properties of the beams and the floor loads are statistically independent, the total number of independent random variables is 27. It is therefore not feasible to use the point estimate method. The problem can be solved by the MVFO method by considering the ten beams separately. Ten probabilistic finite element analyses were performed in each of which the appropriate parameters were perturbed (e.g. in the first analysis only the distributed load acting on beam 1 and its elastic modulus and moment of area were perturbed; in the third analysis only the elastic modulus and moment of area of beam 3 were perturbed as there is no load acting on this beam). The distributed load acting on beam 4 was perturbed with the distributed load on beam 1. A

fast probability integration analysis was then performed involving the results of these ten perturbed analyses from which the mean, standard deviation and coefficient of variance at the points of maximum deflection and bending moment were evaluated.

This process was performed for the Taylor series perturbation and iterative perturbation schemes, and involving in each case positive and negative perturbation of all the random parameters and perturbation of the random parameters in the direction which would cause the highest deflection. The results of these analyses are presented under condition A in Table 7.3.

There is almost no difference between the MVFO results for the different perturbation schemes and the results for the two types of Taylor series perturbation are identical. This is because the variance in the deflection and bending moment is largely load controlled and both the Taylor series and iterative perturbation give the full perturbation result if the load is perturbed. The coefficient of variance of the deflection at A and the moment at B are both higher than that of the wind load. The coefficient of variance of the moment at C is lower than that of the wind load.

The FPI program can produce the MVFO cumulative distribution data for the response and the most probable points for each response level. These most probable points can be used to re-analyse the structure to find better estimates of the response at a particular probability level through the AMVFO procedures. Figures 7.3 to 7.5 plot the MVFO and selected AMVFO results. The AMVFO re-analysis was performed only for the upper tail of the CDF as only this region is of interest. The AMVFO results indicate that the extreme values of the response of the structure are higher than indicated by the MVFO analysis.

The CDF plots indicate that the structural response can reach levels which approach the mean failure criteria, but at very low levels of probability. The CDF plots do not take variance of the failure criteria into account.

While the CDF plots are convenient to the designer in providing initial estimates of the probabilistic response of a structure and to decide on the required minimum "strength" of the materials for construction, they are not sufficiently refined to estimate the probability of failure of a structure if this probability of failure is low. Repeated AMVFO techniques must then be used to find the probability of failure by an iterative procedure. This process was performed using the Taylor series perturbation scheme involving positive perturbation of the random parameters. This perturbation scheme was chosen because the difference between the different perturbation schemes is negligible in this problem, and the Taylor series perturbation is computationally more efficient than the iterative perturbation scheme when the stiffness is perturbed.

Condition	Probabilistic method	Deflection at A (mm)			Moment at B (kNm)			Moment at C (kNm)		
		Mean	STD	COV	Mean	STD	COV	Mean	STD	COV
A	MVFO - iterative perturbation									
	w, E, I: positive and negative	7.68	1.578	20.6%	119.6	26.50	22.2%	83.4	14.64	17.6%
	w: positive; E, I: negative	7.68	1.582	20.6%	119.6	26.60	22.2%	83.4	14.74	17.7%
	MVFO - Taylor series perturbation									
	w, E, I: positive and negative	7.68	1.578	20.6%	119.6	26.75	22.4%	83.4	14.87	17.8%
	w: positive; E, I: negative	7.68	1.578	20.6%	119.6	26.75	22.4%	83.4	14.87	17.8%
B	MVFO - iterative perturbation									
	w: positive; E, I: negative	7.68	1.731	22.5%	119.6	33.80	28.3%	83.4	19.14	22.9%
C	MVFO - iterative perturbation									
	w, E, I: positive and negative	7.68	1.882	24.5%	119.6	23.92	20.0%	83.4	13.09	15.7%
	w: positive; E, I: negative	7.68	1.942	25.3%	119.6	23.91	20.0%	83.4	13.07	15.7%
	PEM - iterative perturbation	7.84	1.928	24.6%	119.6	23.90	20.0%	83.4	14.36	17.2%
	PEM - Taylor series perturbation	7.68	1.880	24.5%	117.2	24.30	20.7%	81.7	14.61	17.9%

Table 7.3: MVFO and PEM results – plane frame structure

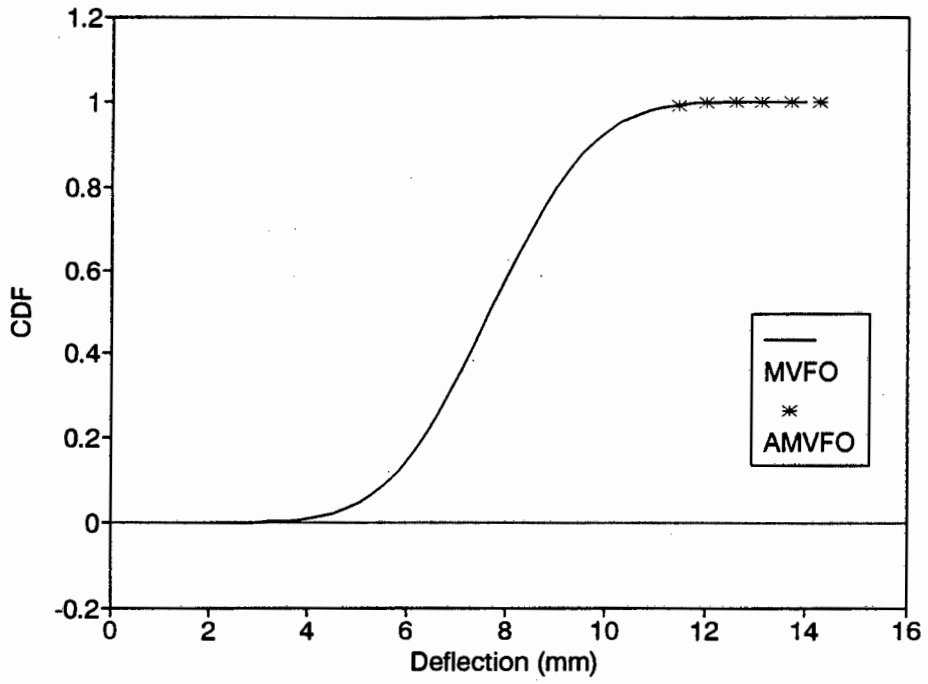

Figure 7.3: Cumulative distribution plot of deflection at A

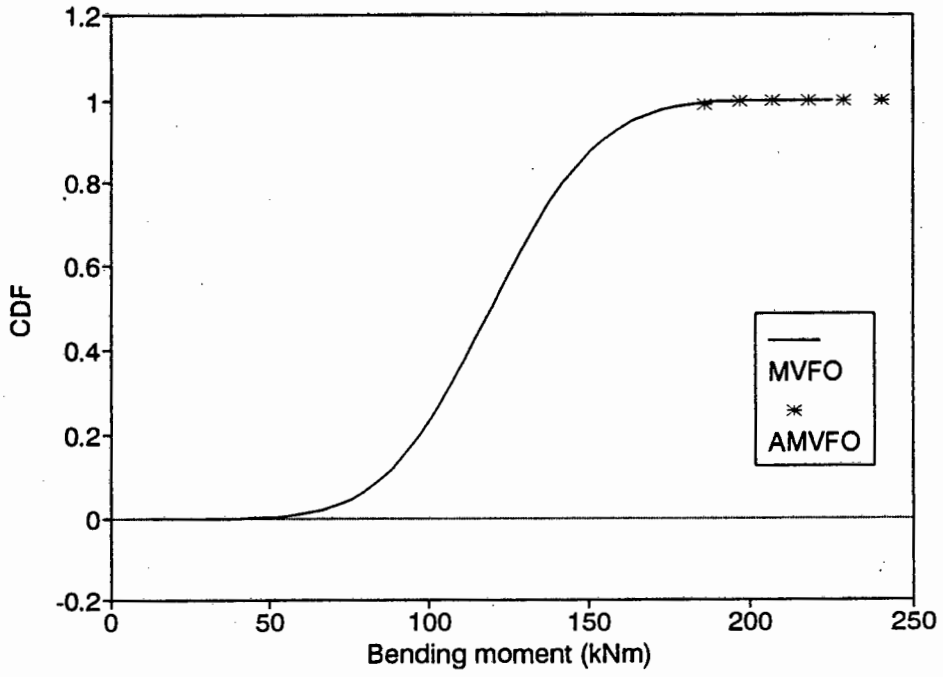

Figure 7.4: Cumulative distribution plot of bending moment at B

The results of the repeated AMVFO procedure are shown in Table 7.4 which lists the probability of failure for the three failure criteria and the most probable points for failure to occur. The repeated AMVFO procedure converged by the third iteration for each case. The probability of failure is smaller than the design specification in each instance.

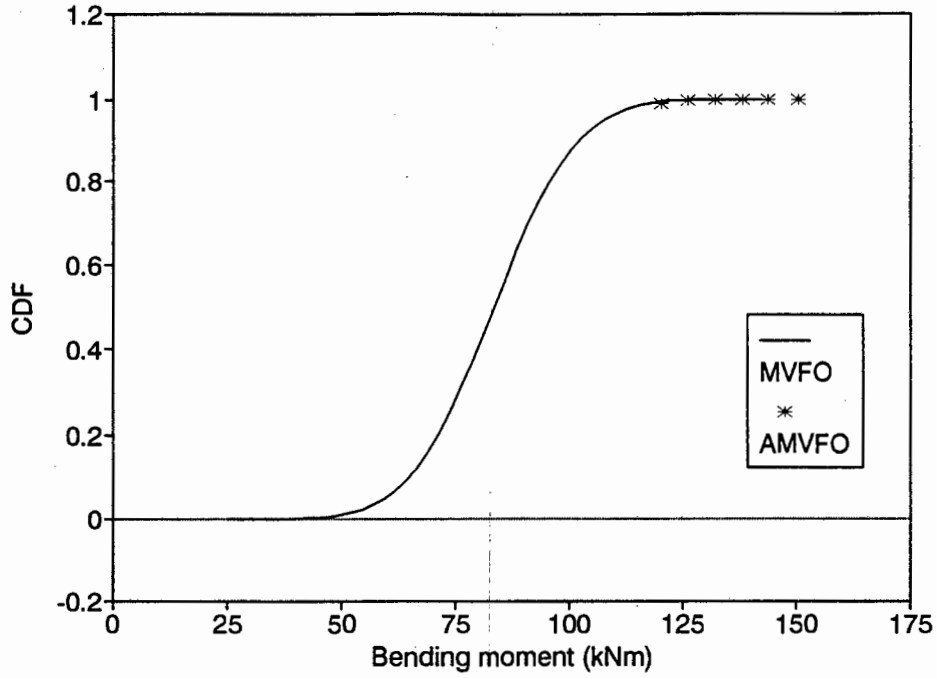

Figure 7.5: Cumulative distribution plot of bending moment at C

The values for the most probable points show that in each instance the variance in the wind load and the failure criterion itself are the dominant factors through which failure can occur. This feature was noted after the first iteration in the repeated AMVFO procedure, and further perturbation steps involved only the parameters for which the most probable points were significantly different from their mean value (i.e. those parameters which contributed significantly to the standard deviation of the structural response). In this way the number of random parameters could be reduced thus reducing the computational requirements. This simplification is consistent with the proposals of Hasofer and Lind (1974).

The conclusion that failure of the building is dependent largely on extreme values of the wind load and the "strength" of the structure is consistent with the expected behaviour of the structure: damage to fixtures and failure of structural members is associated with storms and other extreme weather conditions. Variation of the wind load has an effect over the entire structure whereas variation of the floor loads, elastic modulus and moment of area has only a localised effect since these random parameters are not correlated between the different beams. The coefficient of variance of the wind load is also higher than for the floor loads and stiffness parameters.

The effect of a higher coefficient of variation of the stiffness parameters on the structural response was investigated. The coefficients of variation of the elastic modulus and moment of area were increased to 20% and an MVFO probabilistic analysis was performed using the iterative perturbation scheme. The results are presented under condition B in Table 7.3.

	Deflection at A	Moment at B	Moment at C
β	2.864	3.481	3.576
p_f	$2.1\text{x}10^{-3}$	$2.5\text{x}10^{-4}$	$1.7\text{x}10^{-4}$
Z_f^*	9.33mm	210.87kNm	136.51kNm
w_1^* (kN/m)	18.07	22.74	22.98
w_5^*	2.50	2.50	2.50
w_6^*	2.50	2.50	2.50
w_7^*	2.50	2.51	2.50
w_8^*	2.50	2.50	2.50
w_9^*	2.50	2.50	2.50
w_{10}^*	2.50	2.49	2.58
E_1^* (GPa)	199	193	194
E_2^*	198	222	195
E_3^*	199	193	200
E_4^*	200	200	200
E_5^*	179	180	180
E_6^*	179	180	180
E_7^*	179	177	173
E_8^*	179	180	180
E_9^*	179	180	180
E_{10}^*	179	177	201
I_1^* ($\text{x}10^{-6}\text{m}^4$)	796	773	778
I_2^*	792	887	780
I_3^*	795	773	800
I_4^*	798	800	800
I_5^*	598	600	600
I_6^*	596	600	600
I_7^*	596	589	577
I_8^*	598	600	600
I_9^*	596	600	600
I_{10}^*	597	589	670

Table 7.4: Most probable points and probability of failure – plane frame structure

Increasing the coefficient of variance of the stiffness parameters from 10% to 20% raises the coefficient of variance of the structural response, and these effects are more pronounced in the bending moments at B and C. This is because a positive change in stiffness in a single beam causes that beam to carry a higher portion of the applied loading. The wind load and failure criteria remain the dominant parameter to cause failure. A coefficient of variation of 20% in the stiffness parameters is unlikely to occur in practice is since high deviations from the design specification would be noticed during construction.

The effect of full correlation between the beams was investigated, and full correlation of the floor loads and stiffness parameters between the different beams was assumed. This would correspond to the situation when a mistake in construction affected all the columns

and beams, and the maximum floor load of the building was exceeded throughout. The coefficients of variance listed in Table 7.1 were used but the random parameters were perturbed together in the probabilistic analysis. An MVFO analysis involving iterative perturbation and a PEM analysis were performed. The results are listed under condition C in Table 7.3. This condition increases the coefficient of variance of the deflection at A since a change in stiffness is effected throughout the structure. It lowers the coefficient of variance of the bending moment at B and C since a change in stiffness does not cause any particular member to carry a disproportionate amount of the applied load. The MVFO and PEM results agree except for the coefficient of variance of the bending moment at C, for which PEM predicts higher values.

7.2 Reactor Pressure Vessel Nozzle

A reactor pressure vessel nozzle connects a cylindrical reactor pressure vessel with an elliptical dome to an inlet pipe. The nozzle is connected to the inlet pipe by a flange and to the dome by a weld. The nozzle is shown schematically in Figure 7.6. The geometry is based on an existing pressure vessel, but other problem parameters have been modified for the purpose of this case study.

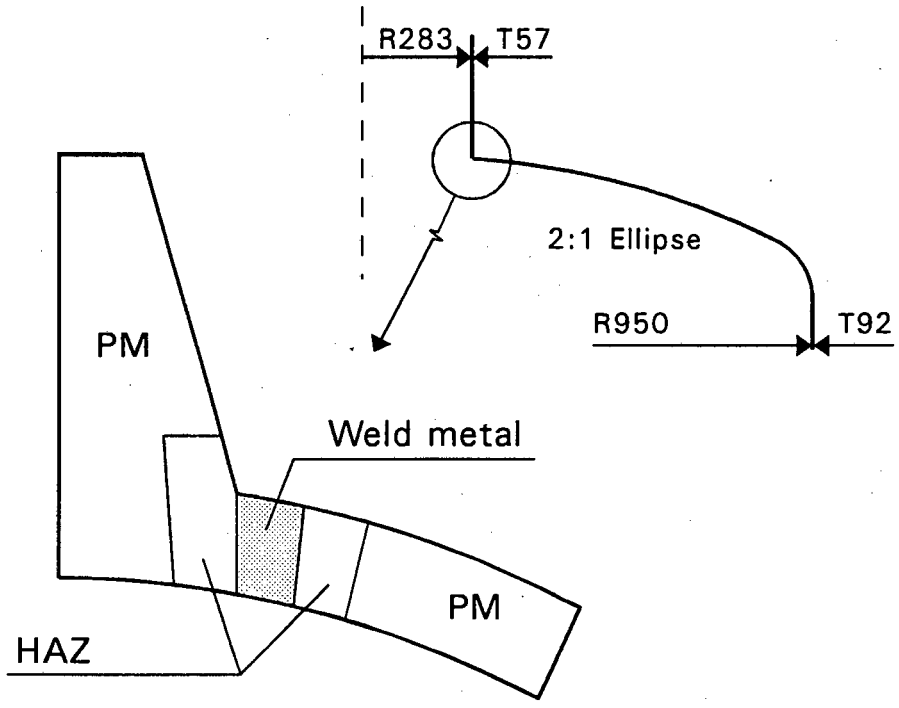

Figure 7.6: Reactor pressure vessel nozzle

The pressure vessel operates at a nominal pressure of 3MPa and a nominal temperature of 500°C. The material of construction is a 1%CrMo steel, typically used for high temper-

ature applications in the 1960's and 1970's. The vessel has been in operation for 170,000 hours. Non-destructive examination of the weld region using replicas has revealed that creep has caused degradation of the nozzle material in the weld metal/heat affected zone interface on the nozzle side where oriented cavitation and micro-cracking were found. This examination indicates that creep cracking through the linking of micro-voids has initiated and that vessel integrity is starting to deteriorate. However no cracks were detected by ultrasonic measurements during the last shutdown.

The location of the maximum creep damage corresponds to the findings of Price and Alberry (1988). Creep damage has a tendency to accumulate more quickly in the weld metal/heat affected zone interface, and in this problem the effect is compounded by the fact that this is also the region of highest stress. The approximate regions of weld metal (WM), heat-affected zone (HAZ) and parent metal (PM) are indicated in Figure 7.6. The material parameters describing these regions can be considered statistically independent.

A deterministic creep stress and fracture analysis was performed and it is anticipated that vessel integrity will not be impaired until the next shutdown, provided no extreme pressure/temperature excursions occur. Of concern is the probability that an extreme load excursion coupled with reduced strength of the steel may lead to sudden and catastrophic failure, either through exceedance of the static strength of the material, or through the combination of an undetected crack, increased stress and uncertain critical fracture toughness.

The yield/ultimate strength of metallic materials reduces due to the creep process (Penny, 1974), but the remanent strength of the pressure vessel is unknown because the extent of damage is uncertain (only surface measurements were made by the replica technique). The non-destructive measurements found no cracks in the pressure vessel nozzle, but non-destructive techniques are known to be uncertain (Le May et al., 1993), and the presence and future growth of cracks in the nozzle must be considered. The available data for fracture toughness values shows a considerable amount of scatter, and varies with temperature and stress. The remanent "strength" of the nozzle must therefore be considered as a random parameter. The magnitude of the mean strength of the nozzle must be estimated from available data and the magnitude of the variance of the strength must be assigned by engineering judgement.

The mean remanent strength of the nozzle to resist static collapse is assumed to be the mean ultimate strength of the steel at the nominal operating temperature and values for this steel were obtained from Woolman and Mottram (1964). It is also assumed that the original, un-aged values have degraded by 20% in the weld metal and heat affected zone and this strength has a coefficient of variance of 10%. Failure is assumed to occur when the Mises stress exceeds this strength.

The strength of the nozzle to resist sudden fracture can be estimated by using the fracture mechanics result:

$$K > \sigma \sqrt{\pi a}\, f(\alpha)$$

where α is the ratio of crack depth to nozzle thickness. An expression for $f(\alpha)$ can be obtained from Tada et al. (1985). Rewriting this expression in terms of a failure criterion involving stress gives:

$$\sigma_f = \frac{K_{I_c}}{\sqrt{\pi a_c}\, f(\alpha)}$$

An equivalent failure criterion can be derived by assigning a limiting value to the right hand side of the above expression. The mean of this value was estimated by considering a range of crack lengths (between 5mm and 20mm) and typical fracture toughness values from Neale (1978) and Chell and Gates (1978). Failure is assumed to occur when the maximum principal stress in the nozzle exceeds this failure criterion. It is assumed that this fracture strength failure criterion has a coefficient of variance of 12%.

Loading on the pressure vessel nozzle is due to internal pressure, piping system reactions and thermal effects. For the problem of sudden failure due to pressure/temperature excursions the internal pressure and piping system reaction moment are likely to dominate. It is assumed that the internal pressure and piping system reaction moment are statistically correlated. Historical records indicate a coefficient of variance of approximately 7% for the internal pressure of the reactor. A coefficient of variance of 15% has been assumed here to take into account the possibility of an extreme pressure/temperature excursion during future operation. The mean piping system reaction moment at the flange has been estimated on the basis of a piping system reaction analysis. The problem parameters are summarised in Table 7.5.

The bending moment at the flange can be represented by equivalent loading which varies sinusoidally around the circumference. The maximum value of the equivalent loading can be calculated by integration:

$$M = \int_0^{2\pi} (P_o r \sin\theta)(r \sin\theta)\, \mathrm{d}\theta$$

where P_o is the maximum equivalent loading, r the mean radius and θ is the angular position in the flange. Simplifying and evaluating the integral gives:

$$P_o = \frac{M}{\pi r^2}$$

Parameter	Description	Mean	STD	COV
p	Internal pressure (MPa)	3	0.45	15%
M	Piping system reaction moment (kNm)	150	22.5	15%
E	Elastic modulus (GPa) (PM, HAZ & WM)	160	24	15%
σ_y^o	Initial yield stress (MPa) (PM)	250	37.5	15%
σ_y^o	Initial yield stress (MPa) (HAZ & WM)	200	30	15%
H	Hardening modulus (GPa) (PM, HAZ & WM)	1	0.15	15%
σ_{f_s}	Static strength failure criterion (MPa)	350	35	10%
σ_{f_f}	Fracture strength failure criterion (MPa)	300	36	12%

Table 7.5: Problem parameters – reactor pressure vessel nozzle

Since the maximum stresses in the nozzle are of interest in this problem, the nozzle can be modelled axisymmetrically by applying this equivalent maximum loading. The maximum stresses at other points in the nozzle will be lower. The nozzle was modelled by 1032 axisymmetric eight-noded elements. The finite element mesh is shown in Figure 7.7. The regions of parent metal, heat-affected zone and weld metal are indicated in the figure.

An MVFO finite element analysis involving three independent zones was performed for the pressure vessel nozzle and the Mises stress and maximum principal stress were evaluated. The mean, standard deviation and reliability index were calculated by fast probability integration for the entire model. These results are presented as contour plots in Figures 7.8 to 7.13. The portion of the model shown in these plots corresponds to the detail shown in Figure 7.7. Figures 7.8, 7.9 and 7.10 show the mean Mises stress, its standard deviation and the corresponding reliability index for static failure respectively. Figures 7.11, 7.12, and 7.13 show similar results, but for the maximum principal stress and failure by sudden fracture. Each contour plot shows the contour levels on the left hand of the figure. The units in the plots for mean and standard deviation are Pascal (Pa). The reliability index is a non-dimensional number.

It is possible to produce contour plots of the probability of failure but these do not convey information in a convenient format. To establish the probability of failure it is more convenient to work with the reliability index, realising that a large positive reliability index indicates a small probability of failure. The reliability index can be related to a value for the probability of failure through Table B.1 in Appendix B. For the values found in this problem however, the series expansion used to calculate probability of failure from the reliability index is unstable, and reliability indices larger than 4 indicate a probability of failure smaller than $1\text{x}10^{-4}$.

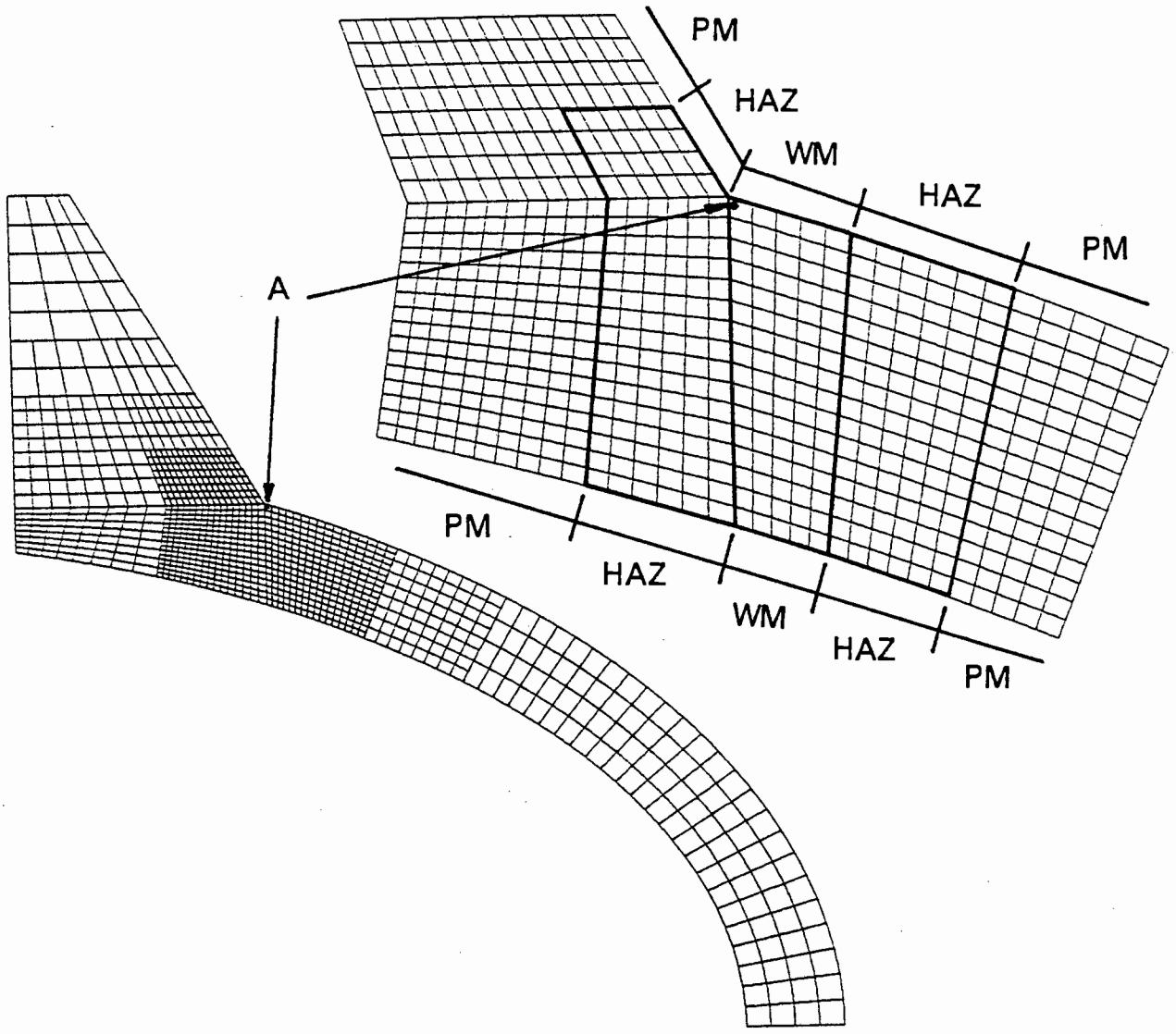

Figure 7.7: Finite element mesh – reactor pressure vessel nozzle

The maximum values for the mean and standard deviation of the stresses in the model and the minimum reliability occur consistently at point A indicated in Figure 7.7 and this should be the point for further investigation. The maximum value of the mean maximum principal stress in the model agrees with the results of Penny and Leckie (1963). The die-away length of the high stresses is short, and approximately 60% of the maximum values is reached two thicknesses away from the weld.

Repeated AMVFO analyses were then performed using the most probable points calculated for the element corresponding to point A. The centre integration point of this element was used. This point does not give the maximum stresses in the model, but it represents a good average for the high stress region. The reliability index and most probable points for failure calculated for the two failure criteria are listed in Table 7.6.

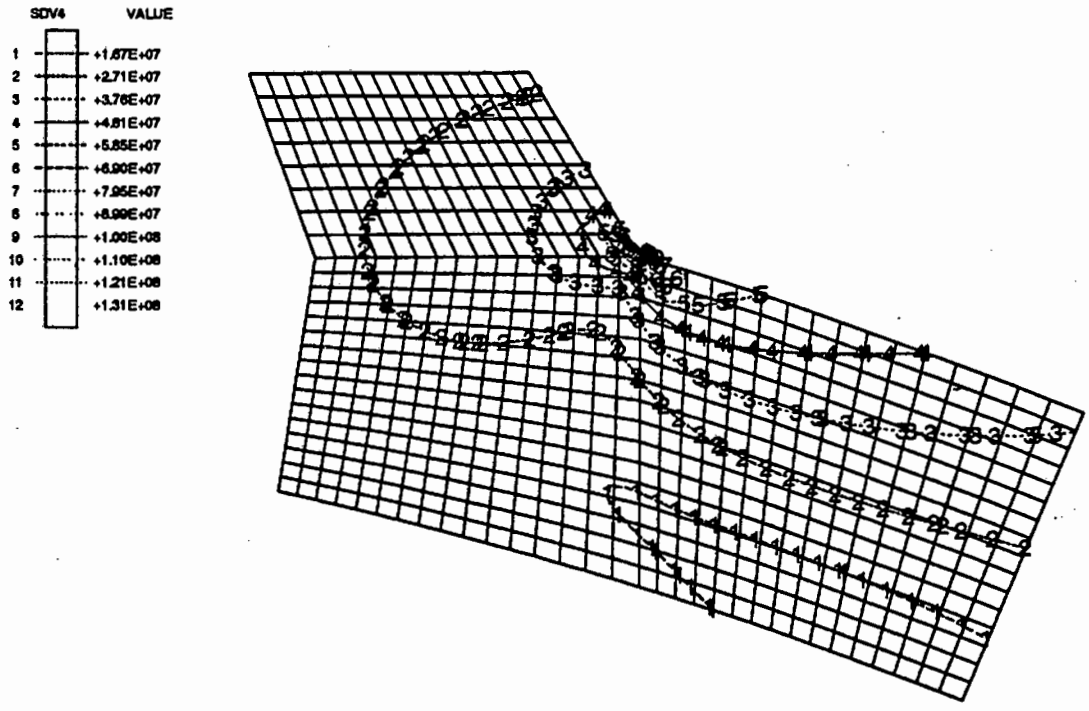

Figure 7.8: Mean Mises stress contour plot
reactor pressure vessel nozzle

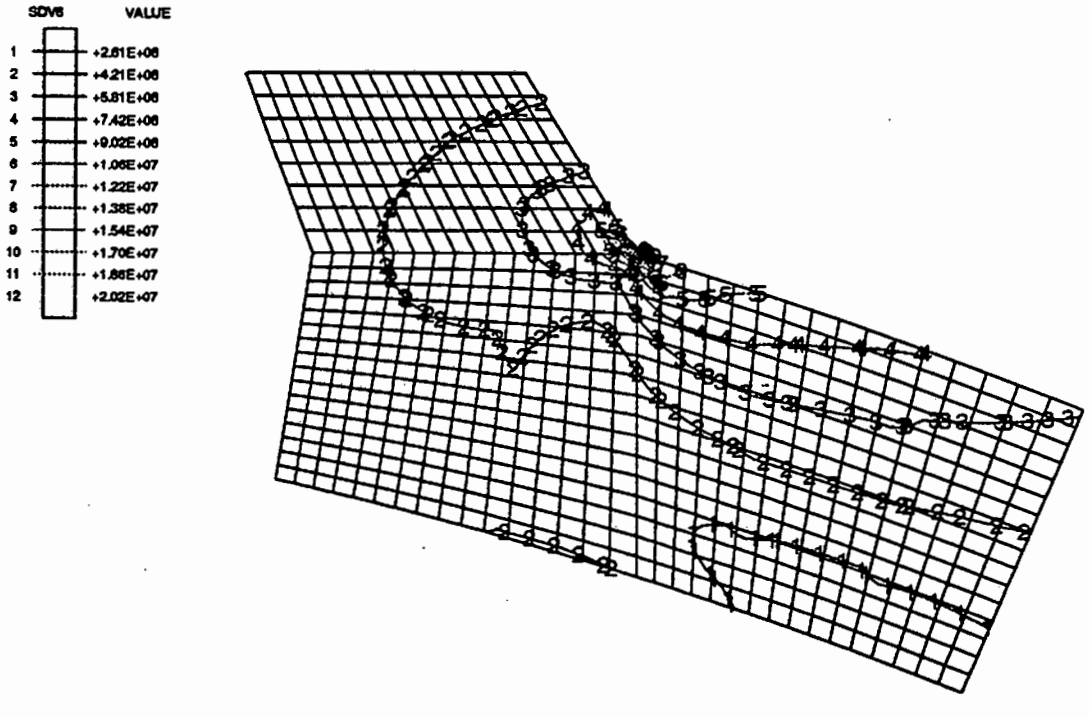

Figure 7.9: Standard deviation of Mises stress contour plot
reactor pressure vessel nozzle

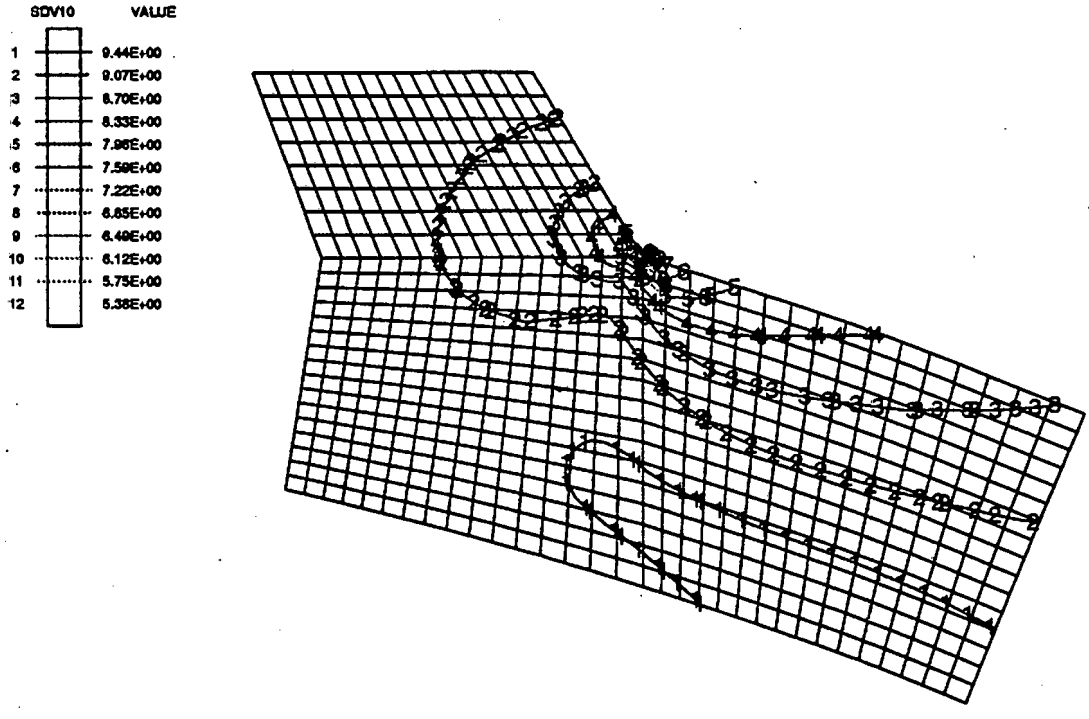

Figure 7.10: Static failure reliability index contour plot
reactor pressure vessel nozzle

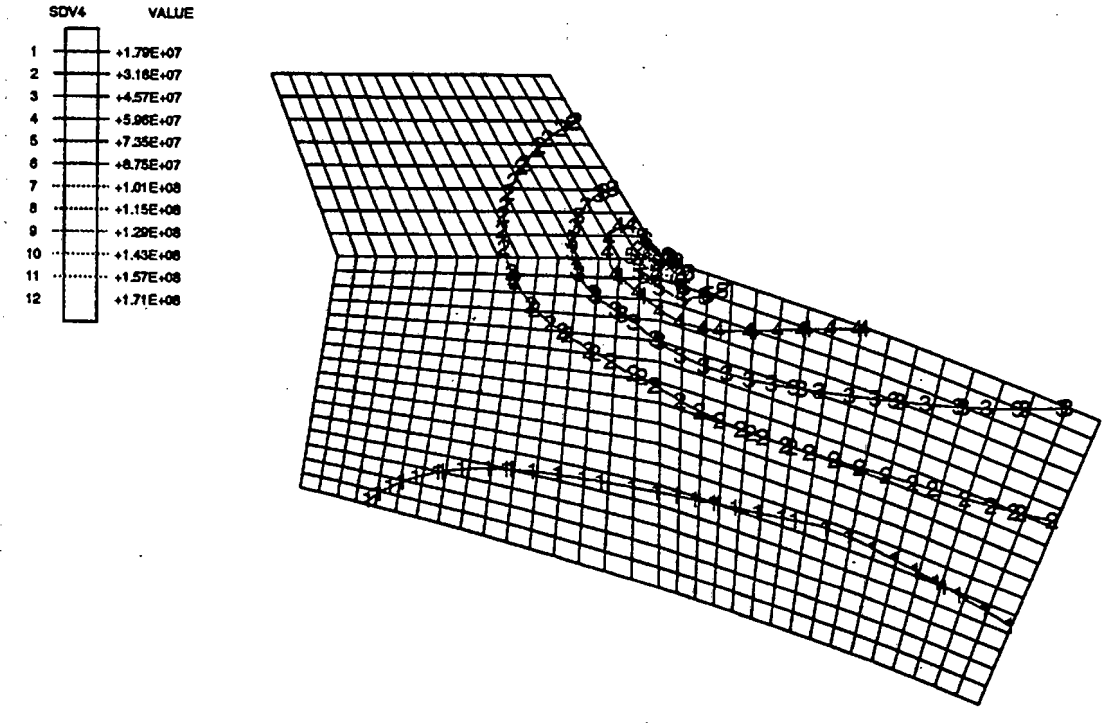

Figure 7.11: Mean maximum principal stress contour plot
reactor pressure vessel nozzle

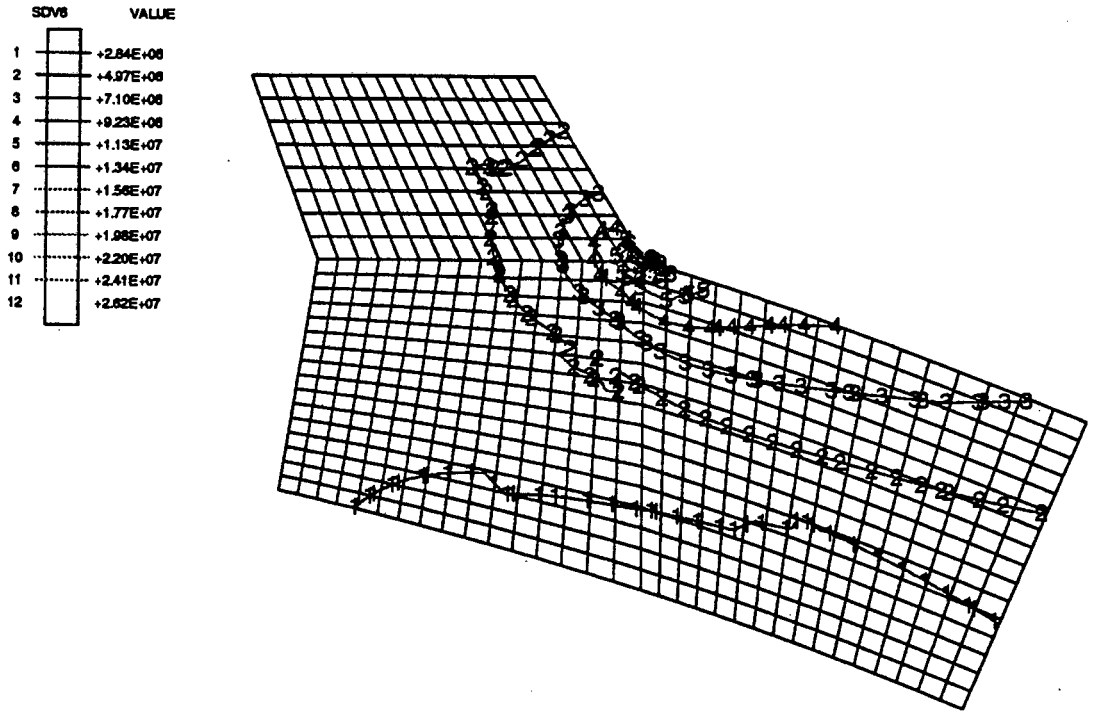

Figure 7.12: Standard deviation of maximum principal stress contour plot reactor pressure vessel nozzle

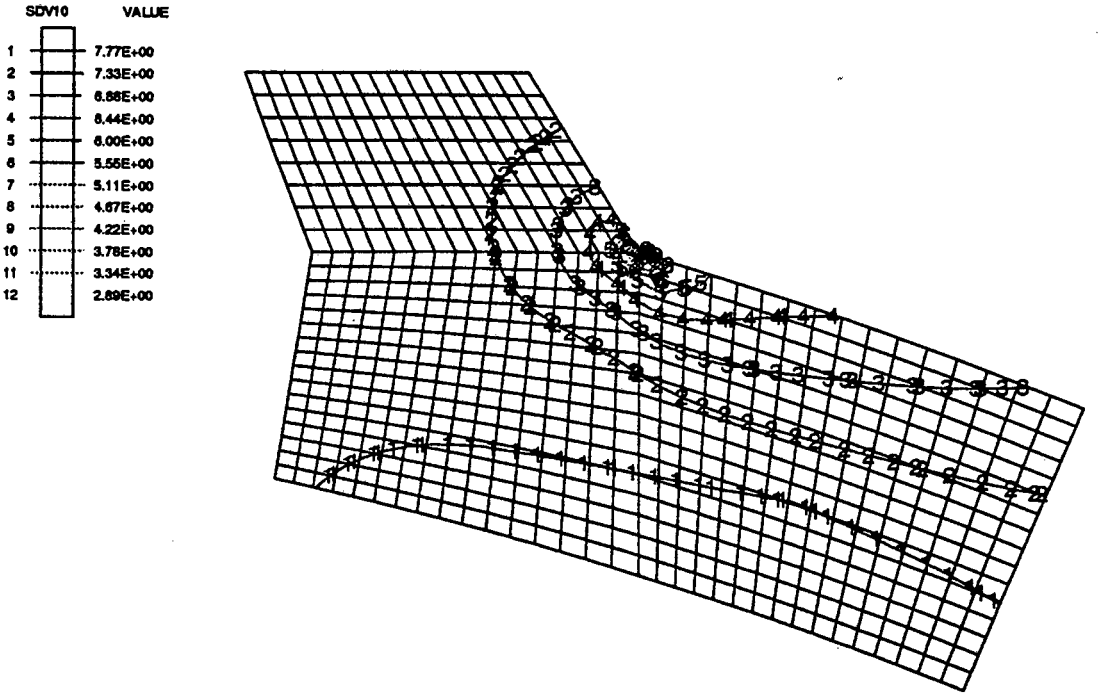

Figure 7.13: Sudden fracture failure reliability index contour plot reactor pressure vessel nozzle

	Static failure	Fracture failure
β	7.188	5.214
σ_f^* (MPa)	114	122
p^* (MPa)	4.07	3.81
E_{PM}^* (GPa)	153	155
E_{HAZ}^* (GPa)	161	161
E_{WM}^* (GPa)	166	164
σ_{yPM}^* (MPa)	250	250
σ_{yHAZ}^* (MPa)	200	200
σ_{yPM}^* (MPa)	196	200

Table 7.6: Most probable points and reliability index – reactor pressure vessel nozzle

For static failure, the variation in internal pressure and the failure criterion are the dominant factors. A small excursion into the plastic zone occurred only after the first iteration of the repeated AMVFO procedures, and only when the initial yield strength was perturbed negatively in the weld metal zone. The most probable points for the static failure criterion indicate that failure would occur at stress levels below the mean yield strength. Unless creep damage is so far advanced that there is almost no remaining strength in the steel, this situation is unlikely to occur, and even then failure would probably occur through sudden fracture. The reliability index indicates that the probability of failure is very small, and the most probable point for the internal pressure is sufficiently high that warning systems installed on the reactor would shut down the system before these pressure levels are reached.

For failure through sudden fracture, the variation in internal pressure and the failure criterion are again the dominant factors, and no excursions into the plastic zone were encountered in the perturbed analyses. The reliability index indicates that the probability of failure is higher than for static failure, but this is less than $1x10^{-4}$. The pressures at which this would occur are higher than the shutdown levels monitored by the warning systems.

The conclusion of this probabilistic analysis of the reactor pressure vessel nozzle is that although creep damage is known to exist in the nozzle, the likelihood of failure is very small, and operation of the reactor can be continued until the next shutdown at which time the state of material damage at the nozzle weld can be established, and a decision for further operation can be made.

8 Summary and Conclusions

The probabilistic finite element routines developed in this thesis have met the objectives which were set. Two different probabilistic methods for structural analysis, namely the point estimate method and the mean value first order method, have been integrated into a standard finite element program. Both methods involve the perturbation of the random parameters. They enable improvements in the computational requirements of traditional methods for probabilistic structural analysis by obtaining estimates of the probabilistic response from a limited set of perturbed evaluations corresponding to a systematic perturbation sequence, and by perturbation schemes which are computationally efficient.

The probabilistic routines have been implemented for a three-dimensional beam element and a two-dimensional plane element in the ABAQUS general purpose finite element program through its user element subroutine facility. The beam element can be reduced to a truss element. The plane element involves plane stress, plane strain and axisymmetric formulations. Each element gives the user a number of options with respect to number of nodes, integration order and load types.

It has been shown in this thesis that computer-time saving techniques which were developed for mean value first order methods can also be used for the point estimate method. These are the Taylor series perturbation and iterative perturbation schemes. Both solve for the perturbed response using the deterministic response which must be calculated, and are able to re-use the inverse of the deterministic stiffness matrix. Consequently only matrix manipulations are required to calculate the perturbed response and this results in significant savings in computer-time.

The Taylor series perturbation scheme neglects the higher order cross-multiplication terms and results in a linear problem requiring a single set of matrix manipulations for each perturbed evaluation. The iterative perturbation scheme solves for the full perturbation problem but requires iterative matrix manipulation if the stiffness terms are perturbed. Both schemes solve for the full perturbation problem in a single iteration if only the load is perturbed.

In problems where the variance of the load dominates, the Taylor series perturbation scheme can give results equivalent to the iterative perturbation scheme but with greater computational efficiency in the evaluation of the response due to perturbed stiffness. This has been shown in the plane frame structure case study. The user will have to exercise judgement however in problems where stiffness effects are not negligible: although the Taylor series scheme is more efficient in calculating the response gradients with respect to stiffness, more steps are usually required for the repeated AMVFO procedure to converge. This was found in the plane frame verification problem.

The Taylor series perturbation and iterative perturbation schemes are not readily compatible with nonlinear problems: if the problem requires derivation of a consistent tangent stiffness matrix, these schemes are inherently unstable and display poor convergence characteristics. By using the deterministic solution to find the perturbed solution, they can lead to erroneous results since the path leading to the deterministic solution is different from the path leading to the perturbed solution and full perturbation is required.

The point estimate method can obtain estimates of the mean and standard deviation of component response directly within the finite element analysis, from which estimates of the cumulative distribution, reliability index and probability of failure can be made. The method requires the evaluation of a number of point estimates which are obtained by the combined perturbation of the random parameters. The perturbation sequence corresponds to all the permutations of positive and negative perturbations of the random parameters. A total of 2^n point estimates are required for n random parameters. The results of the individual point estimates need not be stored.

The point estimate method can incorporate the correlation between different random parameters in a systematic way, but cannot, in the way the method is implemented in this thesis, deal with random parameters for which one part of the structure is independent of another. This would result in highly complex perturbation sequences which would vary from problem to problem. Nevertheless the point estimate method is a powerful method for probabilistic structural analysis. Its limitation has been that the number of perturbed evaluations required doubles for every additional random parameter and this results in a significant number of evaluations even if the number of random parameters is small. The computational requirements can then become too large for the method to be efficient.

The mean value first order method requires the evaluation of the perturbed response corresponding to the individual perturbation of the random parameters. The method requires the results of the individual perturbations to be stored for later access by a fast probability integration post-processing program. This program can calculate the mean and standard deviation of the response from which the cumulative distribution, reliability index and probability of failure are calculated. The program also estimates the most probable point to cause failure which is that combination of values for the random parameters which is most likely to lead to failure. From these most probable points better estimates of the cumulative distribution can be made through advanced mean value first order techniques. Repeating this procedure allows the probability of failure to be found.

Because the random parameters are perturbed individually in the mean value first order method, it is possible to repeat a probabilistic analysis for a number of independent zones. In each analysis the random parameters are perturbed only in the zone of interest. This procedure is then repeated for each independent zone. In this way problems involving

random parameters which are independent for different parts of the structure can be solved without having to implement this explicitly in the probabilistic finite element program.

The concept of independent zones is consistent with, and corresponds to, the concept of element sets by which the user defines different regions of the model. The procedure has been used successfully in a number of verification problems and in the case studies. The procedure will be useful in the analysis, for instance, of framed structures where each frame element (i.e. the beams and columns) must be considered statistically independent of the others, both in terms of the material and section properties which describe the stiffness and in terms of the loads acting on them. This has been illustrated in the plane frame structure case study. Another example is in the detailed analysis of welded structures where the material properties in the parent metal, heat affected zone and weld metal are, firstly, nominally different, and, secondly, degrade at differing rates.

The mean value first order method, as implemented in this thesis, does not limit the number of independent zones that can be considered. This number is limited by the storage capacity available on a computer, since the results of each independent analysis need to be stored until a fast probability integration analysis involving all the perturbed random parameters and independent zones is performed. Since the larger workstations and mainframe computers can accommodate large amounts of data, albeit temporarily, this limitation should not constitute a problem on these systems.

Usually finite element programs installed on smaller workstations or personal computers do not have a large storage capacity. For these systems even the MVFO method involving a few random parameters may lead to problems, especially if the number of elements in the model is large, since the quantity of data that needs to be stored relative to a deterministic analysis is multiplied by the number of random parameters. The point estimate method does not lead to this problem, since the amount of storage required is at most trebled, regardless of the number of random parameters. Here the problem size is limited by the number of perturbed analyses which must be performed.

The purpose of the probabilistic finite element routines is to track through the appropriate perturbation sequence. The standard pseudo-time incrementation schemes of finite element programs can be used for this where one increment corresponds to one perturbed evaluation. If the deterministic problem requires more than one load increment in the solution procedure (as, for instance, in nonlinear problems), each perturbed evaluation follows the same load path as the deterministic evaluation.

The finite element expressions which govern the probabilistic routines are similar to the deterministic finite element expressions, and consequently existing program structures can be maintained. The finite element expressions for the different perturbations schemes

(i.e. full, Taylor series and iterative perturbation) involve only different arrays but are not affected by the specific probabilistic method used. Consequently both probabilistic methods (i.e. PEM and MVFO) can be implemented within the same program code.

The difference between the point estimate method and the mean value first order method lies in the perturbation sequence which the two methods follow and in whether the random parameters are perturbed in combination. The conversion of deterministic finite element routines to probabilistic routines requires that the appropriate perturbation sequence be followed and that the correct random parameters are perturbed by the correct amount at the correct time. This is achieved by the addition of a perturbation control module which accounts for the different probabilistic methods and perturbation schemes.

This module sets a number of perturbation control flags and arrays which are passed through to the standard element subroutines. The deterministic program structure and subroutine code can be maintained. Only minimal additional code is required which is in a standard format throughout the program code. This method for converting deterministic to probabilistic routines requires that the random parameters are perturbed in a specific order, but as this order is transparent to the user, this should not lead to problems.

The operation of the probabilistic finite element programs implemented in this thesis follows a similar format to that of deterministic finite element programs, although some additional information is required from the user. The standard mesh generation and refinement techniques are used. When the material and section parameters and the load magnitudes are entered, the user specifies the mean and the perturbation amount. This perturbation amount is usually one standard deviation. The user also specifies the particular probabilistic method and the perturbation scheme that should be followed. The format in which this information is required corresponds to the format in which information is specified in deterministic finite element programs, and the user should not expect any undue problems in adapting from a deterministic to a probabilistic finite element program. The user will require some understanding of the two probabilistic methods and of the fast probability integration method prior to using the probabilistic routines and a description of the methods should be included in the program manuals.

If the methods described in this thesis for converting existing deterministic finite element programs to probabilistic finite element programs are implemented, both the point estimate method and the mean value first order method should be integrated within the same program, as should the full, Taylor series and iterative perturbation schemes. The majority of commercially available finite element programs is developed for use on a range of computer systems, from personal computers to mainframes, and a probabilistic finite element routine which incorporates a range of probabilistic methods and perturbation schemes will be most beneficial to a wide range of users.

9 References

References are given by the combination of the author surname and the date of publication. If the reference has two authors, both author surnames are given with the date. If the reference has more than two authors, the lead author surname followed by *et al.* is given with the date. If the reference has no specific author, a characteristic title is given with the date. If there are multiple references with the same author and date combination, these are differentiated by lower case suffixes to the date (e.g. 1988a, 1988b). The list of references is ordered alphabetically by lead author/characteristic title and date. Reference titles are given in italics. If a referenced article is part of a book, the article title is given in italics and the book title within quotation marks.

(1) *ABAQUS Theory Manual - Version 4.8* (1989), Hibbit, Karlsson and Sorensen Inc., Providence, Rhode Island.

(2) *ABAQUS User's Manual - Version 4.8* (1989), Hibbit, Karlsson and Sorensen Inc., Providence, Rhode Island.

(3) *ABAQUS User's Manual - Version 5.2* (1992), Hibbit, Karlsson and Sorensen Inc., Providence, Rhode Island.

(4) *ABAQUS Verification Manual - Version 5.2* (1992), Hibbit, Karlsson and Sorensen Inc., Providence, Rhode Island.

(5) Ang, A.H-S., and Tang, W.H. (1975), *Probability concepts in engineering planning and design - Volume I: Basic principles*, John Wiley, New York.

(6) Ang, A.H-S., and Tang, W.H. (1984), *Probability concepts in engineering planning and design - Volume II: Design, risk and reliability*, John Wiley, New York.

(7) Arbabi, F., Sherbourne, A.N. and El-Ghazaly, H.A. (1991), *Strength and stability of railway tracks - I. Probabilistic finite element analysis*, Computers & Structures, Vol. 39, No. 1/2, pp. 9-21.

(8) Arbabi, F. and Loh, C.U. (1991), *Reliability analysis of railroad tracks*, J. Struct. Eng., Vol. 117, No. 5, pp. 1435-1447.

(9) Arnbjerg-Nielsen, T. and Bjerager, P. (1988), *Finite element reliability method with improved efficiency by sensitivity analysis*, in "Computational probabilistic methods", AMD-Vol. 93, ASME, pp. 15-25.

(10) ASME Ad Hoc Task Group on Reliability (1990), *Report prepared for Main Committee of ASME Boiler and Pressure Vessel Code*, ASME.

(11) Balkey, K.R., Meyer, T.A. and Witt, F.J. (1986), *Chances are ...*, Mechanical Engineering, Vol. 108, No. 7, pp. 56-62.

(12) Benaroya, H. and Rehak, M. (1988), *Finite element methods in probabilistic structural analysis: A selective review*, Appl. Mech. Rev., Vol. 41, No. 5, pp. 201-213.

(13) Besterfield, G.H., Liu, W.K., Lawrence, M.A. and Belytschko, T.B. (1990), *Brittle fracture reliability by probabilistic finite elements*, J. Eng. Mech., Vol. 116, No. 3, pp. 642-659.

(14) Besterfield, G.H., Liu, W.K., Lawrence, M.A. and Belytschko, T.B. (1991), *Fatigue crack growth reliability by probabilistic finite elements*, Comp. Meth. in Appl. Mech. and Eng., Vol. 86, No. 3, pp. 297-320.

(15) Bjerager, P. (1989), *Probability computation methods in structural and mechanical reliability*, in "Computational mechanics of probabilistic and reliability analysis", Liu, W.K. and Belytschko, T.B. (Eds.), Elmepress Intl., Lausanne, pp. 47-68.

(16) Bulleit, W.M. and Yates, J.L. (1991), *Probabilistic analysis of wood trusses*, J. Struct. Eng., Vol. 117, No. 10, pp. 3008-3025.

(17) Carter, A.D.S. (1972), *Mechanical reliability*, MacMillan, London.

(18) Casciati, F. (1982), *Probabilistic analysis of inelastic structures*, Nucl. Eng. and Des., Vol. 71, pp. 271-276.

(19) Chell, G.G. and Gates, R.S. (1978), *A study of failure in the post yield regime using single edge-notched tension specimens*, Intl. J. Fracture, Vol. 14, No. 2, pp. 233-247.

(20) Clough, R.W. (1960), *The finite element method in plane stress analysis*, Proc. 2nd Conf. on Electronic Computation, ASCE, Pittsburgh, Pennsylvania, pp. 345-378.

(21) Cowper, G.R. (1966), *The shear coefficient in Timoshenko's beam theory*, J. Appl. Mech., Vol. 33, No. 2, pp. 335-340.

(22) Cruse, T.A., Burnside, O.H., Wu, Y.-T., Polch, E.Z. and Dias, J.B. (1988a), *Probabilistic structural analysis methods for select space propulsion system structural components (PSAM)*, Computers & Structures, Vol. 29, No. 5, pp. 891-901.

(23) Cruse, T.A., Wu, Y.-T., Dias, J.B. and Rajagopal, K.R. (1988b), *Probabilistic structural analysis methods and applications*, Computers & Structures, Vol. 30, No. 1/2, pp. 163-170.

(24) Cruse, T.A., Chamis, C.C. and Millwater, H.R. (1989), *An overview of the NASA (LeRC) - SwRI probabilistic structural analysis (PSAM) program*, in Proc. 5th

Intl. Conf. on Structural Safety and Reliability (ICOSSAR '89), San Francisco, California, August 1989, pp. 2267-2274.

(25) Cruse, T.A., Unruh, J.F., Wu, Y.-T. and Harren, S.V. (1990), *Probabilistic structural analysis for advanced space propulsion systems*, Trans. ASME, J. Eng. Gas Turb. and Power, Vol. 112, No. 2, pp. 251-260.

(26) Dawe, D.J. (1984), *Matrix and finite element displacement analysis of structures*, Clarendon, Oxford.

(27) Decker, K.M. (1991), *The Monte Carlo method in science and engineering: Theory and application*, Comp. Meth. in Appl. Mech. and Eng., Vol. 89, Nos. 1-3, pp. 463-483.

(28) Deodatis, G. (1990), *Bounds on response variability of stochastic finite element systems*, J. Eng. Mech., Vol. 116, No. 3, pp. 565-585.

(29) Der Kiureghian, A. and Moghtaderi-Zadeh, M. (1982), *An integrated approach to the reliability of engineering systems*, Nucl. Eng. and Des., Vol. 71, pp. 349-354.

(30) Der Kiureghian, A. and Ke, J.-B. (1985), *Finite-element based reliability analysis of frame structures*, in "Structural Safety and Reliability - Vol. 1" (Proc. ICOSSAR '85, Kobe, Japan), Konishi, I., Ang, A.H-S. and Shinozuka, M. (Eds.), IASSAR, New York, pp. 395-404.

(31) Der Kiureghian, A. and De Stefano, M. (1991), *Efficient algorithm for second-order reliability analysis*, J. Eng. Mech., Vol. 117, No. 12, pp. 2904-2923.

(32) Dias, J.B. and Nakazawa, S. (1988), *An approach to probabilistic finite element analysis using a mixed-iterative formulation*, in "Computational probabilistic methods", AMD-Vol. 93, ASME, pp. 75-86.

(33) Dias, J.B., Nagtegaal, J.C. and Nakazawa, S. (1989), *Iterative perturbation algorithms in probabilistic finite element analysis*, in "Computational mechanics of probabilistic and reliability analysis", Liu, W.K. and Belytschko, T.B. (Eds.), Elmepress Intl., Lausanne, pp. 211-230.

(34) Ditlevsen, O. (1981), *Uncertainty modelling*, McGraw-Hill, New York.

(35) Ditlevsen, O. (1982), *Extended second moment algebra as an efficient tool in structural reliability*, Nucl. Eng. and Des., Vol. 71, pp. 317-323.

(36) Faravelli, L. (1989), *Response-surface approach for reliability analysis*, J. Eng. Mech., Vol. 115, No. 12, pp. 2763-2781.

(37) FEA Report No. FEAL807 (1988), *The backward Euler return algorithm with consistent elastoplastic tangent moduli for the von Mises yield criterion*, FEA Ltd, Surrey, UK.

(38) Garribba, S. (1982), *Methods for probabilistic analysis*, Nucl. Eng. and Des., Vol. 71, pp. 363-365.

(39) Gopalakrishna, H.S. and Donaldson, E. (1987), *Structural reliability assessment with the ANSYS program*, ANSYS 1987 Conf. Proc., Swanson Analysis Systems.

(40) Gopalakrishna, H.S. and Donaldson, E. (1991), *Practical reliability analysis using a general purpose finite element program*, Fin. Elem. in Anal. and Des., Vol. 10, No. 1, pp. 75-87.

(41) Handa, K. and Andersson, K. (1981), *Application of finite element methods in the statistical analysis of structures*, in "Structural Safety and Reliability" (Proc. ICOSSAR '81, Trondheim, Norway), Moan, T. and Shinozuka, M. (Eds.), Elsevier, Amsterdam, pp. 409-417.

(42) Harr, M.E. (1987), *Reliability-based design in civil engineering*, McGraw-Hill, New York.

(43) Harren, S.V. (1989), *Probabilistic analysis of structures composed of path dependent materials*, in Proc. 5th Intl. Conf. on Structural Safety and Reliability (ICOSSAR '89), San Francisco, California, August 1989, pp. 2291-2298.

(44) Hasofer, A.M. and Lind, N.C. (1974), *Exact and invariant second-moment code format*, J. Eng. Mech., Vol. 100, No. EM1, pp. 111-121.

(45) Haugen, E.B. (1968), *Probabilistic approaches to design*, John Wiley, New York.

(46) Hien, T.D. and Kleiber, M. (1989), *Computational aspects in structural design sensitivity analysis for statics and dynamics*, Computers & Structures, Vol. 33, No. 4, pp. 939-950.

(47) Hien, T.D. and Kleiber, M. (1990), *Finite element analysis based on stochastic Hamilton variational principle*, Computers & Structures, Vol. 37, No. 6, pp. 893-902.

(48) Hien, T.D. and Kleiber, M. (1991a), *Stochastic structural design sensitivity of static response*, Computers & Structures, Vol. 38, No. 5/6, pp. 659-667.

(49) Hien, T.D. and Kleiber, M. (1991b), *Stochastic design sensitivity in structural dynamics*, Int. J. Num. Meth. Eng., Vol. 32, No. 6, pp. 1247-1265.

(50) Hinton, E. and Owen, D.R.J. (1977), *Finite element programming*, Academic Press, London.

(51) Hinton, E. and Owen, D.R.J. (1979), *An introduction to finite element computations*, Pineridge Press, Swansea, UK.

(52) Hisada, T. and Nakagiri, S. (1981), *Stochastic finite element method developed for structural safety and reliability*, in "Structural Safety and Reliability" (Proc. ICOSSAR '81, Trondheim, Norway), Moan, T. and Shinozuka, M. (Eds.), Elsevier, Amsterdam, pp. 395-408.

(53) Hisada, T. and Nakagiri, S. (1985), *Role of the stochastic finite element method in structural safety and reliability*, in "Structural Safety and Reliability - Vol. 1" (Proc. ICOSSAR '85, Kobe, Japan), Konishi, I., Ang, A.H-S. and Shinozuka, M. (Eds.), IASSAR, New York, pp. 385-394.

(54) Hisada, T. and Noguchi, H. (1989), *Development of a nonlinear stochastic FEM and its application*, in Proc. 5th Intl. Conf. on Structural Safety and Reliability (ICOSSAR '89), San Francisco, California, August 1989, pp. 1097-1104.

(55) Hohenbichler, M. and Rackwitz, R. (1981), *Non-normal dependent vectors in structural safety*, J. Eng. Mech., Vol. 107, No. EM6, pp. 1227-1238.

(56) Hopkins, R.B. (1970), *Design analysis of shafts and beams*, McGraw-Hill, New York.

(57) Hrennikoff, A. (1941), *Solution of problems in elasticity by the framework method*, Trans. ASME, J. Appl. Mech., Vol. 8, pp. A169-A175.

(58) Irons, B. M. (1970), *A frontal solution program*, Int. J. Num. Meth. Eng., Vol. 2, No. 1, pp. 5-32.

(59) Irons, B.M. and Ahmad, S. (1980), *Techniques of finite element analysis*, John Wiley, New York.

(60) Kapur, K.C. and Lamberson, L.R. (1977), *Reliability in engineering design*, John Wiley, New York.

(61) Kleiber, M. and Hien, T.D. (1992), *The stochastic finite element method*, John Wiley, Chichester.

(62) Kleinlogel, A. (1952), *Rigid Frame Formulas*, Crosby Lockwood & Son, London.

(63) Klingmüller, O. (1982), *Some mechanical aspects of the probability of failure*, Nucl. Eng. and Des., Vol. 71, pp. 277-279.

(64) Knuth, D.E. (1969), *The art of computer programming: Volume 2 – Seminumerical algorithms*, Addison-Wesley, Reading, Massachusetts.

(65) Krieg, R.D. and Krieg, D.B. (1977), *Accuracies of numerical solutions for the elastic-perfectly plastic model*, J. Press. Vess. Tech., Vol. 99, No. 4, pp. 510-515.

(66) Lawrence, M.A. (1986), *A basis random variable approach to stochastic structural analysis*, PhD Thesis, University of Illinois at Urbana-Champaign.

(67) Lawrence, M.A. (1987). *Basis random variables in finite element analysis*, Int. J. Num. Meth. Eng., Vol. 24, No. 10, pp. 1849-1863.

(68) Lawrence, M.A. (1989), *An introduction to reliability methods*, in "Computational mechanics of probabilistic and reliability analysis", Liu, W.K. and Belytschko, T.B. (Eds.), Elmepress Intl., Lausanne, pp. 9-46.

(69) Le May, I., da Silveira, T.L. and Cheung-Mak, S.K.P. (1993), *Uncertainties in the evaluation of high temperature damage in power stations and petrochemical plant*, Proc. 2nd Intl. Conf. on Ageing of Materials and Life Assessment (CAPE '93), Somerset West, South Africa, March/ April 1993.

(70) Levy, S. (1947), *Computation of influence coefficients for aircraft structures with discontinuities and sweepback*, J. Aeron. Sci., Vol. 14, No. 10, pp. 547-560.

(71) Levy, S. (1953), *Structural analysis and influence coefficients for Delta wings*, J. Aeron. Sci., Vol. 20, No. 7, pp. 449-454.

(72) Liaw, D.G. and Yang, H.T.Y. (1989), *Reliability of randomly imperfect beam-columns*, J. Eng. Mech., Vol. 115, No. 10, pp. 2251-2270.

(73) Liu, P.-L. and Der Kiureghian, A. (1991), *Finite element reliability of geometrically nonlinear uncertain structures*, J. Eng. Mech., Vol. 117, No. 8, pp. 1806-1825.

(74) Liu, W.K., Belytschko, T.B. and Mani, A. (1986), *Random field finite elements*, Intl. J. Num. Meth. Eng., Vol. 23, No. 10, pp. 1831-1845.

(75) Liu, W.K., Belytschko, T.B. and Mani, A. (1987), *Applications of probabilistic finite element methods in elastic/plastic dynamics*, Trans. ASME, J. Eng. for Ind., Vol. 109, No. 1, pp. 2-8.

(76) Liu, W.K., Besterfield, G. and Belytschko, T.B. (1988), *Transient probabilistic systems*, Comp. Meth. in Appl. Mech. and Eng., Vol. 67, No. 1, pp. 27-54.

(77) Liu, W.K. and Belytschko, T.B. (Eds.) (1989), *Computational mechanics of probabilistic and reliability analysis*, Elmepress Intl., Lausanne.

(78) Mahadevan, S. and Haldar, A. (1991), *Stochastic FEM-based validation of LRFD*, J. Struct. Eng., Vol. 117, No. 5, pp. 1393-1412.

(79) Martin, H.C. and Carey, G.F. (1973), *Introduction to finite element analysis*, McGraw-Hill, New York.

(80) Martin, J.B. (1975), *Plasticity: Fundamentals and general results*, MIT Press, Cambridge, Massachusetts.

(81) Millwater, H.R., Wu, Y.-T., Dias, J.B., McClung, R.C., Raveendra, S.T. and Thacker, B.H. (1989), *The NESSUS software system for probabilistic structural analysis*, in Proc. 5th Intl. Conf. on Structural Safety and Reliability (ICOSSAR '89), San Francisco, California, August 1989, pp. 2283-2291.

(82) Millwater, H.R., Harren, S.V. and Thacker, B.H. (1991), *A probabilistic methodology for random stress-strain curves*, in "Reliability, stress analysis and failure prevention", Service, T.H. (Ed.), DE-Vol. 30, ASME, pp. 37-41.

(83) Millwater, H.R., Wu, Y.-T., Torng, Y., Thacker, B., Riha, D. and Leung, C. (1992), *Recent developments of the NESSUS probabilistic structural analysis computer program*, in Proc. 33rd AIAA/ASME/AHS/ASC Structures, Structural Dynamics and Materials Conf., Dallas, Texas, April 1992, pp. 614-624.

(84) Mitchell, G.P. and Owen, D.R.J. (1988), *Numerical solutions for elastic-plastic problems*, Engineering Computations, Vol. 5, No. 4, pp. 274-284.

(85) Nakagiri, S. (1987), *Fluctuation of structural response, why and how*, JSME Intl. J., Vol. 30, No. 261, pp. 369-374.

(86) Nakagiri, S., Hisada, T. and Nagasaki, T. (1989), *Stochastic stress analysis of assembled structures*, Trans. ASME, J. Press. Vess. Tech., Vol. 111, No. 1, pp. 72-78.

(87) NBS Special Publication 577 (1980), *Development of a probability based load criterion for American National Standard A58*, National Bureau of Standards, US Government Printing Office, Washington.

(88) Neale, B.K. (1978), *An investigation into the effect of thickness on the fracture behaviour of compact tension specimens*, Intl. J. Fracture, Vol. 14, No. 2, pp. 203-212.

(89) Oden, J.T. (1972), *Finite elements of nonlinear continua*, McGraw-Hill, New York.

(90) Ortiz, M. and Simo, J.C. (1986), *An analysis of a new class of integration algorithms for elastoplastic constitutive relations*, Int. J. Num. Meth. Eng., Vol. 23,

No. 2, pp. 353-366.

(91) Owen, D.R.J. and Hinton, E. (1980), *Finite elements in plasticity: Theory and practice*, Pineridge Press, Swansea, UK.

(92) Paulsen, W.C. (1986), *Finite elements on the PC: No excuses left*, Mechanical Engineering (Interviewed by Weinrib, J.), Vol. 108, No. 7, pp. 36-40.

(93) Pearce, H.T. (1983), *Finite element methods in structural reliability - A review*, UCT Nonlinear Structural Mechanics Research Unit, Technical Report No. 38.

(94) Penny, R.K. and Leckie, F.A. (1963), *Solutions for the stresses in nozzles in pressure vessels*, Welding Research Council Bulletin No. 90.

(95) Penny, R.K. and Marriott, D.L. (1971), *Design for creep*, McGraw-Hill, London.

(96) Penny, R.K. (1974), *The usefulness of engineering damage parameters during creep*, J. Metals and Materials, Vol. 8, pp. 278-283.

(97) Penny, R.K. (1989), *Simulation of effects of material randomness on structural behaviour*, in "Proc. 6^{th} SAS-world Conf. on Structural Analysis and Optimisation (FEMCAD '89, Paris)", Liebowitz, H. and Davies, G.A.O. (Eds.), IITT Intl., Gourney-sur-Marne, France, pp. 99-106.

(98) Price, A.T. and Alberry, P.J. (1988), *Welding - the critical link*, CEGB Research, No. 21, pp. 15-25.

(99) Przemieniecki, J.S. (Ed.) (1966), *Proc. 1st Conf. on Matrix Methods in Structural Mechanics*, Wright-Patterson AFB, AFFDL, October 1965.

(100) Przemieniecki, J.S. (1968), *Theory of matrix structural analysis*, McGraw-Hill, New York.

(101) Rackwitz, R. and Fiessler, B. (1978), *Structural reliability under combined random load sequences*, Computers & Structures, Vol. 9, No. 5, pp. 489-494.

(102) Rajagopal, K.R., DebChaudhury, A. and Newell, J.F. (1989), *Verification of NESSUS code on space propulsion components*, in Proc. 5th Intl. Conf. on Structural Safety and Reliability (ICOSSAR '89), San Francisco, California, August 1989, pp. 2299-2306.

(103) Rao, S.S. (1982), *The finite element method in engineering*, Pergamon, Oxford.

(104) Riha, D.S., Millwater, H.R. and Thacker, B.H. (1992), *Probabilistic structural analysis using a general purpose finite element program*, Fin. Elem. in Anal. and Des., Vol. 11, No. 3, pp. 201-211.

(105) Rosenblatt, M. (1952), *Remarks on a multivariate transformation*, Annals of Mathematical Statistics, Vol. 23, pp. 470-472.

(106) Rosenblueth, E. (1975), *Point estimates for probability moments*, Proc. Nat. Acad. Sci. USA, Vol. 72, No. 10, pp. 3812-3814.

(107) Ryu, Y.S., Haririan, M., Wu, C.C. and Arora, J.S. (1985), *Structural design sensitivity analysis of nonlinear response*, Computers & Structures, Vol. 21, No. 1/2, pp. 245-255.

(108) SABS-0160 (1989), *South African Standard: Code of Practice for the general procedures and loadings to be adopted in the design of buildings*, South African Bureau of Standards, Pretoria.

(109) SABS-0162 (1984), *South African Standard: Code of Practice for the structural use of steel*, South African Bureau of Standards, Pretoria.

(110) SABS-219 (1978), *Standard specification for the design and manufacture of welded steel cylinders for low pressure service*, South African Bureau of Standards, Pretoria.

(111) Schuëller, G.I. and Stix, R. (1987), *A critical appraisal of methods to determine failure probabilities*, Structural Safety, Vol. 4, pp. 293-309.

(112) Schütz, W. (1993), *Fatigue life prediction - A review of the state of the art*, in "Structural failure, product liability and technical insurance, IV", Rossmanith, H.P. (Ed.), Elsevier, Amsterdam, pp. 49-60.

(113) Shinozuka, M. (1987), *Structural response variability*, J. Eng. Mech., Vol. 113, No. 6, pp. 825-842.

(114) Sih, G.C. (Ed.) (1973), *Methods of analysis and solution of crack problems*, Noordhoff, Leyden.

(115) Simo, J.C. and Taylor, R.L. (1985), *Consistent tangent operators for rate-independent plasticity*, Comp. Meth. in Appl. Mech. and Eng., Vol. 48, No. 1, pp. 101-108.

(116) Simo, J.C. and Taylor, R.L. (1986), *A return mapping algorithm for plane stress elastoplasticity*, Int. J. Num. Meth. Eng., Vol. 22, No. 3, pp. 649-670.

(117) Sire, R.A., Kokarakis, J.E., Wells, C.H. and Taylor, R.K. (1992), *A probabilistic structure life prediction system for container ship repair and inspection*, Proc. 1st Intl. Conf. on Ageing of Materials and Life Assessment (CAPE '91), Intl. J. Press. Vess. and Piping, Vol. 50, Nos. 1-3, pp. 297-315.

(118) Spiegel, M.R. (1968), *Mathematical Handbook*, McGraw-Hill, New York.

(119) Tada, H., Paris, P.C. and Irwin, G.R. (1985), *Stress analysis of cracks handbook*, Paris Productions, St. Louis, Missouri.

(120) Teigen, J.G., Frangopol, D.M., Sture, S. and Felippa, C.A. (1991a), *Probabilistic FEM for nonlinear concrete structures. I: Theory*, J. Struct. Eng., Vol. 117, No. 9, pp. 2674-2689.

(121) Teigen, J.G., Frangopol, D.M., Sture, S. and Felippa, C.A. (1991b), *Probabilistic FEM for nonlinear concrete structures. II: Applications*, J. Struct. Eng., Vol. 117, No. 9, pp. 2690-2707.

(122) Thacker, B.H., McClung, R.C. and Millwater, H.R. (1990), *Application of the probabilistic approximate analysis method to a turbopump blade analysis*, in Proc. 31st AIAA/ASME/ASCE/AHS/ASC Structures, Structural Dynamics and Materials Conf., Long Beach, California, April 1990, pp. 1039-1047.

(123) Thacker, B.H., Harren, S.V. and Millwater, H.R. (1991), *Combined stress and resistance modelling with the NESSUS software system*, in "Reliability, stress analysis and failure prevention", Service, T.H. (Ed.), DE-Vol. 30, ASME, pp. 49-54.

(124) Timoshenko, S.P. and Young, D.H. (1968), *Elements of strength of materials*, D. Van Nostrand, New York.

(125) Timoshenko, S.P. and Goodier, J.N. (1970), *Theory of elasticity*, McGraw-Hill, New York.

(126) Tortorelli, D.A. (1991), Private discussion, Urbana-Champaign.

(127) Tsai, C.-H. and Wu, W.-F., *On the application of probabilistic fracture mechanics to the reliability and inspection of pressure vessels*, Proc. 2nd Intl. Conf. on Ageing of Materials and Life Assessment (CAPE '93), Somerset West, South Africa, March/ April 1993.

(128) Turner, M.J., Clough, R.W., Martin, H.C. and Topp, L.J. (1956), *Stiffness and deflection analysis of complex structures*, J. Aeron. Sci., Vol. 23, No. 9, pp. 805-824.

(129) Vanmarcke, E.H. (1982), *Developments in random field modeling*, Nucl. Eng. and Des., Vol. 71, pp. 325-327.

(130) Weber, M.A. (1990), *The study of creep in machine elements using finite element methods*, M.Sc. Dissertation, University of Cape Town.

(131) Weber, M.A. and Penny, R.K. (1991), *Probabilistic stress analysis methods*, in "Reliability, stress analysis and failure prevention", Service, T.H. (Ed.), DE-Vol. 30, ASME, pp. 21-28.

(132) Wirsching, P.H. and Wu, Y.-T. (1987), *Advanced reliability methods for structural evaluation*, Trans. ASME, J. Eng. Ind., Vol. 109, No. 1, pp. 19-23.

(133) Wong, F.S. (1985), *First-order, second-moment methods*, Computers & Structures, Vol. 20, No. 4, pp. 779-791.

(134) Woolman, J. and Mottram, R.A. (Eds.) (1964), *The mechanical properties of the British Standard En steels (BS 970 - 1955), Volume 1*, Pergamon, Oxford.

(135) Wu, Y.-T. (1987), *Demonstration of a new, fast probability integration method for reliability analysis*, J. Eng. for Ind., Vol. 109, No. 1, pp. 24-28.

(136) Wu, Y.-T., Burnside, O.H. and Dominguez, J. (1987), *Efficient probabilistic fracture mechanics analysis*, Proc. 4th Intl. Conf. on Num. Meth. in Fract. Mech., San Antonio, Texas, March 1987.

(137) Wu, Y.-T. and Wirsching, P.H. (1987), *New algorithm for structural reliability estimation*, J. Eng. Mech., Vol. 113, No. 9, pp. 1319-1336.

(138) Wu, Y.-T., Burnside, O.H. and Cruse, T.A. (1989), *Probabilistic methods for structural response analysis*, in "Computational mechanics of probabilistic and reliability analysis", Liu, W.K. and Belytschko, T.B. (Eds.), Elmepress Intl., Lausanne, pp. 181-196.

(139) Wu, Y.-T. and Wirsching, P.H. (1989), *Advanced reliability methods for probabilistic structural analysis*, in Proc. 5th Intl. Conf. on Structural Safety and Reliability (ICOSSAR '89), San Francisco, California, August 1989, pp. 2275-2281.

(140) Wu, Y.-T., Millwater, H.R. and Cruse, T.A. (1990), *Advanced probabilistic structural analysis method for implicit performance functions*, AIAA J., Vol. 28, No. 9, pp. 1663-1669.

(141) Yamazaki, F., Shinozuka, M. and Dasgupta, G. (1988), *Neumann expansion for stochastic finite element analysis*, J. Eng. Mech., Vol. 114, No. 8, pp. 1335-1354.

(142) Young, W.C. (1989), *Roark's formulas for stress and strain (6th edition)*, McGraw-Hill, New York.

(143) Zienkiewicz, O.C. and Cheung, Y.K. (1967), *The finite element method in structural and continuum mechanics*, McGraw-Hill, London.

A Deterministic Finite Element Formulation

A.1 Preamble

The objective of the finite element method is to model components or structures numerically by finite element equations of the general form:

$$\mathbf{Ku} = \mathbf{f} \tag{A.1}$$

where $\mathbf{K}$ is a general stiffness matrix, $\mathbf{u}$ is a vector containing the unknown solution variables, $\mathbf{f}$ is a general load vector and a solution for $\mathbf{u}$ is required subject to applied boundary conditions. In this thesis the unknown solution variables are displacements. Once the displacements have been calculated, further solution variables such as strains and stresses can be calculated.

This appendix describes the general definition of the solution variables, the calculation of the element stiffness matrix and load vector for iso-parametric three-dimensional beam elements and two-dimensional plane elements, the definition of the matrices required in these calculations, the updating procedures for the strain and stress vectors, and the convergence checking procedures.

The beam element is based on a Timoshenko beam which takes into account axial, transverse and shear deformations, and axial torsional and transverse bending rotations (Timoshenko and Young, 1968). This beam element is versatile and can be used to analyse not only thin beams with negligible shear deformation but also thick beams in which shear effects cannot be ignored. It has the advantage that it can be implemented as a C(0) continuity element. Conventional beam formulations require C(1) continuity resulting in cubic interpolation (Hinton and Owen, 1979). The Timoshenko formulation can result in "locking" of the element (i.e. "overstiff" deflections are calculated for very thin beams). The problem can be avoided by reduced integration (i.e. a two-noded beam is integrated at one point only while a three-noded beam is integrated at two points). The beam element can be reduced to a truss element by releasing the rotational degrees of freedom at the pin-jointed nodes. Only linear elastic material behaviour is considered in this thesis.

The plane element can be used to analyse plane stress, plane strain and axisymmetric problems. These elements are implemented to allow either full or reduced integration. The material behaviour considered for these elements is either linear elastic or, if yield criteria are exceeded, elastic-plastic with isotropic hardening.

The programs developed in this thesis use the element formulations described in this appendix. Features of these elements are listed in Table A.1.

Element type	3D Beam element	2D Plane element
Element formulation	Timoshenko beam Truss	Plane stress, Plane strain or Axisymmetric
Node number	2 (linear interpolation) or 3 (quadratic interpolation)	4 (linear interpolation) or 8 (quadratic interpolation)
Degrees of freedom	6 per node	2 per node
Integration order	1 or 2	1, 2 or 3
Integration type	Gaussian quadrature	Gaussian quadrature
Shape functions	Iso-parametric	Iso-parametric
Material behaviour	Linear elastic	Elastic-plastic
Material/section parameters	Elastic modulus Poisson's ratio Cross-sectional area Second moment of area (about y and z axes) Polar moment of area Shear correction factor (in y and z directions) Beam principal axes rotation	Elastic modulus Poisson's ratio Initial yield stress Plastic hardening modulus Element thickness (req. for plane stress)
Load types	Concentrated loads and moments and distributed loads in global directions Transverse distributed loads Axial thermal expansion/misfit	Concentrated loads Distributed normal and tangential loads
Solution variables	Displacement at nodes Stress (axial force, shear force, bending moment, torque)	Displacement at nodes Total strain and stress Mises equivalent stress Maximum principal stress Equivalent plastic strain

Table A.1: Element features

A.2 Element Solution Vectors

The local directions xyz for an iso-parametric beam element are shown in Figure A.1. The directions y and z are the principal axes of the beam cross-section. The figure

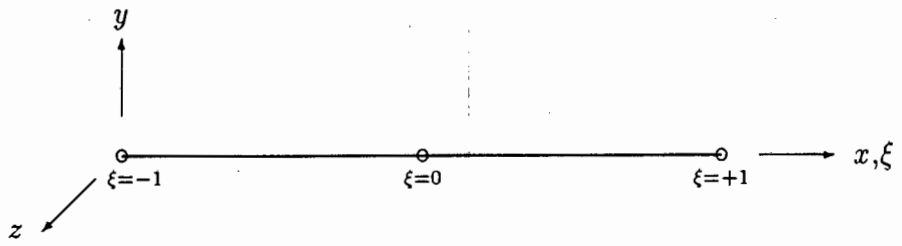

Figure A.1: Beam element: local and iso-parametric coordinate systems

also indicates the iso-parametric coordinate system with its curvilinear coordinate ξ. The element solution vectors, displacements $\mathbf{u}_i$ (evaluated at each node), strains $\boldsymbol{\varepsilon}_i$ and stresses $\boldsymbol{\sigma}_i$ (evaluated at each integration point) can be defined as:

$$\mathbf{u}_i = \begin{Bmatrix} u_x \\ u_y \\ u_z \\ \theta_x \\ \theta_y \\ \theta_z \end{Bmatrix} \quad \text{where} \quad \begin{array}{l} u_x \text{ is the axial displacement} \\ \\ u_y \text{ and } u_z \text{ are transverse displacements} \\ \theta_x \text{ is the torsional rotation} \\ \\ \theta_y \text{ and } \theta_z \text{ are bending rotations} \end{array}$$

$$\boldsymbol{\varepsilon}_i = \begin{Bmatrix} \varepsilon_x \\ \phi_y \\ \phi_z \\ \dfrac{\partial \theta_y}{\partial x} \\ \dfrac{\partial \theta_z}{\partial x} \\ \phi_x \end{Bmatrix} \quad \text{where} \quad \begin{array}{l} \varepsilon_x \text{ is the axial strain} \\ \phi_y \text{ and } \phi_z \text{ are effective shear rotations and} \\ \phi_y = -\dfrac{\mathrm{d}u_y}{\mathrm{d}x} + \theta_y \;;\; \phi_z = -\dfrac{\mathrm{d}u_z}{\mathrm{d}x} + \theta_z \\ \\ \dfrac{\partial \theta_y}{\partial x} \text{ and } \dfrac{\partial \theta_z}{\partial x} \text{ are pseudo-curvatures} \\ \phi_x \text{ is the torsional shear rotation} \end{array} \tag{A.2}$$

$$\boldsymbol{\sigma}_i = \begin{Bmatrix} F_x \\ S_y \\ S_z \\ M_y \\ M_z \\ T_x \end{Bmatrix} \quad \text{where} \quad \begin{array}{l} F_x \text{ is the axial force} \\ \\ S_y \text{ and } S_z \text{ are transverse shear forces} \\ \\ M_y \text{ and } M_z \text{ are bending moments} \\ T_x \text{ is the axial torque} \end{array}$$

The (co-incident) local and global directions xyz and XYZ for a two-dimensional plane element are shown in Figure A.2. The z axis is the direction of thickness in plane strain and plane stress problems. In axisymmetric problems the z axis represents the circumferential

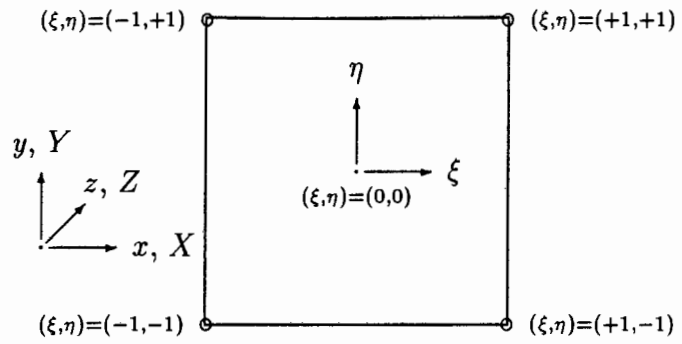

Figure A.2: Plane element: global, local and iso-parametric coordinate systems

(or hoop) direction. The y axis is the axis of symmetry in these problems. The figure also indicates the iso-parametric coordinate system with the curvilinear coordinate variables ξ and η. Axes x and ξ (and y and η) are not necessarily parallel. The element solution vectors, displacements $\mathbf{u}_i$ (evaluated at each node), strains $\boldsymbol{\varepsilon}_i$ and stresses $\boldsymbol{\sigma}_i$ (evaluated at each integration point) can be defined as:

$$\mathbf{u}_i = \left\{ \begin{array}{c} u_x \\ u_y \end{array} \right\} \; ; \; \boldsymbol{\varepsilon}_i = \left\{ \begin{array}{c} \varepsilon_{xx} \\ \varepsilon_{yy} \\ \varepsilon_{zz} \\ \gamma_{xy} \end{array} \right\} \; ; \; \boldsymbol{\sigma}_i = \left\{ \begin{array}{c} \sigma_{xx} \\ \sigma_{yy} \\ \sigma_{zz} \\ \tau_{xy} \end{array} \right\} \tag{A.3}$$

where the ε_{xx}, ε_{yy} and ε_{zz} terms are direct total strains, the σ_{xx}, σ_{yy} and σ_{zz} terms are direct stresses and the γ_{xy} and τ_{xy} terms are the shear total strain and stress respectively. In plane stress problems the σ_{zz} term is zero, while in plane strain problems the ε_{zz} term is zero.

A.3 Stiffness Matrix

The stiffness matrix for a three-dimensional beam element can be defined as:

$$\begin{aligned} \mathbf{K} &= \int_{len} \mathbf{R}^T\mathbf{B}^T\mathbf{D}\mathbf{B}\mathbf{R}\, \mathrm{d}x \\ &= \int \mathbf{R}^T\mathbf{B}^T\mathbf{D}\mathbf{B}\mathbf{R}\, \det\mathbf{J}\, \mathrm{d}\xi \end{aligned} \tag{A.4}$$

where $\mathbf{R}$ is the rotation matrix, $\mathbf{B}$ is the strain-displacement matrix, $\mathbf{D}$ is the constitutive matrix, $\mathbf{J}$ is the Jacobian matrix, x is the local coordinate and ξ is the iso-parametric coordinate, indicated in Figure A.1. Definitions for $\mathbf{R}$, $\mathbf{B}$, $\mathbf{D}$ and $\mathbf{J}$ are given in following

Integration Order	Integration Point	Gauss Point	Weighting Factor
1	1	$\xi_1 = 0$	$a_1 = 2$
2	1	$\xi_1 = -1/\sqrt{3}$	$a_1 = 1$
	2	$\xi_2 = +1/\sqrt{3}$	$a_2 = 1$

Table A.2: Beam element: integration points and weighting factors

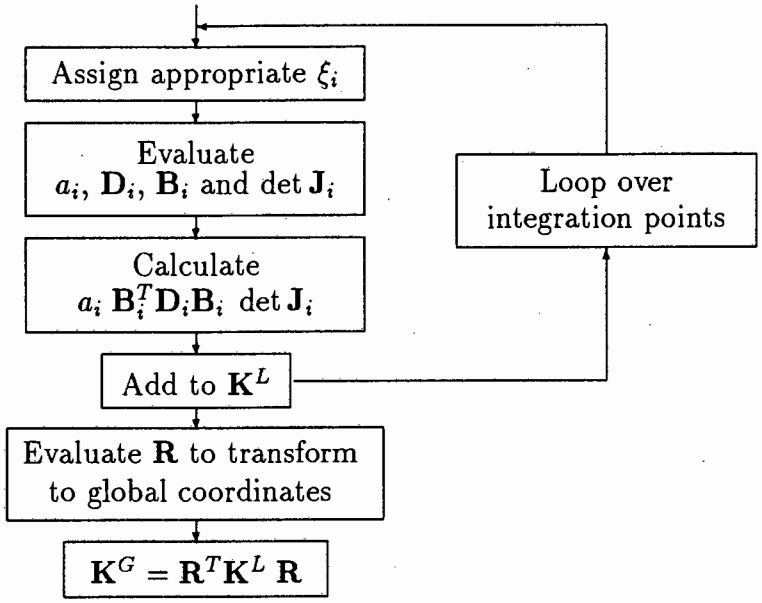

Figure A.3: Numerical integration of beam element stiffness matrix

sections. The stiffness matrix can be numerically integrated using Gaussian quadrature as follows (Hinton and Owen, 1977):

$$\mathbf{K} = \mathbf{R}^T \left(\sum_{i=1}^{NGAUS} a_i\, \mathbf{B}_i^T \mathbf{D}_i \mathbf{B}_i\, \det \mathbf{J}_i \right) \mathbf{R} \tag{A.5}$$

where subscript i represents Gauss (and integration) point, a_i is the integration weighting factor and *NGAUS* is the integration order. The integration order is one for a two-noded element and two for a three-noded element. The integration points and weighting factors for the beam element are listed in Table A.2 and the numerical integration procedure is illustrated in Figure A.3.

The stiffness matrix for a two-dimensional plane element is defined as:

$$\begin{aligned}\mathbf{K} &= \int_{vol} \mathbf{B}^T\mathbf{D}\mathbf{B}\, dvol \\ &= \iint \mathbf{B}^T\mathbf{D}\mathbf{B}\, t\, dx\, dy \\ &= \iint \mathbf{B}^T\mathbf{D}\mathbf{B}\, t\, \det\mathbf{J}\, d\xi\, d\eta\end{aligned} \tag{A.6}$$

where $\mathbf{B}$ is the strain-displacement matrix, $\mathbf{D}$ is the constitutive matrix, $\mathbf{J}$ is the Jacobian matrix, t is the element thickness in plane stress problems, $t = 1$ in plane strain problems and $t = 2\pi r$ in axisymmetric problems (where r is the radius), x and y are the local coordinates and ξ and η are the iso-parametric coordinates, indicated in Figure A.2. Definitions for $\mathbf{B}$, $\mathbf{D}$ and $\mathbf{J}$ are given in following sections. The stiffness matrix can be numerically integrated using Gaussian quadrature as follows:

$$\mathbf{K} = \sum_{i=1}^{NGAUS} \sum_{j=1}^{NGAUS} a_i a_j\, \mathbf{B}_{ij}^T\mathbf{D}_{ij}\mathbf{B}_{ij}\, t\, \det\mathbf{J}_{ij} \tag{A.7}$$

where subscripts i and j represent Gauss point combinations, a_i and a_j are the corresponding integration weighting factors, $t = 2\pi r$ is evaluated at the integration points in axisymmetric problems and $NGAUS$ is the integration order. The standard integration order for a four-noded element is two and is one for reduced integration; the standard integration order for an eight-noded element is three and is two for reduced integration. Combinations of the integration points and weighting factors for the plane element are listed in Table A.3 and the numerical integration procedure is illustrated in Figure A.4.

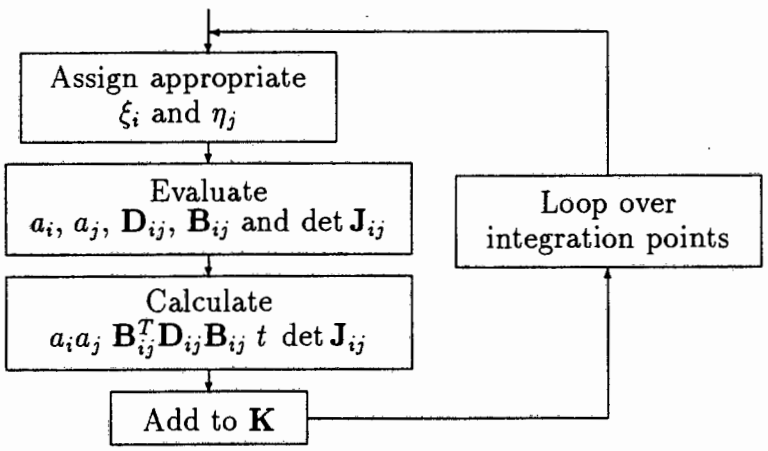

Figure A.4: Numerical integration of plane element stiffness matrix

Integration Order	Integration Point	Gauss Point Combination		Weighting Factor Combination	
1	1	$\xi_1 = 0$	$\eta_1 = 0$	$a_1 = 2$	$a_1 = 2$
2	1	$\xi_1 = -1/\sqrt{3}$	$\eta_1 = -1/\sqrt{3}$	$a_1 = 1$	$a_1 = 1$
	2		$\eta_2 = +1/\sqrt{3}$		$a_2 = 1$
	3	$\xi_2 = +1/\sqrt{3}$	$\eta_1 = -1/\sqrt{3}$	$a_2 = 1$	$a_1 = 1$
	4		$\eta_2 = +1/\sqrt{3}$		$a_2 = 1$
3	1	$\xi_1 = -\sqrt{0.6}$	$\eta_1 = -\sqrt{0.6}$	$a_1 = 5/9$	$a_1 = 5/9$
	2		$\eta_2 = 0$		$a_2 = 8/9$
	3		$\eta_3 = +\sqrt{0.6}$		$a_3 = 5/9$
	4	$\xi_2 = 0$	$\eta_1 = -\sqrt{0.6}$	$a_2 = 8/9$	$a_1 = 5/9$
	5		$\eta_2 = 0$		$a_2 = 8/9$
	6		$\eta_3 = +\sqrt{0.6}$		$a_3 = 5/9$
	7	$\xi_3 = +\sqrt{0.6}$	$\eta_1 = -\sqrt{0.6}$	$a_3 = 5/9$	$a_1 = 5/9$
	8		$\eta_2 = 0$		$a_2 = 8/9$
	9		$\eta_3 = +\sqrt{0.6}$		$a_3 = 5/9$

Table A.3: Plane element: integration points and weighting factors

The positions and numbering of integration points (the x's) and nodes (the o's) are shown schematically in Figure A.5 for two- and three noded beam elements and four- and eight noded plane elements with standard integration. The numbering scheme is chosen to match the corresponding standard ABAQUS elements.

A.4 Shape Functions

Shape functions are interpolation functions used to relate variables within an element, denoted $\mathbf{x}^e$, to the known nodal variable values, denoted $\mathbf{x}$, as follows (Hinton and Owen, 1979):

$$\mathbf{x}^e = \mathbf{N}\mathbf{x} \tag{A.8}$$

where the components of the single row array $\mathbf{N}$ are defined below in terms of the iso-parametric coordinate ξ for the beam element and iso-parametric coordinates ξ and η for the plane elements.

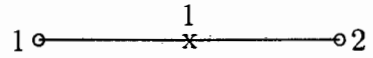

(a) 2 nodes; integration order 1

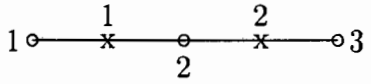

(b) 3 nodes; integration order 2

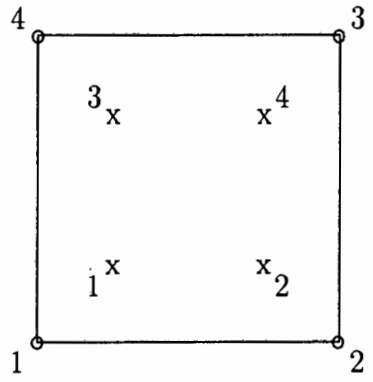

(c) 4 nodes; integration order 2

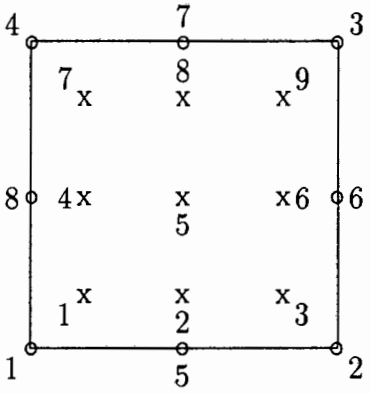

(d) 8 nodes; integration order 3

Figure A.5: Position of integration points (x's) and nodes (o's)

The linear shape functions for a two-noded beam element are:

$$\begin{aligned} N_1(\xi) &= \tfrac{1}{2}(1-\xi) \\ N_2(\xi) &= \tfrac{1}{2}(1+\xi) \end{aligned} \tag{A.9}$$

The quadratic shape functions for a three-noded beam element are:

$$\begin{aligned} N_1(\xi) &= -\tfrac{1}{2}\xi(1-\xi) \\ N_2(\xi) &= (1-\xi)(1+\xi) \\ N_3(\xi) &= \tfrac{1}{2}\xi(1+\xi) \end{aligned} \tag{A.10}$$

The linear shape functions for a four-noded plane element are:

$$\begin{aligned} N_1(\xi,\eta) &= \tfrac{1}{4}(1-\xi)(1-\eta) \\ N_2(\xi,\eta) &= \tfrac{1}{4}(1+\xi)(1-\eta) \\ N_3(\xi,\eta) &= \tfrac{1}{4}(1+\xi)(1+\eta) \\ N_4(\xi,\eta) &= \tfrac{1}{4}(1-\xi)(1+\eta) \end{aligned} \tag{A.11}$$

The quadratic shape functions for an eight-noded plane element are:

$$\begin{aligned}
N_1(\xi,\eta) &= \tfrac{1}{4}(\xi-1)(1-\eta)(1+\xi+\eta) \\
N_2(\xi,\eta) &= \tfrac{1}{4}(1+\xi)(1-\eta)(\xi-\eta-1) \\
N_3(\xi,\eta) &= \tfrac{1}{4}(1+\xi)(1+\eta)(\xi+\eta-1) \\
N_4(\xi,\eta) &= \tfrac{1}{4}(1-\xi)(1+\eta)(-\xi+\eta-1) \\
N_5(\xi,\eta) &= \tfrac{1}{2}(1-\xi^2)(1-\eta) \\
N_6(\xi,\eta) &= \tfrac{1}{2}(1+\xi)(1-\eta^2) \\
N_7(\xi,\eta) &= \tfrac{1}{2}(1-\xi^2)(1+\eta) \\
N_8(\xi,\eta) &= \tfrac{1}{2}(1-\xi)(1-\eta^2)
\end{aligned} \tag{A.12}$$

A.5 Jacobian Matrix

The Jacobian matrix of a beam element can be defined as (Hinton and Owen, 1977):

$$\mathbf{J} = \frac{\partial x}{\partial \xi} = \sum_{i=1}^{NNODE} \frac{\partial N_i}{\partial \xi} x_i \tag{A.13}$$

where $NNODE$ is the number of nodes and the shape function derivatives are evaluated from equations (A.9) or (A.10) as appropriate. For the iso-parametric formulation used here, the Jacobian matrix and its determinant reduce to:

$$\mathbf{J} = \det \mathbf{J} = \frac{L}{2} \text{ where } L \text{ is the element length} \tag{A.14}$$

The Jacobian matrix of a plane element can be defined as (Hinton and Owen, 1977):

$$\mathbf{J} = \begin{bmatrix} \dfrac{\partial x}{\partial \xi} & \dfrac{\partial y}{\partial \xi} \\ \dfrac{\partial x}{\partial \eta} & \dfrac{\partial y}{\partial \eta} \end{bmatrix} = \sum_{i=1}^{NNODE} \begin{bmatrix} \dfrac{\partial N_i}{\partial \xi} x_i & \dfrac{\partial N_i}{\partial \xi} y_i \\ \dfrac{\partial N_i}{\partial \eta} x_i & \dfrac{\partial N_i}{\partial \eta} y_i \end{bmatrix} \tag{A.15}$$

where the shape function partial derivatives are evaluated from equations (A.11) or (A.12) as appropriate and from which the determinant of the Jacobian matrix can be evaluated as:

$$\det \mathbf{J} = \frac{\partial x}{\partial \xi}\frac{\partial y}{\partial \eta} - \frac{\partial y}{\partial \xi}\frac{\partial x}{\partial \eta} \tag{A.16}$$

A.6 Rotation Matrix

In the three-dimensional beam element formulation the rotation matrix **R** is required to transform from the local coordinate system xyz to the global coordinate system XYZ. The two coordinate systems are illustrated in Figure A.6.

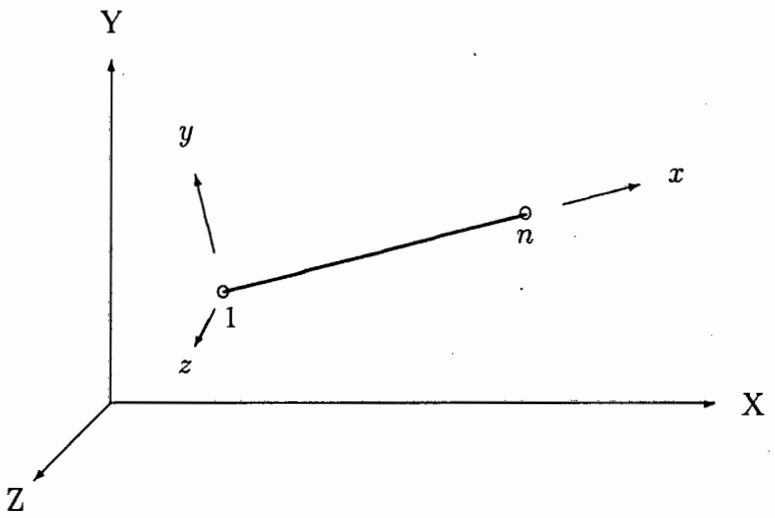

Figure A.6: Beam element: local and global coordinate systems

The rotation matrix **R** can be generally defined by a diagonal matrix with zero off-diagonal terms as (Dawe, 1984):

$$\mathbf{R} = \begin{bmatrix} \mathbf{MN} & \cdots & \cdots & \mathbf{0} \\ \vdots & \ddots & & \vdots \\ \vdots & & \ddots & \vdots \\ \mathbf{0} & \cdots & \cdots & \mathbf{MN} \end{bmatrix} \tag{A.17}$$

where there are four rows in the case of a two-noded element and six rows in the case of a three-noded element. The matrix **N** is a 3x3 matrix of direction cosines and can be evaluated from (Dawe, 1984):

$$\mathbf{N} = \begin{bmatrix} e & f & g \\ \dfrac{-ef}{\sqrt{e^2+g^2}} & \sqrt{e^2+g^2} & \dfrac{-fg}{\sqrt{e^2+g^2}} \\ \dfrac{-g}{\sqrt{e^2+g^2}} & 0 & \dfrac{e}{\sqrt{e^2+g^2}} \end{bmatrix} \quad \text{where} \quad \begin{aligned} e &= \frac{X_n - X_1}{len} \\ f &= \frac{Y_n - Y_1}{len} \\ g &= \frac{Z_n - Z_1}{len} \end{aligned} \tag{A.18}$$

In the above derivation, it is assumed that the principal axes of the cross-section lie in horizontal and vertical planes and that the z axis is chosen to be horizontal and perpendicular to the x axis. This assumption is insufficient when the element is vertical (i.e. when the local x axis runs parallel to the global Y axis) since the z axis will then not be uniquely defined. In this special case, the $\mathbf{N}$ matrix can be derived as (Rao, 1982):

$$\mathbf{N} = \begin{bmatrix} 0 & 1 & 0 \\ -1 & 0 & 0 \\ 0 & 0 & 1 \end{bmatrix} \quad \text{or} \quad \mathbf{N} = \begin{bmatrix} 0 & -1 & 0 \\ 1 & 0 & 0 \\ 0 & 0 & 1 \end{bmatrix} \tag{A.19}$$

depending on whether the local x axis runs in the positive or negative global Y direction respectively.

If the condition that the principal axes of the cross-section must lie in horizontal and vertical planes is relaxed, as shown in Figure A.7, the local $x_p y_p z_p$ system (where $x_p \equiv x$) must be rotated first through an angle ϕ_p to the earlier defined xyz system by the matrix $\mathbf{M}$ where $\mathbf{M}$ is defined as (Dawe, 1984):

$$\mathbf{M} = \begin{bmatrix} 1 & 0 & 0 \\ 0 & \cos\phi_p & -\sin\phi_p \\ 0 & \sin\phi_p & \cos\phi_p \end{bmatrix} \tag{A.20}$$

The angle ϕ_p is specified directly as part of the element section property data. If ϕ_p is zero, $\mathbf{M}$ reduces to the identity matrix.

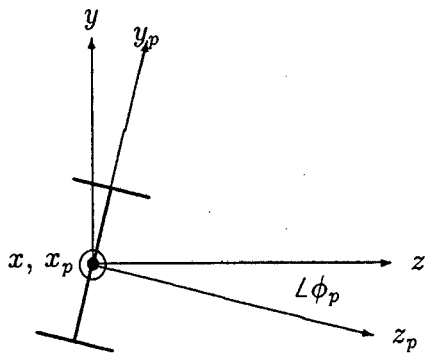

Figure A.7: xyz and $x_p y_p z_p$ coordinate systems

A.7 Strain-Displacement Matrix

The strain-displacement matrix $\mathbf{B}$ relates the strain vector $\boldsymbol{\epsilon}$ at an integration point to the nodal displacement vector $\mathbf{u}$ as follows:

$$\boldsymbol{\epsilon} = \mathbf{B}\mathbf{u} \tag{A.21}$$

In an incremental analysis the strain-displacement matrix is used to calculate the incremental strains, $\Delta\boldsymbol{\epsilon}$, from the incremental displacements, $\Delta\mathbf{u}$, after which the strain at the end of the n^{th} increment can be calculated:

$$\begin{aligned} \Delta\boldsymbol{\epsilon} &= \mathbf{B}\,\Delta\mathbf{u} \\ \boldsymbol{\epsilon}^n &= \boldsymbol{\epsilon}^{n-1} + \Delta\boldsymbol{\epsilon} \end{aligned} \tag{A.22}$$

If a beam element is subject to thermal expansion or misfit, the corresponding free movement strain is added to the axial strain component directly, either in full in the first increment, or gradually in each increment, depending on the problem.

The strain-displacement matrix for an iso-parametric beam element is (Hinton and Owen, 1977):

$$\mathbf{B}_i = \begin{bmatrix} \dfrac{\partial N_i}{\partial x} & 0 & 0 & 0 & 0 & 0 \\ 0 & -\dfrac{\partial N_i}{\partial x} & 0 & 0 & 0 & N_i \\ 0 & 0 & -\dfrac{\partial N_i}{\partial x} & 0 & N_i & 0 \\ 0 & 0 & 0 & 0 & \dfrac{\partial N_i}{\partial x} & 0 \\ 0 & 0 & 0 & 0 & 0 & \dfrac{\partial N_i}{\partial x} \\ 0 & 0 & 0 & \dfrac{\partial N_i}{\partial x} & 0 & 0 \end{bmatrix} \tag{A.23}$$

where for a two-noded beam element $\mathbf{B} = [\mathbf{B}_1, \mathbf{B}_2]$ while for a three-noded beam element $\mathbf{B} = [\mathbf{B}_1, \mathbf{B}_2, \mathbf{B}_3]$.

The strain-displacement matrices for plane stress and plane strain elements, and axisymmetric elements are, respectively (Hinton and Owen, 1977):

$$\mathbf{B}_i = \begin{bmatrix} \dfrac{\partial N_i}{\partial x} & 0 \\ 0 & \dfrac{\partial N_i}{\partial y} \\ 0 & 0 \\ \dfrac{\partial N_i}{\partial y} & \dfrac{\partial N_i}{\partial x} \end{bmatrix} \quad \text{and} \quad \mathbf{B}_i = \begin{bmatrix} \dfrac{\partial N_i}{\partial x} & 0 \\ 0 & \dfrac{\partial N_i}{\partial y} \\ \dfrac{N_i}{r} & 0 \\ \dfrac{\partial N_i}{\partial y} & \dfrac{\partial N_i}{\partial x} \end{bmatrix} \tag{A.24}$$

where for a four-noded plane element $\mathbf{B} = [\mathbf{B}_1, \mathbf{B}_2, \mathbf{B}_3, \mathbf{B}_4]$ while for a eight-noded plane element $\mathbf{B} = [\mathbf{B}_1, \mathbf{B}_2, \ldots, \mathbf{B}_8]$ and r is the radius of the integration point.

A.8 Elastic Constitutive Matrix

The elastic constitutive matrix $\mathbf{D}^{el}$ relates the stress vector $\boldsymbol{\sigma}$ at an integration point to the strain vector $\boldsymbol{\epsilon}$ at that integration point as follows:

$$\boldsymbol{\sigma} = \mathbf{D}^{el}\boldsymbol{\epsilon} \tag{A.25}$$

In a linear elastic incremental analysis the elastic constitutive matrix is used to calculate the incremental stresses, $\Delta\boldsymbol{\sigma}$, from the incremental strains, $\Delta\boldsymbol{\epsilon}$, after which the stress at the end of the n^{th} increment can be calculated:

$$\begin{aligned} \Delta\boldsymbol{\sigma} &= \mathbf{D}^{el}\,\Delta\boldsymbol{\epsilon} \\ \boldsymbol{\sigma}^{n} &= \boldsymbol{\sigma}^{n-1} + \Delta\boldsymbol{\sigma} \end{aligned} \tag{A.26}$$

The elastic constitutive matrix for a beam element with an underlying Timoshenko beam formulation is (Hinton and Owen, 1977):

$$\mathbf{D}^{el} = \begin{bmatrix} EA & 0 & 0 & 0 & 0 & 0 \\ 0 & \dfrac{GA}{\alpha_y} & 0 & 0 & 0 & 0 \\ 0 & 0 & \dfrac{GA}{\alpha_z} & 0 & 0 & 0 \\ 0 & 0 & 0 & EI_y & 0 & 0 \\ 0 & 0 & 0 & 0 & EI_z & 0 \\ 0 & 0 & 0 & 0 & 0 & GJ \end{bmatrix} \tag{A.27}$$

where

E is the elastic modulus
G is the shear modulus
A is the cross-sectional area
I_y and I_z are second moments of area about y and z axes
α_y and α_z are shear correction factors for y and z axes
J is the polar moment of area about the x axis

Expressions for shear correction factors and polar moments of area for a wide range of cross-sectional geometries can be found in Cowper (1966) and Hopkins (1970).

The elastic constitutive matrices for a plane stress element, and plane strain and plane axisymmetric elements are, respectively (Owen and Hinton, 1980):

$$\mathbf{D}^{el} = \frac{E}{1-\nu^2}\begin{bmatrix} 1 & \nu & 0 & 0 \\ \nu & 1 & 0 & 0 \\ 0 & 0 & 0 & 0 \\ 0 & 0 & 0 & \dfrac{1-\nu}{2} \end{bmatrix} \tag{A.28}$$

and

$$\mathbf{D}^{el} = \frac{E(1-\nu)}{(1+\nu)(1-2\nu)}\begin{bmatrix} 1 & \dfrac{\nu}{1-\nu} & \dfrac{\nu}{1-\nu} & 0 \\ \dfrac{\nu}{1-\nu} & 1 & \dfrac{\nu}{1-\nu} & 0 \\ \dfrac{\nu}{1-\nu} & \dfrac{\nu}{1-\nu} & 1 & 0 \\ 0 & 0 & 0 & \dfrac{1-2\nu}{2(1-\nu)} \end{bmatrix} \tag{A.29}$$

where E is the elastic modulus and ν is Poisson's ratio. Additionally, in plane stress problems, the ε_{zz} term is defined as:

$$\varepsilon_{zz} = \frac{-\nu(\varepsilon_{xx}+\varepsilon_{yy})}{1-\nu} \tag{A.30}$$

A.9 Consistent Tangent Constitutive Matrix and Radial Return Stress Update

The consistent tangent constitutive matrix is calculated whenever the elastic predictor step indicates that the Mises equivalent stress has exceeded the yield surface. The elastic predictor stresses are then adjusted by a radial return procedure. The equations used in the programs developed in this thesis are listed below as a sequential procedure but their formal derivation and the underlying plasticity theory is not included here in detail. A bibliography of the publications referenced includes Martin (1975), Krieg and Krieg (1977), Simo and Taylor (1985, 1986), Ortiz and Simo (1986), Mitchell and Owen (1988), ABAQUS Theory Manual (1989) and FEA Report No. FEAL807 (1988); since there is some overlap between these papers, not all papers will be specifically referred to in the derivation.

The following definitions govern the plasticity equations below. The total strain, $\boldsymbol{\varepsilon}$, contains elastic and plastic terms as follows:

$$\boldsymbol{\varepsilon} = \boldsymbol{\varepsilon}^{el} + \boldsymbol{\varepsilon}^{pl} \tag{A.31}$$

The volumetric plastic strain is zero, from which it follows that the direct and deviatoric plastic strains are equal. Plasticity is governed by an *associative flow* rule:

$$\mathrm{d}\boldsymbol{\varepsilon}^{pl} = \mathrm{d}\lambda \frac{\partial g}{\partial \boldsymbol{\sigma}} \tag{A.32}$$

where $g(\boldsymbol{\sigma}, H)$ is the plastic flow potential and $\mathrm{d}\lambda$ is a scalar whose value is determined by the requirement to satisfy the consistency condition $f(\boldsymbol{\sigma}, H) = 0$ for plastic flow of a rate independent model. An associative flow model is used where the direction of flow is the same as the outward normal to the yield surface:

$$\frac{\partial g}{\partial \boldsymbol{\sigma}} = c \frac{\partial f}{\partial \boldsymbol{\sigma}} \tag{A.33}$$

where c is a scalar. In the derivations below, the shear modulus, G, bulk modulus, K, plastic hardening modulus, H, and yield stress, σ_y, are used and are defined here:

$$\begin{aligned} G &= \frac{E}{2(1+\nu)} \\ K &= \frac{E}{3(1-2\nu)} \\ H &= \frac{\mathrm{d}\sigma_y}{\mathrm{d}\tilde{e}^{pl}} \qquad \text{and } H \text{ is illustrated in Figure A.8} \\ \sigma_y &= \sigma_y^o + H\tilde{e}^{pl} \qquad \text{and } \sigma_y^o \text{ is illustrated in Figure A.8} \end{aligned} \tag{A.34}$$

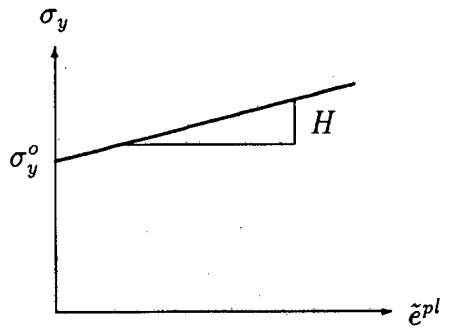

Figure A.8: Plastic hardening modulus; initial yield stress

The first step in the process is to calculate the elastic predictor strain increment, $\Delta\hat{\boldsymbol{\varepsilon}}$, the elastic predictor stress increment, $\Delta\hat{\boldsymbol{\sigma}}$, the elastic predictor stresses, $\hat{\boldsymbol{\sigma}}$, the corresponding deviatoric stresses, $\hat{\mathbf{s}}$, from them the Mises equivalent stress, $\hat{\sigma}^*$, and check whether the equivalent stress exceeds the yield stress, σ_y, at that integration point (superscripts $n-1$ refer to a previously converged solution, i.e. at the end of the previous increment) (Simo and Taylor, 1985):

$$\begin{aligned}
\Delta\hat{\boldsymbol{\varepsilon}} &= \mathbf{B}\,\Delta\mathbf{u} \\
\Delta\hat{\boldsymbol{\sigma}} &= \mathbf{D}^{el}\left(\boldsymbol{\varepsilon}^{el,n-1} + \Delta\hat{\boldsymbol{\varepsilon}}\right) \\
\hat{\boldsymbol{\sigma}} &= \boldsymbol{\sigma}^{n-1} + \Delta\hat{\boldsymbol{\sigma}} \\
\hat{\mathbf{s}} &= \hat{\boldsymbol{\sigma}} - \tfrac{1}{3}\,\mathrm{trace}(\hat{\boldsymbol{\sigma}})\,\mathbf{I} = \hat{\boldsymbol{\sigma}} - \hat{\sigma}_{vol}\,\mathbf{I} \\
\hat{\sigma}^* &= \sqrt{\tfrac{3}{2}\hat{\mathbf{s}}\cdot\hat{\mathbf{s}}} = \sqrt{\tfrac{3}{2}\left(\hat{s}_{xx}^2 + \hat{s}_{yy}^2 + \hat{s}_{zz}^2 + 2\hat{s}_{xy}^2\right)}
\end{aligned} \tag{A.35}$$

$$\begin{aligned}
&\text{if} \quad \hat{\sigma}^* > \sigma_y \quad \Rightarrow \quad \text{plasticity calculation required for this element} \\
&\text{if} \quad \hat{\sigma}^* \le \sigma_y \quad \Rightarrow \quad \text{elastic calculation sufficient for this integration point} \\
&\qquad\qquad\qquad\quad\ \ \text{(elastic predictor stresses used at end of increment)}
\end{aligned} \tag{A.36}$$

At this point the algorithm proceeds differently for plane strain and axisymmetric problems than for plane stress problems.

A.9.1 Plane strain and axisymmetric problems

In plane strain and axisymmetric problems, the yield function and flow rule are defined respectively as (Mitchell and Owen, 1988):

$$\begin{aligned}
f &= \sigma^* - \left(\sigma_y^o + H\tilde{e}^{pl}\right) \\
\mathrm{d}\mathbf{e}^{pl} &= \mathrm{d}\tilde{e}^{pl}\frac{3}{2}\frac{\mathbf{s}}{\sigma^*}
\end{aligned} \tag{A.37}$$

The next step in the algorithm is to calculate the deviatoric strains, $\mathbf{e}$, the elastic predictor deviatoric strains, $\hat{\mathbf{e}}$, and their equivalent strain, $\tilde{e}$.

$$\begin{aligned}
\mathbf{e} &= \boldsymbol{\varepsilon} - \tfrac{1}{3}\,\mathrm{trace}(\boldsymbol{\varepsilon})\,\mathbf{I} = \boldsymbol{\varepsilon} - \varepsilon_{vol}\,\mathbf{I} \\
\hat{\mathbf{e}} &= \mathbf{e}^{el,n-1} + \Delta\mathbf{e} \\
\tilde{e} &= \sqrt{\tfrac{3}{2}\hat{\mathbf{e}}\cdot\hat{\mathbf{e}}} = \sqrt{\tfrac{3}{2}\left(\hat{e}_{xx}^2 + \hat{e}_{yy}^2 + \hat{e}_{zz}^2 + 2\hat{e}_{xy}^2\right)}
\end{aligned} \tag{A.38}$$

The third step ensures that the Mises equivalent stress at the end of the iteration is equal to the yield surface. This involves the solution of a non-linear equation in $\Delta\tilde{e}^{pl}$, the equivalent plastic strain increment, using Newton's method:

$$\Delta\tilde{e}^{pl,i} = \Delta\tilde{e}^{pl,i-1} + \frac{f(\Delta\tilde{e}^{pl,i-1})}{f'(\Delta\tilde{e}^{pl,i-1})} = \Delta\tilde{e}^{pl,i-1} + \frac{G\left(2\tilde{e} - 3\Delta\tilde{e}^{pl,i-1}\right) - \sigma_y}{3G + H} \tag{A.39}$$

where G is the shear modulus, H is the plastic modulus, and the yield stress σ_y is updated to the new yield surface at the end of each iteration:

$$\sigma_y = \sigma_y^o + H\left(\tilde{e}^{pl,n-1} + \Delta\tilde{e}^{pl}\right) \quad \text{and} \quad \Delta\tilde{e}^{pl,o} = 0 \tag{A.40}$$

The formal solution is now complete and the elastic predictor stress can be adjusted by the radial return method. The Mises equivalent stress is equated to the current value of the yield surface, the deviatoric stresses are adjusted, the direct stresses, plastic strains and equivalent plastic strain at the end of the increment are calculated (Simo and Taylor, 1985):

$$\begin{aligned}
\sigma^* &= \sigma_y \\
\mathbf{s} &= \frac{2G}{1 + 3G\Delta\tilde{e}^{pl}/\sigma^*}\,\hat{\mathbf{e}} \\
\boldsymbol{\sigma} &= \mathbf{s} + \sigma_{vol}\,\mathbf{I} \\
\Delta\mathbf{e}^{pl} &= \frac{3}{2}\frac{\Delta\tilde{e}^{pl}}{\sigma^*}\mathbf{s} \\
\mathbf{e}^{pl,n} &= \mathbf{e}^{pl,n-1} + \Delta\mathbf{e}^{pl} \\
\tilde{e}^{pl,n} &= \tilde{e}^{pl,n-1} + \Delta\tilde{e}^{pl}
\end{aligned} \tag{A.41}$$

Finally the consistent tangent constitutive matrix is calculated. This matrix is then used to calculate the stiffness matrix used in the next iteration (ABAQUS Theory Manual, 1989):

$$\mathbf{D}^{pl} = \begin{bmatrix}
K + \frac{2}{3}Q - Rs_{xx}^2 & K - \frac{1}{3}Q - Rs_{xx}s_{yy} & K - \frac{1}{3}Q - Rs_{xx}s_{zz} & -Rs_{xx}s_{xy} \\
 & K + \frac{2}{3}Q - Rs_{yy}^2 & K - \frac{1}{3}Q - Rs_{yy}s_{zz} & -Rs_{yy}s_{xy} \\
sym & & K + \frac{2}{3}Q - Rs_{zz}^2 & -Rs_{zz}s_{xy} \\
 & & & \frac{1}{2}Q - Rs_{xy}^2
\end{bmatrix} \tag{A.42}$$

where

$$\begin{aligned}
Q &= \frac{\sigma^*}{\tilde{e}} \\
R &= \frac{3}{2\sigma^*\tilde{e}}\,\frac{1 - \Delta\tilde{e}^{pl}H/\sigma^*}{1 + H/3G}
\end{aligned}$$

A.9.2 Plane stress problems

In plane stress problems, the yield function and flow rule are defined respectively as (FEA Report No. FEAL807, 1988):

$$\begin{aligned} f &= \tfrac{1}{2}\bar{\Phi}^2 - \tfrac{1}{3}R^2 \\ \mathrm{d}\mathbf{e}^{pl} &= \lambda \mathbf{P}\boldsymbol{\sigma} \end{aligned} \tag{A.43}$$

where

$$\begin{aligned} R &= \sigma_y^o + H\tilde{e}^{pl} \\ \left[\bar{\Phi}(\lambda)\right]^2 &= \frac{\left(\hat{\sigma}_{xx}+\hat{\sigma}_{yy}\right)^2}{6\left[1+\dfrac{\lambda E}{3(1-\nu)}\right]^2} + \frac{\left(\hat{\sigma}_{xx}-\hat{\sigma}_{yy}\right)^2}{2\left[1+2\lambda G\right]^2} + \frac{\left(2\hat{\sigma}_{xy}\right)^2}{2\left[1+2\lambda G\right]^2} \\ \mathrm{d}\tilde{e}^{pl} &= \lambda\sqrt{\tfrac{2}{3}\bar{\Phi}^2} \\ \mathbf{P} &= \frac{1}{3}\begin{bmatrix} 2 & -1 & 0 \\ -1 & 2 & 0 \\ 0 & 0 & 6 \end{bmatrix} \end{aligned}$$

The next step satisfies the yield condition. This involves the solution of a non-linear equation in λ using Newton's method:

$$\lambda^i = \lambda^{i-1} + \frac{f(\lambda)}{f'(\lambda)} \quad \text{where } f'(\lambda) = \bar{\Phi}\frac{\partial\bar{\Phi}}{\partial\lambda} - \frac{2}{3}R\frac{\partial R}{\partial\lambda} \text{ and } \lambda^o = 0 \tag{A.44}$$

and the equivalent plastic strain increment and the yield stress σ_y are updated at the end of each iteration as follows:

$$\begin{aligned} \Delta\tilde{e}^{pl} &= \lambda\sqrt{\tfrac{2}{3}\bar{\Phi}^2} \\ \sigma_y &= \sigma_y^o + H\left(\tilde{e}^{pl,n-1} + \Delta\tilde{e}^{pl}\right) \end{aligned} \tag{A.45}$$

The formal solution is now complete and the elastic predictor stress can be adjusted by the radial return method. An *algorithmic* tangent modulus matrix, denoted $\boldsymbol{\Xi}$, is calculated, the Mises equivalent stress is equated to the current value of the yield surface, the direct stresses are adjusted and the plastic strains and equivalent plastic strain at the end of the increment are calculated (Simo and Taylor, 1986):

$$
\begin{aligned}
\boldsymbol{\Xi} &= \left[\left(\mathbf{D}^{el}\right)^{-1} + \lambda \mathbf{P}\right]^{-1} \\
\sigma^* &= \sigma_y \\
\boldsymbol{\sigma} &= \boldsymbol{\Xi}\left(\mathbf{D}^{el}\right)^{-1}\hat{\boldsymbol{\sigma}} \\
\Delta \mathbf{e}^{pl} &= \lambda \mathbf{P}\boldsymbol{\sigma} \\
\mathbf{e}^{pl,n} &= \mathbf{e}^{pl,n-1} + \Delta \mathbf{e}^{pl} \\
\tilde{e}^{pl,n} &= \tilde{e}^{pl,n-1} + \Delta \tilde{e}^{pl}
\end{aligned}
\tag{A.46}
$$

Finally the consistent tangent constitutive matrix is calculated. This matrix is then used to calculate the stiffness matrix used in the next iteration (FEA Report No. FEAL807, 1988):

$$
\mathbf{D}^{pl} = \boldsymbol{\Xi} - \frac{(\boldsymbol{\sigma}\mathbf{P}\boldsymbol{\Xi})^T(\boldsymbol{\Xi}\mathbf{P}\boldsymbol{\sigma})}{\boldsymbol{\sigma}\mathbf{P}\boldsymbol{\Xi}\mathbf{P}\boldsymbol{\sigma} + \frac{4\gamma H\sigma_y^2}{9}} \quad \text{where } \gamma = \left(1 - \frac{2H\lambda}{3}\right)^{-1} \tag{A.47}
$$

A.10 Load Vector

The element load vector for a beam element can be defined as follows:

$$
\mathbf{f}_i = \left\{ \begin{array}{l} F_x \\ S_y \\ S_z \\ T_x \\ M_y \\ M_z \end{array} \right\} \quad \text{where} \quad \begin{array}{l} F_x \text{ is the axial force} \\ \\ S_y \text{ and } S_z \text{ are transverse shear forces} \\ T_x \text{ is the axial torque} \\ \\ M_y \text{ and } M_z \text{ are bending moments} \end{array} \tag{A.48}
$$

where $\mathbf{f}_i$ is evaluated at each node and directions correspond to Figure A.1.

The load vector for a two-dimensional plane element can be defined as:

$$
\mathbf{f}_i = \left\{ \begin{array}{l} f_x \\ f_y \end{array} \right\} \tag{A.49}
$$

where $\mathbf{f}_i$ is evaluated at each node and directions correspond to Figure A.2.

Any loading that is applied to an element must be represented by concentrated loads at the nodal points. Consequently loadings such as pressure acting on a plane element edge

or distributed load transverse to a beam element must be reduced to consistent nodal forces. Point loads acting at nodes can be assigned directly to the load vector at the appropriate degree of freedom.

For a distributed load w acting transverse to a beam element the consistent force f_j at node j is:

$$\begin{aligned} f_j &= \int_{len} w \, \mathrm{d}x \\ &= \int N_j \, w \, \det \mathbf{J} \, \mathrm{d}\xi \\ &= \sum_{i=1}^{NGAUS} a_i \, N_j \, w \, \det \mathbf{J}_i \end{aligned} \tag{A.50}$$

where the f_j term is inserted in the appropriate transverse shear force direction term in equation (A.48). The element force vector is then rotated to the global coordinate system using:

$$\mathbf{f}^G = \mathbf{R}\mathbf{f}^L \tag{A.51}$$

For a distributed load w acting in a global direction, the consistent force f_j at node j is:

$$\begin{aligned} f_j &= \int_{len_p} w \, \mathrm{d}x \\ &= \int N_j \, w \, \det \mathbf{J} \, \frac{len_p}{len} \, \mathrm{d}\xi \\ &= \sum_{i=1}^{NGAUS} a_i \, N_j \, w \, \det \mathbf{J}_i \, \frac{len_p}{len} \end{aligned} \tag{A.52}$$

where len_p is the projected length of the beam in the plane normal to the distributed load and where the f_j term is inserted global load vector in the appropriate global direction term in equation (A.48).

For a normal distributed pressure load p_n and a tangential distributed shear load p_t acting on a plane element edge, the components of the pressure and tangential loads acting in the x and y direction must be determined. If the forces acting on an incremental length $\mathrm{d}l$ of the loaded edge are considered, the components in the x and y direction are:

$$\begin{aligned} \mathrm{d}f_x &= p_t \, t \, \mathrm{d}x - p_n \, t \, \mathrm{d}y = \left(p_t \frac{\partial x}{\partial \xi} - p_n \frac{\partial y}{\partial \xi} \right) t \, \mathrm{d}\xi \\ \mathrm{d}f_y &= p_n \, t \, \mathrm{d}x + p_t \, t \, \mathrm{d}x = \left(p_n \frac{\partial x}{\partial \xi} + p_t \frac{\partial y}{\partial \xi} \right) t \, \mathrm{d}\xi \end{aligned} \tag{A.53}$$

where t is the element thickness in a plane stress problem, $t = 1$ in a plane strain problem and $t = 2\pi r$ in an axisymmetric problem (where r is the radius) and ξ is a curvilinear co-ordinate variable along the loaded edge. Integrating along the loaded edge, the consistent nodal force f_j at node j can be represented by:

$$\begin{aligned} f_{x,j} &= \int_{len} N_j \left(p_t \frac{\partial x}{\partial \xi} - p_n \frac{\partial y}{\partial \xi} \right) t \, \mathrm{d}\xi \\ &= \sum_{i=1}^{NGAUS} a_i \, N_j \, t \left(p_t \frac{\partial x}{\partial \xi} - p_n \frac{\partial y}{\partial \xi} \right) \\ f_{y,j} &= \int_{len} N_j \left(p_n \frac{\partial x}{\partial \xi} + p_t \frac{\partial y}{\partial \xi} \right) t \, \mathrm{d}\xi \\ &= \sum_{i=1}^{NGAUS} a_i \, N_j \, t \left(p_n \frac{\partial x}{\partial \xi} + p_t \frac{\partial y}{\partial \xi} \right) \end{aligned} \tag{A.54}$$

A.11 Convergence

When the element stiffness matrices and load vectors have been calculated, the solution proceeds by assembling the element components and solving for the unknowns. When the nodal displacements have been evaluated, convergence at the end of the increment is checked by ensuring that equilibrium is reached between internal forces and external loads. Firstly the internal stresses at the end of the increment, denoted $\boldsymbol{\sigma}^n$, are evaluated by updating the previous converged internal stresses, $\boldsymbol{\sigma}^{n-1}$ within each element:

$$\boldsymbol{\sigma}^n = \boldsymbol{\sigma}^{n-1} + \Delta\boldsymbol{\sigma} \tag{A.55}$$

where the incremental stress $\Delta\boldsymbol{\sigma}$ is calculated from the incremental displacements directly in the case of a linear increment, or $\boldsymbol{\sigma}^n$ is adjusted by the radial return mapping algorithms described above in the case of an elastic-plastic increment. The internal stresses are then extrapolated to a vector of internal forces at the nodes, denoted $\mathbf{f}^{INT}$. For a beam element the internal forces are:

$$\begin{aligned} \mathbf{f}^{INT} &= \int \mathbf{R}^T \mathbf{B}^T \boldsymbol{\sigma}^n \, \mathrm{d}x \\ &= \sum_{i=1}^{NGAUS} a_i \, \mathbf{R}_i^T \mathbf{B}_i^T \boldsymbol{\sigma}_i^n \, \det \mathbf{J}_i \end{aligned} \tag{A.56}$$

while for plane elements the internal forces are:

$$\begin{aligned} \mathbf{f}^{INT} &= \iint \mathbf{B}^T \boldsymbol{\sigma}^n \, t \, \mathrm{d}x\mathrm{d}y \\ &= \sum_{i=1}^{NGAUS} \sum_{j=1}^{NGAUS} a_i a_j \, \mathbf{B}_{ij}^T \boldsymbol{\sigma}_{ij}^n \, t \, \det \mathbf{J}_{ij} \end{aligned} \tag{A.57}$$

Convergence is checked by calculating the residual vector, denoted $\mathbf{f}^{RES}$, as follows:

$$\mathbf{f}^{RES} = \mathbf{f} + \mathbf{r} - \mathbf{f}^{INT} \tag{A.58}$$

where $\mathbf{r}$ is a vector containing reactions at the boundary conditions. When $\mathbf{f}^{RES}$ contains terms that are sufficiently small, convergence is assumed to have occurred. If convergence is not reached, subsequent iterations are required.

B Standard Normal Cumulative Distribution

The standard normal cumulative distribution function Φ is defined as (Haugen, 1968):

$$\Phi(x) = \frac{1}{\sqrt{2\pi}} \int_{-\infty}^{x} e^{-t^2/2} \, \mathrm{d}t \tag{B.1}$$

The standard normal CDF can be related to the error function through (Spiegel, 1968):

$$\mathrm{erf}(x) = 2\Phi(x\sqrt{2}) - 1 \tag{B.2}$$

since the error function is defined as:

$$\mathrm{erf}(x) = \frac{2}{\sqrt{\pi}} \int_{0}^{x} e^{-t^2} \, \mathrm{d}t \tag{B.3}$$

The error function can be approximated by a series expansion as (Spiegel, 1968):

$$\mathrm{erf}(x) = \frac{2}{\sqrt{\pi}} \left(x - \frac{x^3}{3 \cdot 1!} + \frac{x^5}{5 \cdot 2!} - \frac{x^7}{7 \cdot 3!} + \ldots \right) \tag{B.4}$$

In general as many as 30 terms are required for the series to converge for typical values of $\Phi(x)$. Equations (B.4) and (B.2) were used to generate the standard normal CDF, shown in Table B.1.

x	0.00	0.01	0.02	0.03	0.04	0.05	0.06	0.07	0.08	0.09
0.0	0.5000	0.5040	0.5080	0.5120	0.5160	0.5199	0.5239	0.5279	0.5319	0.5359
0.1	0.5398	0.5438	0.5478	0.5517	0.5557	0.5596	0.5636	0.5675	0.5714	0.5753
0.2	0.5793	0.5832	0.5871	0.5910	0.5948	0.5987	0.6026	0.6064	0.6103	0.6141
0.3	0.6179	0.6217	0.6255	0.6293	0.6331	0.6368	0.6406	0.6443	0.6480	0.6517
0.4	0.6554	0.6591	0.6628	0.6664	0.6700	0.6736	0.6772	0.6808	0.6844	0.6879
0.5	0.6915	0.6950	0.6985	0.7019	0.7054	0.7088	0.7123	0.7157	0.7190	0.7224
0.6	0.7257	0.7291	0.7324	0.7357	0.7389	0.7422	0.7454	0.7486	0.7517	0.7549
0.7	0.7580	0.7611	0.7642	0.7673	0.7704	0.7734	0.7764	0.7794	0.7823	0.7852
0.8	0.7881	0.7910	0.7939	0.7967	0.7995	0.8023	0.8051	0.8078	0.8106	0.8133
0.9	0.8159	0.8186	0.8212	0.8238	0.8264	0.8289	0.8315	0.8340	0.8365	0.8389
1.0	0.8413	0.8438	0.8461	0.8485	0.8508	0.8531	0.8554	0.8577	0.8599	0.8621
1.1	0.8643	0.8665	0.8686	0.8708	0.8729	0.8749	0.8770	0.8790	0.8810	0.8830
1.2	0.8849	0.8869	0.8888	0.8907	0.8925	0.8944	0.8962	0.8980	0.8997	0.9015
1.3	0.9032	0.9049	0.9066	0.9082	0.9099	0.9115	0.9131	0.9147	0.9162	0.9177
1.4	0.9192	0.9207	0.9222	0.9236	0.9251	0.9265	0.9279	0.9292	0.9306	0.9319
1.5	0.9332	0.9345	0.9357	0.9370	0.9382	0.9394	0.9406	0.9418	0.9429	0.9441
1.6	0.9452	0.9463	0.9474	0.9484	0.9495	0.9505	0.9515	0.9525	0.9535	0.9545
1.7	0.9554	0.9564	0.9573	0.9582	0.9591	0.9599	0.9608	0.9616	0.9625	0.9633
1.8	0.9641	0.9649	0.9656	0.9664	0.9671	0.9678	0.9686	0.9693	0.9699	0.9706
1.9	0.9713	0.9719	0.9726	0.9732	0.9738	0.9744	0.9750	0.9756	0.9761	0.9767
2.0	0.9772	0.9778	0.9783	0.9788	0.9793	0.9798	0.9803	0.9808	0.9812	0.9817
2.1	0.9821	0.9826	0.9830	0.9834	0.9838	0.9842	0.9846	0.9850	0.9854	0.9857
2.2	0.9861	0.9864	0.9868	0.9871	0.9875	0.9878	0.9881	0.9884	0.9887	0.9890
2.3	0.9893	0.9896	0.9898	0.9901	0.9904	0.9906	0.9909	0.9911	0.9913	0.9916
2.4	0.9918	0.9920	0.9922	0.9925	0.9927	0.9929	0.9931	0.9932	0.9934	0.9936
2.5	0.9938	0.9940	0.9941	0.9943	0.9945	0.9946	0.9948	0.9949	0.9951	0.9952
2.6	0.9953	0.9955	0.9956	0.9957	0.9959	0.9960	0.9961	0.9962	0.9963	0.9964
2.7	0.9965	0.9966	0.9967	0.9968	0.9969	0.9970	0.9971	0.9972	0.9973	0.9974
2.8	0.9974	0.9975	0.9976	0.9977	0.9977	0.9978	0.9979	0.9979	0.9980	0.9981
2.9	0.9981	0.9982	0.9982	0.9983	0.9984	0.9984	0.9985	0.9985	0.9986	0.9986
3.0	0.9987	0.9987	0.9987	0.9988	0.9988	0.9989	0.9989	0.9989	0.9990	0.9990
3.1	0.9990	0.9991	0.9991	0.9991	0.9992	0.9992	0.9992	0.9992	0.9993	0.9993
3.2	0.9993	0.9993	0.9994	0.9994	0.9994	0.9994	0.9994	0.9995	0.9995	0.9995
3.3	0.9995	0.9995	0.9995	0.9996	0.9996	0.9996	0.9996	0.9996	0.9996	0.9997
3.4	0.9997	0.9997	0.9997	0.9997	0.9997	0.9997	0.9997	0.9997	0.9997	0.9998
3.5	0.9998	0.9998	0.9998	0.9998	0.9998	0.9998	0.9998	0.9998	0.9998	0.9998
3.6	0.9998	0.9998	0.9999	0.9999	0.9999	0.9999	0.9999	0.9999	0.9999	0.9999
3.7	0.9999	0.9999	0.9999	0.9999	0.9999	0.9999	0.9999	0.9999	0.9999	0.9999
3.8	0.9999	0.9999	0.9999	0.9999	0.9999	0.9999	0.9999	0.9999	0.9999	0.9999
3.9	1.0000	1.0000	1.0000	1.0000	1.0000	1.0000	1.0000	1.0000	1.0000	1.0000

Table B.1: Standard normal cumulative distribution

C ABAQUS User Element Subroutine Interface

The ABAQUS general purpose finite element program allows the user to implement a complete finite element in a user element subroutine. The coding of this element must be in the FORTRAN 77 programming language. ABAQUS provides a user element subroutine interface, named UEL, for this purpose, which is essentially the only limitation ABAQUS places on the coding of this user element. The user must ensure that the element will converge when the standard solution procedures within ABAQUS are used.

ABAQUS calls this user element subroutine whenever element calculations are required. The user element subroutine interface provides arrays and variables containing information that may be needed in these calculations. The code which performs these calculations is the responsibility of the user. The UEL interface cards in ABAQUS V5.2 are:

```
      subroutine UEL(RHS,AMATRX,SVARS,ENERGY,NDOFEL,NRHS,NSVARS,
     1    PROPS,NPROPS,COORDS,MCRD,NNODE,U,DU,V,A,JTYPE,TIME,DTIME,
     2    KSTEP,KINC,JELEM,PARAMS,NDLOAD,JDLTYP,ADLMAG,PREDEF,NPREDF,
     3    LFLAGS,MLVARX,DDLMAG,MDLOAD,PNEWDT)
```

The user element code must return RHS, AMATRX, SVARS, ENERGY and PNEWDT to the main ABAQUS program. Not all of the arrays and variables provided in the UEL subroutine interface were used in this thesis and only those of significance are briefly described below. Further detail can be found in the ABAQUS User's Manual (1992).

Arrays evaluated in the user element code:

RHS	An array containing the contributions of this element to the right-hand side vectors of the overall system of equations.
AMATRX	An array containing the contributions of this element to the global stiffness matrix.
SVARS	An array containing the values of the solution state variables associated with this element. ABAQUS provides its values at the end of the previously converged increment. The UEL subroutine must update these to the values at the end of the current increment. The number of state variables is NSVARS.

Arrays and variables passed for information:

PROPS	An array containing the element properties. These element properties are specified by the user in the problem input deck. The number of properties is NPROPS.

COORDS	An array containing the undeformed global coordinates of the nodes of the element. The number of coordinates per node is MCRD.
U, DU	An array containing estimates of the basic solution variables (i.e. displacements and displacement increments) at the end of the current increment. The number of components in these arrays is NDOFEL. The size of the RHS and AMATRX arrays corresponds to this number.
JDLTYP, ADLMAG	Arrays containing information regarding distributed loads acting on the element. The number of distributed loads active on the element is NDLOAD.
NNODE	A scalar indicating the number of nodes on the element. It is specified in the problem input deck.
JTYPE, JELEM	Scalars indicating the element type and element number respectively. These are specified in the problem input deck.
KINC	Scalar indicating the increment number.

One feature of the ABAQUS user element subroutine interface is that solution state variables are not associated with any specific integration point. Consequently the standard post-processing features of ABAQUS are not available, and the user can only print out solution state variable values. The ABAQUS V4.8 user element subroutine interface incorporated features which enabled the user to implement plotting of contour lines from within the UEL subroutine (ABAQUS User's Manual, 1989). These features were rather complex and are no longer included in the ABAQUS V5.2 release.

In this thesis the solution state variables of interest are written to a separate database file in a format which allows recovery of the original integration points. This database file is also used in the probabilistic finite element subroutine.

ABAQUS has the facility to implement a user material subroutine (ABAQUS User's Manual, 1992). This user material subroutine is called at every integration point and requires the calculation of the element constitutive matrix and the solution state variables at the integration points. A dummy user material subroutine was written for the two-dimensional plane elements which reads the database file and performs the fast probability integration algorithms. The subroutine assigns the solution state variables of the element (i.e. the probabilistic response) to the appropriate integration points in the user subroutine. This device allows the generation of contour plots for the user elements.

D Analytical Derivations for Beam Structures

D.1 Angled Bracket

A schematic diagram of an angled bracket is shown below. The two beams are rigidly connected at point B and are rigidly constrained at point A. The out-of-plane vertical point load V acts in the negative Y direction and the in-plane horizontal load H acts in the positive X direction. The beam lengths used in the calculations in this thesis are: $l_1 = l_2 = 2\text{m}$.

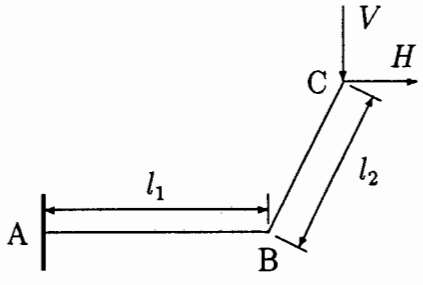

Considering the in-plane horizontal load H, then from equilibrium at points A and B:

$$M_A^Y = M_B^Y = Hl_2 \tag{D.1}$$

Considering the out-of-plane vertical load V, then from equilibrium at points A and B:

$$\begin{aligned} T_A &= T_B = Vl_2 \\ M_A^Z &= Vl_1 \end{aligned} \tag{D.2}$$

D.2 Crossed Beam Structure

A schematic diagram of a crossed beam structure with an overhanging point load is shown below. The beams are at right angles to each other and the displacements, but not the rotations, are equal at point E. The beams are rigidly constrained at points A, B and C. The beam lengths used in the calculations in this thesis are: $l_1 = l_2 = 2\text{m}$.

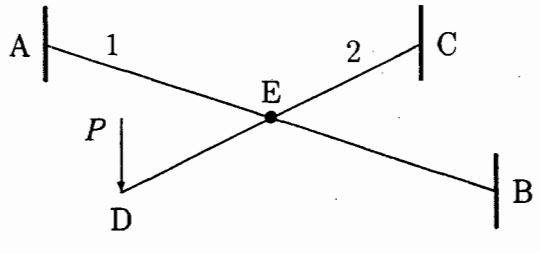

Consider beams 1 and 2 separately to find expressions for the vertical deflection at point E (assume downward deflection is negative) (Young, 1989):

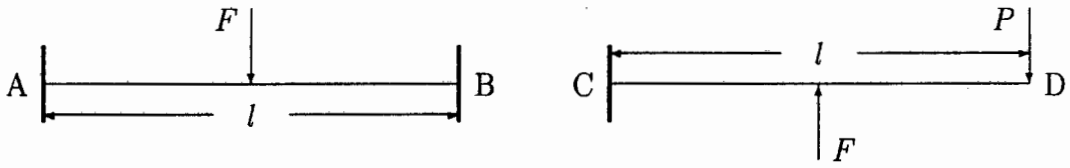

$$\delta_E = -\frac{Fl^3}{192E_1I_1} \qquad \delta_E = \frac{Fl^3}{24E_2I_2} - \frac{5Pl^3}{48E_2I_2}$$

Solve for compatibility of vertical deflection at point E:

$$F = \frac{20PE_1I_1}{(8E_1I_1 + E_2I_2)}$$

Substitute to solve for vertical deflection at point E:

$$\delta_E = \frac{-10Pl^3}{96(8E_1I_1 + E_2I_2)} \tag{D.3}$$

D.3 Co-axial Three Bar Link

A schematic diagram of a co-axial three bar link with an axial end load is shown below. The displacements at point D are equal. The bars are rigidly constrained at points A, B and C. The beam lengths used in the calculations in this thesis are: $l_1 = 1$m; $l_2 = 2$m; $l_3 = 1.5$m. The cross-sections and elastic moduli are equal.

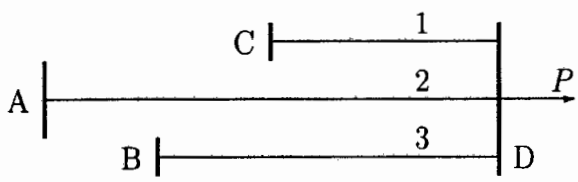

From equilibrium considerations at point D, the sum of the internal forces equals the end load:

$$F_1 + F_2 + F_3 = P$$

From compatibility at point D, the axial extensions of the bars are equal:

$$\delta_1 = \delta_2 = \delta_3 = \delta_D$$

The extension of a bar under tension is (Young, 1989):

$$\delta = \frac{Fl}{AE}$$

Substituting the compatibility equation into equilibrium equation:

$$P = F_1 \left(1 + \frac{A_2 E_2}{A_1 E_1}\frac{l_1}{l_2} + \frac{A_3 E_3}{A_1 E_1}\frac{l_1}{l_3}\right) \tag{D.4}$$

from which it is possible to solve for F_1, F_2, F_3 and δ_D.

D.4 Two Bar Truss System

A schematic diagram of a two bar truss system with a downward point load is shown below. The angle between the trusses at point B is 45°. The trusses are pin-jointed at points A, B and C. The truss lengths used in the calculations in this thesis are: $l_1 = 2.83$m; $l_2 = 2$m. The cross-sections and elastic moduli are equal.

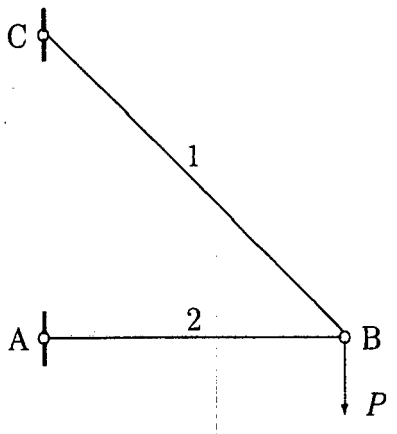

From equilibrium in the vertical direction at point B:

$$F_1 = \frac{P}{\cos 45°} = \sqrt{2}P \tag{D.5}$$

From equilibrium in the horizontal direction at point B:

$$F_2 = -F_1 \cos 45° = -P \tag{D.6}$$

The stiffness matrix governing horizontal and vertical displacement of the nodes of a truss element at angle θ to the horizontal is (Rao, 1982):

$$\mathbf{K} = \frac{AE}{l}\begin{bmatrix} \cos^2\theta & \sin\theta\cos\theta & -\cos^2\theta & -\sin\theta\cos\theta \\ \sin\theta\cos\theta & \sin^2\theta & -\sin\theta\cos\theta & -\sin^2\theta \\ -\cos^2\theta & -\sin\theta\cos\theta & \cos^2\theta & \sin\theta\cos\theta \\ -\sin\theta\cos\theta & -\sin^2\theta & \sin\theta\cos\theta & \sin^2\theta \end{bmatrix}$$

Assembling the global stiffness matrix for the truss system above, setting displacements at the boundary conditions to zero, and inverting the reduced stiffness matrix it is possible to solve for the displacements at point B from:

$$\begin{Bmatrix} u_B \\ v_B \end{Bmatrix} = \frac{l_2}{AE}\begin{bmatrix} 1+\frac{\sqrt{2}}{4} & -\frac{\sqrt{2}}{4} \\ -\frac{\sqrt{2}}{4} & \frac{\sqrt{2}}{4} \end{bmatrix}^{-1}\begin{Bmatrix} 0 \\ P \end{Bmatrix} \tag{D.7}$$

D.5 Combined Beam-Truss System

A schematic diagram of a combined beam-truss system with a downward point load is shown below. The geometry is identical to the two bar truss system above, but here member 2 is a cantilever beam rigidly constrained at point A and connected by a pin-joint at point B to member 1. The lengths used in the calculations in this thesis are: $l_1 = 2.83$m; $l_2 = 2$m.

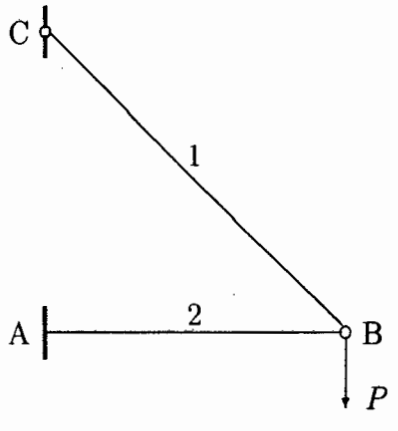

The stiffness matrix governing the horizontal and vertical displacements of member 1 is (from the previous section):

$$\mathbf{K} = \frac{AE\sqrt{2}}{4l_2}\begin{bmatrix} 1 & -1 & -1 & 1 \\ -1 & 1 & 1 & -1 \\ -1 & 1 & 1 & -1 \\ 1 & -1 & -1 & 1 \end{bmatrix} \begin{matrix} u_B \\ v_B \\ u_C \\ v_C \end{matrix}$$

The stiffness matrix governing the horizontal and vertical displacements and rotations of member 2 is (Dawe, 1984):

$$\mathbf{K} = \begin{bmatrix} AE/l & 0 & 0 & -AE/l & 0 & 0 \\ 0 & 12EI/l^3 & 6EI/l^2 & 0 & -12EI/l^3 & 6EI/l^2 \\ 0 & 6EI/l^2 & 4EI/l & 0 & -6EI/l^2 & 2EI/l \\ -AE/l & 0 & 0 & AE/l & 0 & 0 \\ 0 & -12EI/l^3 & -6EI/l^2 & 0 & 12EI/l^3 & -6EI/l^2 \\ 0 & 6EI/l^2 & 2EI/l & 0 & -6EI/l^2 & 4EI/l \end{bmatrix} \begin{matrix} u_A \\ v_A \\ \theta_A \\ u_B \\ v_B \\ \theta_B \end{matrix}$$

Assembling the global stiffness matrix and setting the displacements at the boundary conditions to zero, the displacements and rotation at point B can be solved from:

$$\begin{Bmatrix} u_B \\ v_B \\ \theta_B \end{Bmatrix} = \begin{bmatrix} \frac{AE(1+\sqrt{2}/4)}{l_2} & -\frac{AE\sqrt{2}}{4l_2} & 0 \\ -\frac{AE\sqrt{2}}{4l_2} & \frac{AE\sqrt{2}}{4l_2} + \frac{12EI}{l_2^3} & -\frac{6EI}{l_2^2} \\ 0 & -\frac{6EI}{l_2^2} & \frac{4EI}{l_2} \end{bmatrix}^{-1} \begin{Bmatrix} 0 \\ P \\ 0 \end{Bmatrix} \tag{D.8}$$

D.6 Rectangular Plane Frame

The rigid frame structure shown schematically below was solved by Kleinlogel (1952) in terms of some characteristic coefficients from which the bending moment distributions and reaction forces can be derived for a number of different load configurations (Frame 41 in Kleinlogel (1952) – second moments of area of vertical beams are equal). The load configurations considered here are a distributed load acting transverse to the horizontal beam BC (e.g. the combination of imposed loads and self-weight), a distributed load acting transverse to the left vertical beam AB (e.g. a side wind load), and a uniform increase in temperature of the whole frame. The bending moments at points A, B, C and D and the maximum bending moment and its location are given here. Kleinlogel (1952) gives a more detailed derivation. A schematic diagram of the rectangular plane frame and its characteristic coefficients are given below. The beams are rigidly connected at points

B and C and are rigidly constrained at points A and D. The beam lengths used in the calculations in this thesis are: $h = 5\text{m}$; $l = 8\text{m}$.

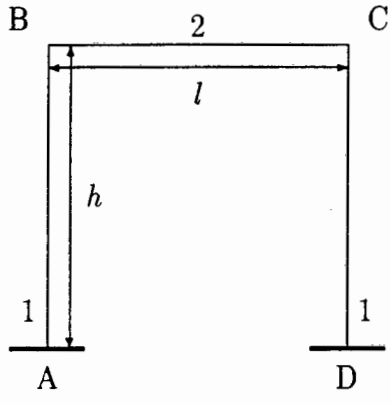

$$k = \frac{I_2}{I_1}\frac{h}{l}$$

$$N_1 = k + 2$$

$$N_2 = 6k + 1$$

For a distributed load w acting transverse to the horizontal beam BC:

$$\begin{aligned} M_A = M_D &= +\frac{wl^2}{12N_1} \\ M_B = M_C &= -\frac{wl^2}{6N_1} \\ M_{max} &= \frac{wl^2}{8} + M_B \text{ acting at the centre of beam 2} \end{aligned} \tag{D.9}$$

For a distributed load w acting transverse to the left vertical beam AB:

$$\begin{aligned} M_A \searrow \\ M_D \nearrow &= \frac{wh^2}{4}\left[-\frac{k+3}{6N_1} \mp \frac{4k+1}{N_2}\right] \\ M_B \searrow \\ M_C \nearrow &= \frac{wh^2}{4}\left[-\frac{k}{6N_1} \pm \frac{2k}{N_2}\right] \\ M_{max} &= M_A \end{aligned} \tag{D.10}$$

For a uniform increase in temperature ΔT of the whole frame (α is the coefficient of thermal expansion):

$$\begin{aligned} C &= \frac{3EI_2\alpha\Delta T}{hN_1} \\ M_A = M_D &= +C\,\frac{k+1}{k} \\ M_B = M_C &= -C \\ M_{max} &= M_A \end{aligned} \tag{D.11}$$

D.7 Gable Plane Frame

The rigid frame structure shown schematically below was solved by Kleinlogel (1952) in terms of some characteristic coefficients from which the bending moment distributions and reaction forces can be derived for a number of different load configurations (Frame 92 in Kleinlogel (1952) - second moments of area of vertical beams are equal and second moment of area of gable beams are equal). The load configuration considered here is a distributed load w acting vertically down onto the gable beams BC and CD (e.g. self-weight of the gable beams). The bending moments at points A, B, C, D and E are given here. Kleinlogel (1952) gives a more detailed derivation. A schematic diagram of the rectangular plane frame and its characteristic coefficients are given below. The beams are rigidly connected at points B, C and D and are rigidly constrained at points A and E. The beam lengths used in the calculations in this thesis are: $h = 5\text{m}$; $s = 5\text{m}$; $l = 8\text{m}$; $f = 3\text{m}$.

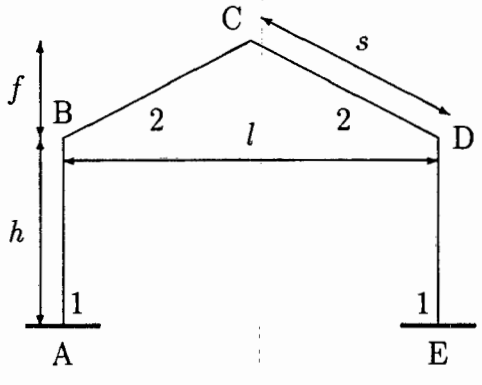

$$k = \frac{I_2}{I_1}\frac{h}{s} \qquad \varphi = \frac{f}{h} \qquad m = 1 + \varphi \qquad B = 3k + 2 \qquad C = 1 + 2m$$

$$K_1 = 2(k + 1 + m + m^2) \qquad K_2 = 2(k + \varphi^2) \qquad R = \varphi C - k$$

$$N_1 = K_1 K_2 - R^2 \qquad N_2 = 3k + B$$

$$\begin{aligned} M_A = M_E &= \frac{wl^2}{16}\frac{k(8 + 15\varphi) + \varphi(6 - \varphi)}{N_1} \\ M_B = M_D &= -\frac{wl^2}{16}\frac{k(16 + 15\varphi) + \varphi^2}{N_1} \\ M_C &= \frac{wl^2}{8} - \varphi M_A + m M_B \end{aligned} \tag{D.12}$$

E Monte Carlo Simulation Program

A general Monte Carlo simulation program was written to simulate the random response of problems which can be represented by simple explicit formulations. The program was designed to be modular so that the program could be easily adapted to cater for new problems: only a few of the modules require minor modifications with each new problem. The program structure is shown in Figure E.1 where those modules which need modification of the source code with a new problem are marked by a star (*) in the top left corner.

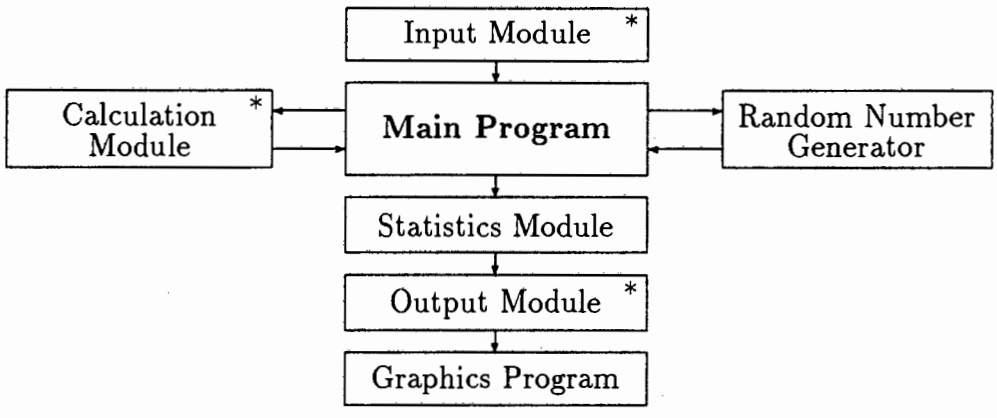

Figure E.1: Schematic of Monte Carlo simulation program structure

The input module is interactive and prompts the user to enter the required information (mean and coefficient of variation of each random parameter, a seed to start the random number generator for each independent random parameter and the number of simulations required). For each new problem only the prompts need to be modified as the information entered by the user is passed to transparent program variables.

The main program receives these program variables from the input module. It starts a loop of simulations and, for each simulation, calls the random number generator for each independent random parameter. The random number generator is based on the theory by Knuth (1969): it returns a random value based on the mean and standard deviation of a random parameter. These values are normally distributed, but can be transformed to other distributions.

The random values are entered into the explicit formulation for the random response in the calculation module. For each new program this explicit formulation needs to be changed. The explicit formulation can include interpolation from a look-up table. Each random response so calculated is stored in an internal array. The size of this internal array limits the maximum number of simulations to 20,000. The number of failures are

recorded (i.e. every time the response exceeds the failure criteria, which themselves may be random).

When the required number of simulations have been performed, the array containing the random responses is passed to the statistics module. This module calculates the mean, standard deviation and skewness of the response, records the minimum and maximum occurrences of the response and builds up probability distribution and cumulative distribution data by a histogram technique (i.e. counting the number of occurrences within a set of small intervals spanning the entire range of the response).

This information is written to a results file in the output module. This module needs minor modifications for each new problem to adapt the descriptive text in the results file to the new problem.

If this is required, the probability distribution and cumulative distribution data can be imported to a separate spreadsheet program to create graphic representations of these.

The program has been adapted to allow a larger number of simulations to be performed. The random responses calculated in the calculation module are then not stored in an internal array and the statistics module is not used. The number of failures is still recorded. This adaptation is useful for the analysis of problem involving very small probabilities of failure, where a large number of trials is required.

Apart from the problems considered in this thesis, Monte Carlo programs have been used for the simulation of butt-welded cylinders where an analytical expression was derived for the stiffening effects of the weld, of flat-ended cylinders which involve the probabilistic simulation of deterministic Code-described calculations, and of a spherical pressure vessel with a flush radial nozzle subject to elastic and creep loading (Weber and Penny, 1991). In the case of the elastic loading, the stress concentration at the nozzle junction was simulated using interpolation from a look-up table based on the stress concentration graphs derived by Leckie and Penny (1963). In the case of creep loading the life-time of the pressure vessel was simulated based on the results of normalised creep analyses performed by Weber (1990).